UNIVERSITY OF LIVERPOOL

TRANSLATIONAL DEVELOPMENTS IN THE STUDY OF SEPSIS:

Investigations into molecular pathways, experimental modelling, & applications of novel biomarkers

Eamon Patrick McCarron

Thesis submitted in accordance with the requirements of the University of Liverpool for the degree of Master of Philosophy

Contents

I Acknowledgments

Zuerst möchte ich Dr Ingeborg Welters danken, für ihre Freundschaft und andauernde Unterstützung über die letzten zwei Jahre. Ohne ihre Entschlossenheit, Leitung und Bereitwilligkeit mich als Student zu fördern, hätte ich diese wunderbare Erfahrung in akademischer Medizin nicht machen können. Dafür bin ich außerordentlich dankbar.

Dr Dominic Williams for accepting me as a student and allowing me to research in the department this year. Thank you for being both patient and understanding when it came to my progress and work. I have gained invaluable experience and have appreciated the opportunity.

Dank gebührt auch Dr Anja Kipar, die trotz ihres vollen Terminkalenders immer die Zeit gefunden hat, mir persönlich feedback zu geben. Danke für die histopathologische Analyse und ihren reichen Erfahrungsschatz im Bereich der Pathologie.

Dr Dan Antoine's experience in HMGB1 and CK18 detection and analysis was invaluable, and I am grateful he took the time to show me these techniques.

Des Weiteren danke ich auch Jana Lemm und der Universität Jena für die Unterstützung meines Projekts und die freundliche Bereitstellung von Proben.

Professor Cheng Hok-Toh & Carol Powell for donating clinical samples.

Valerie Tilston, Phil Roberts & Luke Palmer for their help with the *in vivo* work.

The Association of physicians for Great Britain and Ireland for their generous financial support this year.

I am grateful to have been part of team HMGB1 along with Hannah and Jon. Thank you for allowing me to share in your work and for teaching me the lab basics, cell culture and more.

In my daily work I have been blessed with a friendly and cheerful group of fellow students. Áine made sure that I never starved, by always filling the office cupboard with tasty treats (Go raibh maith agat!). Nicola provided invaluable daily information and teaching on stats, along with a fabulous selection of scarves. Ali and Cosmo for making sure I wasn't homeless by housing me and Babs. Thanks to everyone else in the lab and offices and anyone who I may have missed out, for all your help & friendship throughout the year. I owe a special debt of gratitude to Beatrix and Eugiene, who are a source of constant inspiration in everything I do.

Grazie Gio per avermi insegnato la fondamentale differenza fra il rattus rattus (ratto brutto) e il Wistar ratto (ratto abbastanza). Grazie anche per la tua bella amicizia, il tuo sopporto e aiuto durante l'anno e per il tuo fantastico cibo e caffè. Spero di poterti ritornare il favore un giorno!

Lastly, my loving and supportive parents. Their willingness to support me through the last five years of university and every decision I have made has been appreciated dearly. Go raibh maith agaibh!

II Abbreviations

ACCP	American College of Chest Physicians
AdipoR1&2	Adiponectin receptor 1 &2
ALD	Alcoholic liver disease
ALT	Alanine transaminase
A-MuLV	Abelson murine leukemia virus
AoCF	Acute on chronic failure
APACHE II	Acute Physiology and Chronic Health Evaluation II
APAP	Acetyl-para-aminophenol.
ApC	Adipocyte
APS	Ammonium persulfate
ARF	Acute renal failure
ATP	Adenosine triphosphate
Ba	Bacteria
CARS	Compensatory anti-inflammatory response syndrome
CASP	Colon ascendens stent procedure
CHB	Chronic hepatitis B
CK18	Cytokeratin 18
CLP	Ceacal ligation and puncture
CV	Central vein
DAMPS	Damage associated molecular pathways
Db	Bacterial debris
E.Coli	Escherichia Coli
EC	Endothelial cell
ELISA	Enzyme linked immunosorbant assay
EMEA	European medicines agency
ER	Endoplasmic reticulum
FDA	Food and drug agency

GGT	Gamma glytamyl transpeptidase
Gly	Glycogen
Gly D	Glycogen depletion
H&E	Haematoxylin and eosin
HLA	Human leukocyte antigen
HMGB1	High mobility group box protein – 1
HSP	Heat shock protein
ICU	Intensive care unit
ICU	Intensive care unit
IFN-γ	Interferon gamma
IgG	Immunoglobulin G
IKK	Inhibitory kappa kinase
IL 1, 6, 10, 12, 15, 18	Interleukin 1,6,10,12,15,18
IP	Intra-preitoneally
ITU	Intensive treatment unit
IκB	Inhibitory kappa B protein
LFTS	Liver function tests
LPS	Lipopolysaccharide
LRR	Leucine rich repeat
$MgSo^4$	Magnesium sulphate
MHC	Major Histocompatability complex
NALD	Non-alcholic liver disease
Nec Hep	Necrotic hepatocyte
NFκB	Transcription nuclear factor kappa-light-chain-enhancer of activated B cells
NHS	National Health Service
NHS	National health service
NL	Neutrophil

NLS	Nuclear localization signal
PAMPS	Pathogen associated molecular pathways
PAS	Periodic acid Schiff
PFA	Paraformaldehyde
PSTC	Predictive safety testing consortium
PT	Pro-thrombin time
PV	Portal vein
RHD	Rel homology domain
ROC	Receiver operator characteristic curve
SC	Subcutaneous
SCCM	Society of Critical Care Medicine
SD	Standard deviation
SEM	Standard error of the mean
SIRS	Systemic inflammatory response syndrome
TEMED	Tetramethylethylenediamine
TLR	Toll like receptor
TNFα	Tumour necrosis factor alpha
UK	United Kingdom
V	Vacuole

III Abstract

Sepsis is a significant problem in the United Kingdom with diagnosis, management and prognosis proving difficult for clinicians. This is further exacerbated by the lack of sensitive and specific biomarkers for the disease and complications related with it (i.e. organ dysfunction). The lack of biomarkers and efficacious therapeutic intervention is a result of inadequate understanding of this disconnect between murine and human sepsis on a molecular level and *in vivo*. In this analysis, comparison of molecular signalling pathways involved in inflammation has revealed a possible source for this disconnect. Comparative analysis of two well characterised murine models of sepsis (LPS and faecal peritoneal inoculation) has further demonstrated that the difficulty in recapitulating a similar environment of human sepsis in rodents widens the gap that the translational bridge must cross. Both models showed a similar level of change consistent with an acute systemic inflammatory response, but discrete differences show the superiority of the faecal inoculation as a reproducible, valid and more reliable model of murine sepsis. HMGB1 and cleaved/uncleaved CK18 have been shown to be accurate ways of monitoring the level of inflammation, necrosis and apoptosis in the literature. Their application to defined groups of ICU patients, who could potentially benefit from them, has shown that there is potential for a clinical application. Their use alongside currently used markers of liver function could enhance the overall picture that clinicians have when approaching these patients. However, further research is needed involving larger sample sizes and more scrupulous statically analysis before widespread application can occur.

IV List of Figures

V List of Tables

Chapter 1:

General Introduction

Contents

1 General Introduction

1.1 Sepsis

Sepsis is a life threatening clinical condition defined as a systemic inflammatory response syndrome (SIRS) together with a demonstrable source of infection[1]. It is a major cause of admission to the Intensive care unit (ICU) and carries a high mortality rate of 30%[2], that has been shown to increase in subsequent months after discharge from hospital[3]. Sepsis provides intensivists with significant difficulties regarding management and prognostication, and this is further exacerbated by the lack of specific and sensitive biomarkers available. Studies have already identified the need for the investigation and integration of novel biomarkers with routine clinical chemistry, in order to better diagnose and improve the prognosis of this patient group.[4]

1.1.1American College of Chest Physicians/Society of Critical care Medicine (ACCP/SCCM) definitions [1]

Up until the construction of a general census on the definitions surrounding SIRS, sepsis and related syndromes, there was often diagnostic confusion and misuse of terms in the literature. The ACCP/SCCM set out to construct a clear set of definitions that would allow clinicians and researchers to better diagnosis patients and improve inclusion criteria into studies. Initially they defined the clinical parameters required for the diagnosis of SIRS, an inflammatory process independent of an infectious cause, but related to other aetiologies (i.e. burns, trauma etc.). The committee then developed four recommendations which outlined the terminology surrounding sepsis and sepsis syndromes. Their recommendations are summarised in *table 1.1*.

1.1.2 Epidemiology

In a large multi-centred cohort study *Alberti et al* [5] described that one fifth of patients on admission to ICU had evidence of infection, along with one third of patients who were considered to be "long stay" patients. Altogether eighty per cent of these patients showed evidence of an inflammatory response and would fit in to the *ACCP/SCCM* definition of sepsis[1]. This study also identified that the major sources of infection where respiratory, abdominal, urinary and bloodstream, which is similar to what has been reported before. However, a further study in the UK reported that the majority of patients admitted to ICU with severe sepsis where non-surgical cases suffering with cardiovascular or respiratory aetiologies[6]. Gram negative bacilli (in

45% of patients) and Gram-positive cocci (in 37% of patients) were identified as common causative organisms for infection[5].

The incidence of severe sepsis remains fairly consistent between studies and is reported as ten cases per 100 ICU admissions [7]. The UK, however, has been noted to have a higher incidence (51 per one 100, 00 population per year admitted to ICU with severe sepsis[6]). This has been attributed to the fact that other countries have a lower threshold for admission to ICU, even before patients require organ or ventilator support, whereas in the UK patients that are admitted to ICU frequently present with sepsis and multiple organ failure [7]. Multiple organ failure is associated with a poorer outcome, and this is reflected in an ICU mortality rate for severe sepsis of 35% and overall hospital mortality rate of 47% in the UK[6].

1.1.3 Financial Burden

Angus et al (2) reported that the estimated burden of severe sepsis in the United States (US) was sixteen point seven billion dollars per annum (roughly ten point seven British pounds). Studies estimating the cost in the UK are sparse but scaling this down for the UK population reveals estimated costs of two point six eight billion British pounds. These figures demonstrate the need for further research into novel ways of diagnosing and prognosticating these patients in order to reduce costs and overall National Health Service (NHS) burden.

1.1.4 Pathophysiology of Sepsis

As described by the *ACCP/SCCM*[1] Sepsis is the combination of SIRS with a demonstrable source of infection. Gram negative bacilli and Gram-positive cocci have already been described as causative agents in the provocation of an initial inflammatory response[5]. Inflammation comprises a large portion of the body's innate immune response to infection; so is considered a normal bodily function. Historically, the exaggerated response seen in sepsis, and severe sepsis severity, has been made responsible for the disease. The idea of sepsis as an exaggerated inflammatory response was based on the observation that lipopolysaccharide (LPS), a component of gram-negative bacteria, elicits a sharp increase in pro-inflammatory cytokines, such as TNF-α, IL-6 and IL-1[8]. Consequently, animal models of endotoxaemia have been widely used to better understand the pathophysiology of sepsis. The significantly raised levels of cytokines, in particular TNF-α, led to the

hypothesis that inhibition of these cytokines, could improve outcome. Although this was the case in animal models[9], failure of these antagonistic drugs in humans was at least partly due to the different cytokine profile seen in humans during sepsis [10]. Recent studies suggest that although there is an initial pro inflammatory stage in human sepsis, patients with a prolonged, chronic state of inflammation often progress into a subsequent anti-inflammatory immunodeficent state referred to as "immunoparalysis"[11]. Patients with immunoparalysis often die of secondary nosocomial infection as a result of an ineffective immune response. This has been attributed to the over-production of interleukin 10 (IL-10) and decreased splenocyte production of Interferon gamma (IFN-γ)[12]. This counter-regulatory reaction to the over-zealous SIRS seen in sepsis is referred to as "Compensatory anti-inflammatory response syndrome" or CARS.

1.1.5 Further research

With an increasing cost on ICUs around the UK, the importance of diagnosing, treating and prognosticating sepsis is becoming more important. In order to do that, a better understanding of the molecular pathways involved in inflammation need to be researched. As such, more appropriate models of experimental sepsis need to be developed in order to discover more efficacious and relevant biomarkers that could aid in the diagnosis and treatment of the disease. This work is designed to give an overview of the key inflammatory signalling pathways and events involved in the development of an immune response, demonstrating on a molecular level the dichotomy that can exist between human and murine sepsis. Current models of experimental sepsis will be investigated in order to evaluate current understanding and the successfulness of experimental models in replicating the human disease. This combined with the analysis of new biomarkers in human serum will give a translational overview of developments in the research of sepsis, highlighting the difficulties that are faced, and the clinical benefits of continuing and advancing research in this area.

Recommendation 1	"SIRS should describe the inflammatory process independent of its cause." More than one of the flowing clinical criteria should be met in order reach a definition of SIRS: • Body temperature <36 or >38 degrees Celsius • Hear rate .90 beats per minute • Tachypnoea >20 breaths per minute or arterial partial pressure of carbon dioxide less than 4.3 kPa (32mmHg) • White blood cell count <40000 cells/mm or >120000 cells/mm or the presence of >10% immature neutrophils (band forms
Recommendation 2	*"Whenever SIRS is the result of a confirmed infectious process it is sepsis"*
Recommendation 3	I. "*Infection* shall be defined as a microbial phenomenon characterised by an inflammatory response to the presence of a micro-organism or the invasion of normally sterile host tissue by those organisms." II. "*Bacteraemia* is the presence of viable bacteria in the blood; the presence of virus' or fungi should follow on from this (i.e. viraemia etc)." III. "*Septicaemia* should be eliminated from usage due to its misuse and confusion."
Recommendation 4	I. "*Severe sepsis* will be classified as sepsis with the presence of organ dysfunction or a hypoperfusion abnormality (i.e. lactic acidosis) or hypotension." II. "*Sepsis induced hypotension* should be defined as a systolic pressure of <90mmHg or a reduction by 40mmHg from baseline, in the absence of other causes." III. "*Septic shock* is a subset of severe sepsis and is defined as sepsis induced hypotension, persisting despite adequate fluid resuscitation along with the presence of hypoperfusion abnormalities or organ dysfunction."

Table 1.1: Summary of the recommendation from the ACCP/SCCM consensus committee paper [1]

1.2 The human immune system and the inflammatory response

The human immune system can be divided into two components; innate and acquired immunity. Acquired immunity is characterised by the production and distribution of B and T lymphocytes involved in memory and antibody production. Innate immunity is comprised primarily of the functions of leucocytes in the peripheral blood, namely the inflammatory response. Inflammation is the body's first line of defence to invasion. The majority of the process involves the release of chemical mediators and cytokines which come from plasma proteins or cells including mast cells, platelets, neutrophils and monocytes/macrophages. Chemical mediators bind to specific receptors on target cells and can increase vascular permeability and neutrophil chemotaxis, stimulate smooth muscle contraction, have direct enzymatic activity and induce pain or mediate oxidative damage.

1.2.1Damage and Pathogen associated molecular pathways (DAMPs & PAMPs)

When invading organisms enter the body their specific groups or motifs of exogenous proteins are detected by the immune cells, these are referred to as Pathogen associated molecular pathways or "PAMPS". These along with endogenous alarmins (groups of proteins that are released by immune or damaged cells) are referred to as damage associated molecular pathways "DAMPS". DAMPS are the crucial first step in the development of an inflammatory response. While DAMPS have an exogenous origin, alarmins arise from various endogenous sources including release following non-programmed cell death (i.e. not apoptosis); specialised immune cells can also release them through an endoplasmic reticulum (ER)- Golgi pathway [13].

DAMPs act on immune cells to provoke an inflammatory response through a group of proteins on the cell surface called Toll-Like receptors (TLR). TLRs are type I transmembrane proteins with an extracellular domain, consisting of a leucine-rich repeat (LRR) domain, and a cytoplasmic domain homologous to the cytoplasmic domain of the human interleukin (IL)-1 receptor [14]. *Medzhitov et al* [14] not only first described the Toll proteins, but also identified that TLR 4 was the main receptor for LPS and led to downstream activation of transcription factor NFκB (nuclear factor kappa-light-chain-enhancer of activated B cells). Once activated the TLRs interact with adaptor proteins resulting in a downstream activation of signalling cascades, leading to activation of NFκB, which controls induction of pro-inflammatory

cytokines and chemokines [15]. Further studies[16]; have shown that there is a significant up-regulation of TLR 2 and 4 during human and experimental sepsis. Eleven TLRs in total have been identified; 1,2,4,5 & 6 mainly detect bacterial products while 3, 7 & 8 are involved in viral detection. *Table 1.2* from *Tsujimoto et al* [17] describes the various exogenous and endogenous ligands that signal through TLRs.

1.2.2 Nuclear factor kappa-light-chain-enhancer of activated B cells (NFκB) signalling pathway

In humans, the NFκB signalling pathway is a group of five members; NFκB1 (p105/p50), NFκB2 (p100/p52), RelA (p65), RelB and c-Rel which collectively have been shown to be ubiquitously expressed. Rel-related transcription factors serve as critical regulators for the inducible expression of several genes[18, 19]. Each of the five proteins contains a rel-homology domain (RHD), which is a conserved amino acid-terminal region containing a nuclear localisation sequence (NLS) important in gene transcription. Inactivation of the NFκB signalling pathway is through complexing of the RHD with Inhibition of NFκB (IκB) proteins resulting in inactivation of the NLS.

Inactive NFκB proteins reside in the cytoplasm of cells complexed with IκB. Degradation of this complex through phosphorylation of IκB by IκB kinase (IKK) complex is under the mediation of TLR receptors. Activation allows NFκB to translocate from the cytoplasm to the nucleus, inducing target gene transcription through the NLS. As discussed previously, the TLRs are stimulated by DAMPs and pro-inflammatory cytokines. The most common signalling pathway of NFκB translocation is described as the "classical pathway" and is summarised in *figure 1.1*. Activation of this pathway mostly leads to the translocation of the p50-p65 heterodimer and increased transcription of genes coding for cytokines needed to mount an inflammatory response. The composition of the NFκB dimers exerts substantially different effects on gene transcription [20].

1.2.3 Key pro-inflammatory cytokines in the development of Inflammation

There are three important cytokines that are produced and released from activated immune cells (typically mononuclear cells) as part of the initial pro-inflammatory or "acute-phase" response; these are IL-1, IL-6 and TNF-α. These molecules are the earliest to be released and are followed later by IL-12, IL-15, IL-18 and an array of other molecules (i.e. chemokines, lipid mediators and oxygen free radicals) [21]. *Table 1.3*[22-30] summarises the major cytokines involved in the inflammatory response; including information about their release, where they act and the response they evoke (with relation to inflammation only).

TNF-α has been identified as a crucial mediator in the development of septic shock in animal models [9] and has a similar role in patients [31]. A poorer outcome of patients with meningococcal sepsis was associated with higher levels of the cytokine. It has an important synergistic relationship with IL-1[25]. IL-6 alone does not appear to have a causal effect in provoking an inflammatory response but combined with IL-1 and TNF-α, potentiates it[25]. Significant rises in serum IL-6 also correlate with poorer outcome in septic patients[10]. The initial rise in pro-inflammatory cytokines is accompanied by a rise in compensatory anti-inflammatory cytokines and high serum levels have also been correlated with a poorer outcome [32]. IL-1, IL-6 and TNF-α are all referred to as "acute phase" cytokines, as they are the first cytokines released in response to invasion. IL-12, 15 & 18 are "late phase", and along with the more recently characterised cytokine Human mobility group box protein-1 (HMGB1) are involved in maintaining and regulating the state of inflammation.

1.2.4 High mobility group box protein as an inflammatory cytokine

HMGB1 is a 30KDa inflammatory cytokine and nuclear transcription factor that has a delayed onset of activation in comparison to other pro-inflammatory cytokines. Its nomenclature is derived from its high mobility in electrophoretic polyacrylamide gels[33]. It is a 214 amino acid long protein that has specific regions including an A box, B box, acidic tail and 43 lysine residues – these all contribute towards the molecule's varied functions [34]. Research has shown that HMGB1 release is largely divided into two pathways, either active secretion by monocytes as a pro inflammatory cytokine or passive release from apoptotic and necrotic cells [35]. Its action, in inflammation, is largely on TLR receptors, most importantly TLR 2 and

TLR 4[33]. As mentioned above, this pathway leads to the activation of NFκB, which is crucial for the transcription of other pro-inflammatory cytokines such as IL-1, IL-6 or TNF-α. *In vitro* analysis showed that after stimulation with LPS measurable levels of HMGB1 mRNA could be detected after 24 hours[36]. Mass spectroscopy has demonstrated that depending on the mode of release various "sub-forms" of HMGB-1 exist. Necrosis releases HMGB-1 in a reduced form that mediates the massive release of TNF-α, which is shown to be lethal in mice models[37]. However, cells that undergo apoptosis do not cause a release of TNF-α; and this is largely due to the oxidation of cysteine at position 106 on the B box arm of the HMGB-1 molecule[38]. Therapeutic antagonism of HMGB-1 using polyclonal antibodies against HMGB1 reduces severity and fatality of sepsis in several mice models[39].

1.2.5 Drug toxicity and inflammation

Acetaminophen (APAP) hepatotoxicity because of overdose is the most common cause of acute liver failure in the western world [40]. Metabolic activation of APAP and toxic metabolite formation, mitochondrial dysfunction, oxidant stress, peroxynitrite formation and nuclear DNA fragmentation are critical intracellular events in hepatocytes. However, the early cell necrosis causes the release of a number of mediators such as high-mobility group box 1 protein (DAMPs), which can be recognized by toll-like receptors on macrophages, and leads to their activation with cytokine and chemokine formation. Although pro-inflammatory mediators recruit inflammatory cells (neutrophils, monocytes) into the liver, neither the infiltrating cells nor the activated resident macrophages cause any direct cytotoxicity[41]. *Larson et al* concluded that the extensive sterile inflammatory response during APAP hepatotoxicity is predominantly beneficial by limiting the formation and the impact of pro-inflammatory mediators and by promoting tissue repair.

	Ligands	
TLR	*Exogenous*	*Endogenous*
1	Triacyl lipopetide	
2	Peptidoglycan lipoprotein	Necrotic cells
3	Double-stranded RNA	HSPs (HSP-60, HSP-70,Gp-96) Biglycan
4	LPS Taxol (mouse TLR-4 only)	Extra domain A-contain fibronectin • Fibrinogen • Polysaccharide fragments of heparin sulphate • Oligosaccharides of hyalouronic acid • ß Defensin 2 • Oxidized low-density lipoprotein • HSPs • Surfactant protein A in the lung • epithelium 1 • Neutrophil elastase • High mobility group box 1 protein • Biglycan
5	Flagellin	
6	Diacyl lipopeptide	
7	Single –stranded RNA	
8	Single – stranded RNA	
9	Unmethylated CpG DNA	Chromatin IgG complex
10	Unkown	
11	Uropathogenic Escherichia Coli (E-Coli)	

Table 1.2: Table taken from Tsujimoto et al [17]. Table showing exogenous and endogenous ligands that act on TLRs. IgG indicates immunoglobulin; TLR, toll-like receptor; HSP, heat shock protein; CpG, deoxy-cystidylate-phospate-deoxy-guanylate.

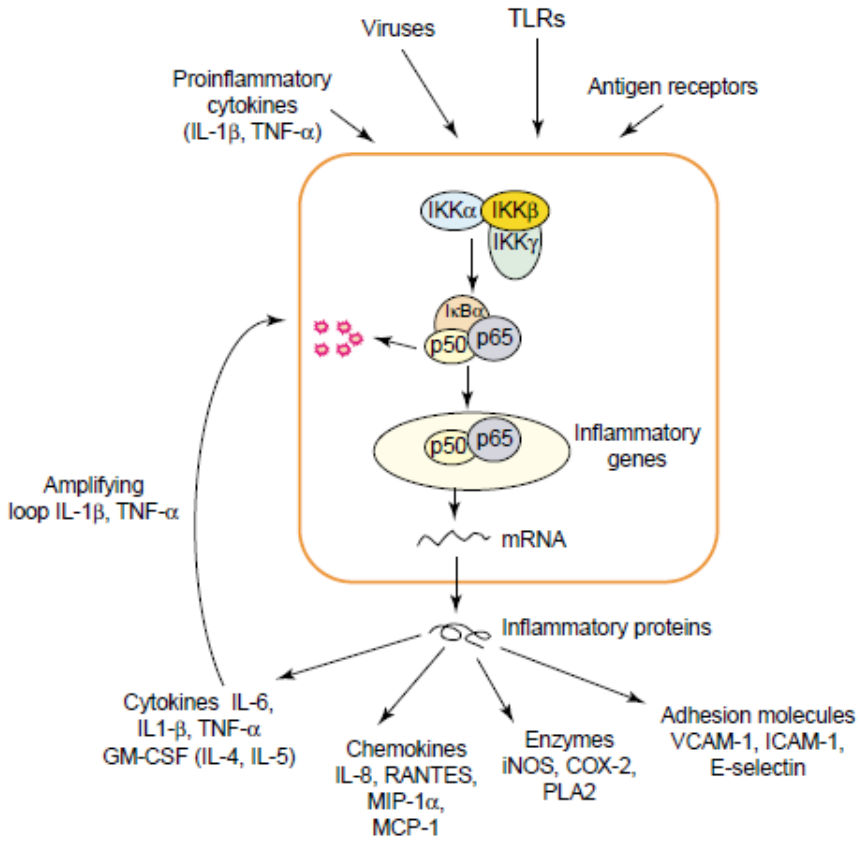

*Figure 1.1: Figure taken from Bonizzi et al [19] NFκB "Classical" signalling pathway. Various endogenous and exogenous ligands act on the TLRs causing a signal transduction that results in the degradation, phosphorylation and ubiquitination of IκB by the IKK complex. The final step involves the release of the NLS on NKκB leaving it free to translocate to the nucleus and induce transcription of mRNA which can go on to code for various cytokines, chemokines, enzymes and adhesion molecules. (*IκB, I-kappa-B, IKK-IκB kinase, NLS, nuclear localization signal).*

Cytokine	Primary Release	Action	Response
Early or "Acute phase" Cytokines			
TNFα	Macrophages, Monocytes & Dendritic cells	TNF Receptor family: TNFR1 – found in most tissues whereas; TNFR2 – is only expressed in immune cells	Endogenous pyrogen Activation of NFκB signalling and Mitogen-activated protein kinase pathways which lead to production and release of cytokines. TNF has also been shown to be important in cell death signalling
IL-1α IL-1ß	Macrophages, Monocytes, & Dendritic cells	IL-1 Receptor family: Type I: Proinflammatory Type II: Anti-inflammatory through competitive IL-1 binding.	Endogenous pyrogen IL1 results in increased gene expression in the cell of release and neighbouring cells. IL I-induced production of itself, IL 2, and B lymphocyte growth factors augments the immune response to antigens whereas IL 1-induced interferonγ production results in an anti-inflammatory action.
IL-6	Macrophages and Activated T cells	IL-6 Cell surface type 1 cytokine receptor complex (gp80 and IL-6Rα sub units)	Induces differentiation of activated B cells; culminating in the production of immunoglobulin. Stimulates proliferation of thymic and peripheral T cells and induces differentiation into cytotoxic T cells.
Late cytokines			
IL-12	Macrophages, Monocytes, Neutrophils & Dendritic cells	IL-12 Receptor which consists of a IL-12ß2 subunit that is only found on activated T cells.	Most of IL-12 pro-inflammatory effects are mediated through IFN-γ. It induces increased proliferation and colony formation of Natural killer and T cells as well as increasing their cytoxicity and expression of cytotoxic mediators. It stimulates the differentiation of cells into those that produce cytokines.
IL-15	Macrophages, Monocytes & Dendritic cells	IL-15 Receptor	Natural killer cell proliferation.
IL-18	Macrophages, Monocytes, & Dendritic cells	IL-18 Receptor heterodimer consisting of a α &ß subunit.	Like IL-12, some of the effects of IL-18 are mediated through IFN-γ production. It is also important in T and Natural Killer cell maturation along with production of inflammatory cytokines.
HMGB1	Macrophages, Monocytes	TLR 2 & 4	Activation of NFκB and production of cytokines. Upregulation of endothelial adhesion molecules, stimulation of epithelial cell barrier failure, and mediation of fever and anorexia

Table 1.3: Table showing the major pro-inflammatory cytokines including information about their release, action and response in relation to the inflammatory response only [22-30]

1.3 Animal models of sepsis

Sepsis in humans often has polymicrobial aetiology, along with often being heterogeneous in focus. These factors seem to be the major difficulties when similar conditions are attempted to be recreated in some experimental animal models [42] . In order for experimental sepsis to be translatable to clinical medicine, it needs to replicate the key events seen in humans to include the hemodynamic and immunological changes seen. *Marshall et al* [43] concluded that although there was no ideal model of sepsis, various models offer different recapitulations of discrete features of the disorder. *Redl et al* [44] suggested that the most appropriate model will depend largely on aspect of interest. The widely used endotoxin model is now being replaced by those that induce an inflammatory response more similar to the "polymicrobial" intra-abdominal sepsis event in humans, i.e. caecal ligation and puncture (CLP), colon acendens stent procedure (CASP) and various methods of faecal or tissue inoculation in the peritoneal cavity. Four key papers comparing and contrasting the major models of sepsis are summarised in *Table 1.4* [45-48]

1.3.1 Translational disconnect

Mathiak et al [45] demonstrated that by intra-peritoneal inoculation of E. coli the human cytokine profile of sepsis could be replicated in a rat. However, inoculation with murine faecal material induced changes in mice which mimicked more appropriately the metabolic, hormonal and energy derangements observed in human sepsis. More advanced techniques include CLP and CASP; CLP was shown to be superior to LPS in replicating a consistent model[46, 47], as LPS induces a sharp, but transient rise in cytokines that is usually not sustained and different to that seen in humans. *Maier et al*[46] found CASP to be a superior model compared to CLP in that it was more consistent with the pathological diffuse abdominal peritonitis, whereas CLP mice were found to develop intra-abdominal abscesses after the procedure. Problems with techniques such as CLP or CASP include the time for training and skills required for the actual procedure. Other worries surrounding the use of these models involve reproducibility, variability and also a so called "double-hit" of cytokines, where a surgical procedure will see a rise in cytokines independent of the intervention intended to causes sepsis. *Gonnert et al* [48] identified that in using a batch of stool for peritoneal inoculation, reproducibility was possible and variability

between experiments could be reduced. Experimental modelling of sepsis is largely accepted to be the main failure of efficacy of developed therapeutic agents.

Study	Year	Methods	Results	Conclusion
Caecal ligation and puncture (CLP) versus colon ascendens stent peritonitis (CASP): Two distinct animal models for polymicrobial sepsis. *Maier et al* SHOCK, 21(6); 505–511, 2004 [46]	2004	8-12 week old female mice were sorted into two groups and given either of the two interventions: • CASP – a venous catheter (venflon) was inserted into the ascending colon and contents were allowed to flow into the abdominal cavity. • CLP – the cecum was ligated with 15mm of prolene and then punctured using a needle.	Comparison of the models suggests that CLP results in the formation of an intra-abdominal abscess, Whereas diffuse peritonitis was only observed in the CASP model. Evaluation of the abdomen of CASP mice after 24 hours revealed that there is still an opening in the luminal site with increasing signs of systemic infection and inflammation. In CLP only moderate levels of increase were found. CASP mice also demonstrated earlier involvement of the lungs and liver.	The closer the model is adapted to human disease, the more reliable will be the results. Thus, for evaluation of new treatment approaches for diffuse peritonitis, the CASP model appears advantageous over CLP, whereas for other intra-abdominal infections such as abscesses, the CLP model should be preferred.
Comparison of the mortality and inflammatory response of two models of sepsis: lipopolysaccharide versus caecal ligation and puncture. *Remick et al* SHOCK 13 (2);110-116, 2000 [47]	2000	Female mice were sorted into two groups and given either of the interventions: • CLP - the caeum was ligated with prolene 1cm before the distal end. Punctures were made using a needle. • LPS – mice were injected. intraperitoneally with 1ml of normal saline containing 250µg of E-coli type (0111:B4; sigma) LPS.	LPS and CLP appear to be duplicate models of sepsis, with nearly equivalent lethality and loss of activity. LPS causes a deeper decline in peripheral lymphocyte count compared with CLP. LPS causes a more rapid release of cytokines over the initial period post dosing and then begin to decline.	Although the mortality and the morbidity of the two models were similar, the inflammatory responses evoked are distinctly different.
An improved clinically relevant sepsis model in the conscious rat *Mathiak, G et al* Critical Care Medicine 28(6); 1947-1952, 2000 [45]	2000	Male Sprague-Dawley rats where anesthetised and their peritoneum was inoculated with a human derived fibrin-thrombin clot that had been incubated with a strain of E-coli isolated from the respiratory sputum (capsulated and serum resistant, similar to the gram negative sepsis in humans). Control rats were given a sham inoculation. The rats were then observed for three days	This model replicated the cardiac abnormalities seen in human sepsis (i.e. increase in cardiac output). Mice became thrombocytopenic which is also a feature of human sepsis. TNF elevation was only marginal at the higher dosed implantation of clots compared with endotoxin	This model of peritonitis sepsis evokes an inflammatory response similar to that of human sepsis. This is superior to the commonly used endotoxin model and in addition is reproducible and low cost.
Characteristics of clinical sepsis reflected in a reliable and reproducible rodent sepsis model *Gonnert et al* J sur res 170(1);123-134,2011[48]	2011	Male Wistar rats were given an intra-peritoneal injection of faeces from a pooled batch consisting of faces from three healthy vegetarians. Intensive monitoring followed involving insertion of a central jugular vein catheter. A sham experiment involving the IP injection of saline was also given.	None of the septic animals survived 40hours after induction of sepsis. Animals displayed clinical signs of sepsis 2hours after induction. Antibiotic treatment resulted in a 50% increase in survival. Markers of sepsis correlated with organ dysfunction and histopathological changes.	This model provided a reproducible and reliable model of polymicrobial sepsis that was quantifiable and similar to key clinical and molecular changes seen in human sepsis.

Table 1.4: Summary of four major papers that investigate different models of murine sepsis (43-46)

1.4 Sepsis and organ dysfunction

Organ dysfunction is a common occurrence in patients with severe sepsis admitted to ICU, and these patients often require organ replacement therapies or vital organ support. The mechanisms for the dysfunction is largely attributed to the huge increase in systemic cytokine and mediator release which results in immune dysregulation, hormonal alterations, metabolic changes, activation of the coagulation cascades, and mitochondrial, micro-vascular, and epithelial dysfunction [49]. Most tissues contribute to the release of cytokines in inflammation. The differences in organ response lead to the so-called compartmentalisation of the inflammatory response and influence the organ's ability to function during sepsis. The significance of compartmentalisation in sepsis is demonstrated by the observation that in the broncho-alveolar lavage fluid of patients with adult respiratory distress syndrome lower levels of anti-inflammatory cytokines were associated with poorer outcome [50]; whereas high plasma levels of inflammatory and anti-inflammatory cytokines were associated with poorer outcome [51]. The liver has also been identified as a key organ for dysfunction during sepsis. *Gonnert et al* [48] reported that an early increase in markers associated with hepatocellular and cholestatic dysfunction is observed in experimental sepsis and sinusoidal and endothelial-leukocyte changes have been confirmed by histopathology.

Recently, over-activation of neutrophils has been identified as a major contributing cause of organ dysfunction [52]. The activation and increase in numbers of neutrophils provides a functional paradox within patients with sepsis: High numbers of activated neutrophils are needed to clear bacterial products, but collateral tissue damage by reactive oxygen species and cytokine release also increases. Hence, timely removal of neutrophils by apoptosis is key in the resolution of the inflammatory response to avoid leakage of intra-cellular products from necrotic cells however, this mechanism appears to be impaired in systemic patients with SIRS [53]. Apoptosis is the process of programmed cell death [54]. Patients with SIRS have an impaired cellular apoptotic pathway [53]. Therefore being able to assess and quantify the level of apoptosis could prove useful in giving an indication of prognosis and severity of disease.

Keratins are proteins which are found in the cytoskeleton of epithelial tissue. Recently cytokeratin 18 (CK18), a protein of the larger Keratin family, has been discovered as a marker of apoptosis and necrosis. During necrosis, the cytosolic pool

of soluble CK18 is released, whereas apoptosis is associated with significant release of caspase-cleaved CK18 fragments. These results suggested that assessments of different forms of CK18 in patient sera could be used to examine cell death modes. One study [55] has already shown that single serum analysis of septic patients demonstrates higher levels of caspase-cleaved CK18 versus serum of other patients admitted to ICU. The study concluded that CK18 could be useful for monitoring endothelial function in sepsis. Further studies have demonstrated that mutations in CK18 predispose to liver disease through unregulated apoptosis and fibrosis. This mutation could potentiate the pre-existing susceptibility to sepsis that comes with different forms of liver disease, in particular liver cirrhosis [56]. As HMGB1, similar to CK18, is not organ specific, its use as part of a screening panel may help to diagnosis and prognosticate sepsis in ICU patients more efficiently and in a more specific patient group help to differentiate liver dysfunction due to sepsis from decompensation in patients with cirrhosis (i.e. secondary to alcoholic liver disease) due to non-infectious causes, respectively.

1.7 Hypothesis and Aims

Translational medicine is important in the development of new treatments, and making sure these treatments are founded on sound biological science. This work aims to use various techniques and histopathological analysis in order to examine key components of the human inflammatory process and sepsis, looking at how experimental data translates towards the clinical process. Two cell lines, THP1 (human monocytes) and RAW 264.7 (murine macrophages), are used to investigate inflammatory signalling pathways in the development of an inflammatory response, namely the activation of TLRs and NFκB. These experiments will allow a comparison of human and murine inflammatory responses and contribute towards an explanation for the translational disconnect between murine and human sepsis on a molecular level. Furthermore, comparing the widely used LPS model with a more reproducible polymicrobial intra-peritoneal faecal inoculation model will allow for an in-depth histopathological analysis of tissues, in order to examine the differences between the two distinct inflammatory insults and investigate which offers an experimental model that is more similar to human sepsis. Lastly, two proteins, HMGB1 and CK18, will be analysed in patient serum to see if they offer any potential as biomarkers of sepsis and in particular liver dysfunction associated with sepsis.

Three hypotheses have been constructed in order to meet the aims of the thesis.
These are:

1. LPS-induced responses depend on cell type and species: THP1 and RAW 264.7 cells dosed with LPS will exhibit varying levels of activation of the NFκB pathway (via the TLR receptor) and subsequent nuclear translocation of the P65 subunit, depending on the concentration of LPS.
2. LPS induces histopathological changes different from faecal inoculation: Histopathological analysis of cells from Mice dosed IP with LPS or faecal suspension will show differing levels of tissue recruitment and damage of various tissues compared to controls and those dosed with acetaminophen.
3. Serum levels of potential sepsis biomarkers HMGB1 and CK18 vary with the underlying liver condition: Two groups of critically ill patients will be compared: 1. Patients with sepsis and no history of liver disease 2. Patients with sepsis and known liver disease. Results will be compared to healthy

volunteers (controls) and patients admitted to ICU without sepsis or underlying liver disease.

Chapter 2:

In vitro analysis of cell signalling pathways in sterile inflammation

Contents

2. *In vitro* analysis of cell signalling pathways in sterile inflammation

2.1 Introduction

2.1.1Sterile inflammation and the NFκB pathway

Sterile inflammation is defined as a group of stimuli that are non-infectious (absence of living micro-organism) but ultimately lead to the same downstream vascular and cellular manifestations of inflammation [57]. These stimuli can be largely divided into injurious, irritant, or antigenic. LPS, although derived from Gram negative bacteria, are classified as antigenic and irritant so the immune response elicited *in vitro* is therefore classified as "sterile inflammation". Although they are not live stimulants, sterile inflammation elicits a similar pattern recognition and inflammatory response to "infectious" inflammation [58]. Inflammation forms an important part of the human innate immune system and as discussed (section *1.2),* activation of the NFκB signalling pathway through the mediation of the TLRs is an important pathway for the production of inflammatory cytokines (see *1.2.2*). The classical pathway is described in *figure* 1, however *Bonizzi et al* [19] also describe an "alternative pathway" which is dependent on the IKKα homodimer and translocation of different members of the Rel protein family. The pathway is described in *figure 2.1*.

2.1.2 Alternative NFκB pathway

Activation of both NFκB pathways is the result of IKK mediated, phosphorylation induced degradation of the IkB inhibitor, which allows the proteins to translocate to the nucleus. A comparison of the two pathways shows that the classical pathway is dependent on the IKKα- IKKβ heterodimer whereas the alternative pathway is dependent on the IKKβ homodimer. In contrast to the pro-inflammatory role of the classical pathway, the alternative pathway has been described as having a significant role in the maintenance and development of lymphoid organs and adaptive immune system [59], more specifically the survival and maturation of B lymphocytes [60]. The classical NFκB pathway is mainly based on the translocation of p65/p50 dimers, whereas the alternative pathway involves other dimers, including p52, which are released following processing of precursors such as p100 – a progression exclusively seen in the alternative pathway [61].

2.1.3 The role of the monocyte in inflammation

Monocytes are bone marrow (myeloid cell line) derived immune cells that serve to replenish macrophages in the body as well as having the ability to differentiate into dendritic cells and osteoclasts. They circulate in the blood for around 2-3 days as well as being stored in the cords of Billroth in the red pulp of the spleen. Due to their low numbers in the peripheral blood (3-8% of leukocyte population) in comparison to neutrophils they are often not the first cells at the site of inflammation; this, combined with differences in adhesion molecule expressions, usually means they are preceded by neutrophils[62]. Following a persistent state of inflammation, neutrophils become depleted, but by contrast, blood monocytes accumulate and differentiate into inflammatory macrophages, which complete phagocytosis and destruction of the injurious agents, signalling a resolution of an inflammatory state. However in a more chronic state of inflammation neutrophils persist – due to mechanisms including impaired apoptosis[60]. Monocytes can release cytokines without differentiating into dendritic cells and macrophages and this is important in the initiation of the inflammatory response and recruitment of other immune cells. In severe sepsis the ability of monocytes to produce cytokines can be down regulated by unknown mechanisms[63]. Human leukocyte antigen (HLA) expression is also down regulated in monocytes during sepsis and researchers think this plays a crucial role in the development of immunodeficiency and subsequent nosocomial infection[64].

2.1.4 The role of the macrophage in inflammation

Macrophages are monocytes that have undergone migration into tissues and have become differentiated. The activation of macrophages leads to responses that are typical of innate immunity, such as the rapid generation of an inflammatory response, and they play a role as efficient effectors for the clearance of microorganisms. They can also become specialized, so called “tissue macrophages” i.e. in the lung (alveolar macrophages) or liver (Kupffer cells). Macrophages are professional phagocytes and play a crucial role in antigen presentation and recruitment of the adaptive immune system through their use of Major Histocompatibility Complexes (MHC)[65]. Macrophages, monocytes and endothelial cells up regulate their expression of tissue factor during sepsis which leads to a “pro-coagulant state”[66], this can lead to depletion of clotting factors and eventually disseminated intravascular coagulation. Macrophages, in comparison to monocytes, appear to have a longer period of cytokine production and *in vitro* [67] and *in vivo* [64]

studies have shown that various tissue macrophage populations are responsible for the production of an array of cytokines.

2.1.5 Aims of this chapter

Understanding the role of TLRs, NFκB pathways and individual immune cell function has allowed researchers to explore various routes of therapeutic targets in order to manage the inflammatory response in those conditions such as sepsis, where it becomes somewhat overzealous. However as discussed in the general introduction, sometimes these mechanisms are more complex than first perceived and like in the case of TNF-α, IL-1 & IL-6[10], recapitulating an inflammatory response using so called "sterile" techniques can provide information that is dissimilar to the true condition. The aim of this chapter is not to assess the validity of the sterile inflammation model, but use it to examine the relationship between the TLR and activation of the "classical" NFκB pathway. By examining this in two separate cell lines (murine and human) a comparison can be made between species and help understand the contribution of possible differences on the molecular levels can have towards the existing translational disconnect between murine and human sepsis. Comparing two cell populations can also provide information about the role of two separate immune cells in inflammation, their respective sensitivities to LPS and their capacity for cytokine production. *Bonizzi et al* [19] identified the P65-P50 heterodimer, NFκB protein as the most common protein in the "classical" pathway that translocates from the cytoplasm to the nucleus after cellular stimulation with LPS. Therefore these experiments will also determine whether or not p65 detection can be a reliable indicator of activation of the pathway. The hypothesis is stated below:

"LPS-induced responses depend on cell type and species: THP1 and RAW 264.7 cells dosed with LPS will exhibit varying levels of activation of the NFκB pathway (via the TLR receptor) and subsequent nuclear translocation of the P65 subunit, depending on the concentration of LPS."

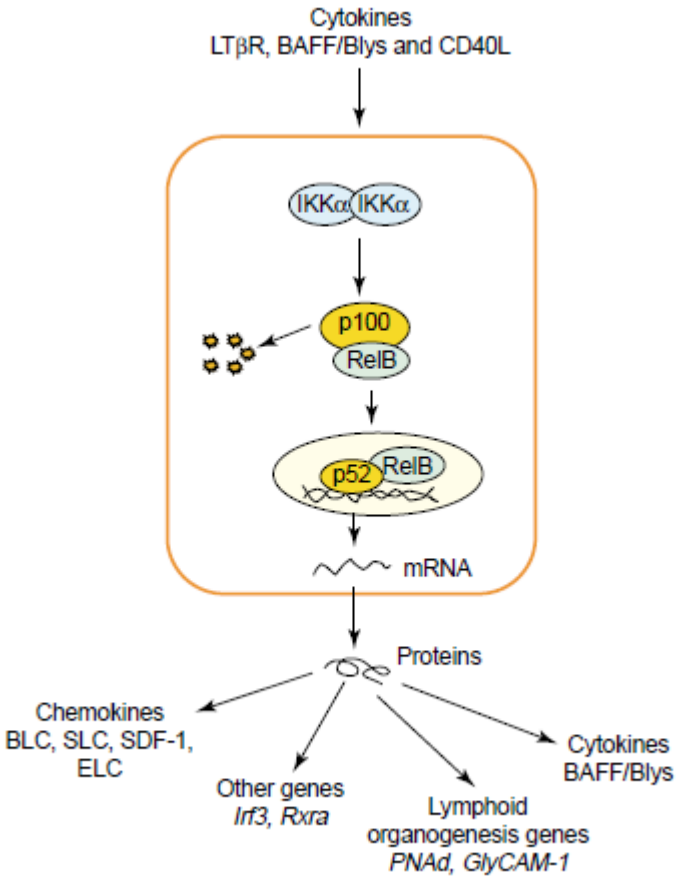

Figure 2.1: The Figure is taken from Bonizzi et al[19] NFκB "alternative" signalling pathway. Activation of the pathway results in the translocation of RelB/p100 from the cytoplasm to the nucleus. This pathway is suggested to be more primarily concerned with the maintenance of secondary lymphoid organs (i.e. the spleen).

2.2 Materials and Methods

2.2.1 Materials

The two cell lines used in these experiments were THP1 human leukemic monocyte and RAW 264.7 murine macrophages. Both were obtained from SIGMA, Aldrich (88081201 & 91062702). THP1 cells are an immortalised cell line derived from the peripheral blood of a 1-year old male with acute monocytic leukaemia. RAW 264.7 cells are a murine cell line isolated from ascites of a tumour induced male mouse by intraperitoneal injection of Abselon Leukaemia virus (A-MuLV). THP-1 cells were cultured in RPMI-1640 (SIGMA, Aldrich R8758) and RAW 264.7 in Dulbecco's modified Eagle media (DMEM, LONZA). LPS used in dosing was obtained by phenol extraction from Escherichia coli 0111:B4 (SIGMA, Aldrich L2630). Materials used in casting acrylamide gels where obtained from Bio-Rad and included ammonium persulfate (APS), tetramethylethylenediamine (TEMED), Protogel (Acrylamide), running buffer and stacking buffer. Three antibodies where used in western blotting; mouse monoclonal IgG against p65 (Santa cruz biotechnology, Inc. sc-109), mouse monoclonal IgG against β-actin (Abcam® mAbcam 8224) and goat derived monoclonal anti-mouse IgG (SIGMA, Aldrich A0168). Chemiluminescence reagents were bought as a Proteoqwest™ kit from SIGMA,Aldrich. Densitometric analysis was done using visionworks® software and data analysis was done in Microsoft excel ® and GraphPad Prism 5 ®.

2.2.2 Cell culture of THP1 and RAW 264.7

All cell culture work was carried out in a sterilized cell culture hood using aseptic technique. THP1 cells were cultured in RPMI-1640 cell culture media treated with 10% foetal bovine serum (FBS), L-glutamine and streptomycin. Frozen THP1 cells where thawed in a water bath at 37°C and added to 15 mls of media in a 15 ml falcon tube. Cells were then centrifuged at 1500 RPM for 5 minutes. Media was poured off and the cells were re-suspended in 1ml of media and trypan exclusion was done to count cells manually on a haemocytometer (improved Neubauer grid) and assess viability (cells were only used if viability was greater than 90%). Cells were then seeded 3-8 x 10^5 per ml of media in a T75 cell culture flask and incubated at 37 °C; 5 - 7% CO^2 in an upright position until the cells reached a critical density and enough were cultured for the experiment. Cells were then centrifuged and counted as described and seeded at $5x10^6$ per ml in 7mls of media within a smaller T25 cell

culture flask and incubated overnight before dosing. 8 flasks in total ($40x10^6$ cells) where required for the experiment; 7 doses and a negative control. Cells were only used for experiment during passage 9-11.

RAW 264.7 cells where cultured in DMEM treated with 10% FBS, L-glutamine and streptomycin. Frozen cells were thawed in a 37°C water bath and added to 15 mls of media in a 15ml flacon tube and centrifuged at 2000 RPM for 5 minutes. Media was poured off and the cells were re-suspended in 1ml of media and trypan exclusion was done to count cells manually on a haemocytometer (improved Neubauer grid) and assess viability (cells were only used if viability was greater than 90%). Cells were then seeded at 20,000 cells per cm^2 in a T75 flask (1.5×10^6 cells per flask) and incubated horizontally at 37 °C; 5 - 7% CO^2 until cells were 60-80% confluent and steps were repeated until enough were cultured for the experiment. As RAW 264.7 cells are semi-adherent a cell scraper and wash media (DMEM) was used to remove adherent cells from the flask. For the experiment cells were seeded at $1x10^6$ cells per ml in 5mls in a T25 flask and incubated overnight before dosing. 7 flasks in total ($35x10^6$ cells) where required for the experiment; 6 doses and a negative control. Cells were only used for experiment during passage 15-20.

2.2.3 Dosing regimen to investigate LPS response on p65 translocation

After being seeded and allowed to settle for 24 hours, cells were dosed. Optimization of the method showed that RAW 264.7 cells required larger doses of LPS in order to elicit a detectable level of p65. The doses for each cell line were as follows:

	Dose of LPS ng/ml							
THP-1	Negative control	0.1	0.3	1	3	10	30	100
RAW 264.7	Negative control	3	10	30	100	300	1000	

Table 2.1 table showing the dosing regimen used to dose cell lines in order to measure p65 translocation.

For each experiment a stock solution of LPS was made up and diluted further in bijous depending on the desired concentration that was to be achieved. Bijous were spun after LPS was added to prevent LPS from sticking to the sides and to ensure that the concentration was consistent. After dosing cells were placed into an incubator for 1 hour before being transferred to 15ml falcon tubes.

2.2.4 Nuclear extraction and protein quantification

Nuclear extraction was carried out on ice in order to prevent degradation of p65. Nuclear extraction buffers were made up as follows:

BUFFER A	BUFFER B	BUFFER C
NaCl	NaCl	NaCl
HEPES (pH 8)	HEPES (pH 8)	HEPES (pH 8)
Sucrose	Glycerol	Glycerol
EDTA	EDTA	EDTA
Spermidine	Spermidine	Spermidine
Spermine	Spermine	Spermine
Triton X-100	dH_2O	dH_2O
dH_2O		

*NaCl – sodium chloride, HEPES- 4-(2-hydroxyethyl)-1-piperazineethanesulfonic acid, EDTA-Ethylenediaminetetraacetic acid, dH20- distilled water.

Table 2.2. Table showing the protocol for making the nuclear extraction buffers for nuclear extraction of proteins following dosing with LPS.

Stock solutions where stored in a fridge at 4^{o}C before being aliquoted for each extraction. Once aliquoted the buffers were supplemented with 2-mercaptoethanol a protease inhibitor cocktail. Once cells had been transferred to a 15ml falcon tube they were spun down (at respective RPMS and times used in cell culture, see 2.2.2) into a pellet and excess media was poured off. The pellet was then re-suspended in 4mls of Hank's balanced salt solution (HBSS). Samples where then centrifuged into a pellet and the salt solution was poured off. Pellets where then re-suspended in 100µl of buffer A in order to rupture the cell membranes and release cytosolic contents. After re-suspension samples in buffer A were transferred to freshly labelled eppendorf tubes. Samples where then spun at 3500 RPM at 4^{o}C for 5 minutes. Excess buffer A was poured off and 100µL of wash buffer B was added and the pellet re-suspended. The samples where again spun and the excess solution poured off. The pellets where then re-suspended in 50µ (RAW 264.7) or 80µl of Buffer C in order to rupture the nucleus. Samples where incubated on ice for 30 minutes before one final spin and the supernatant aliquoted into eppendorf tubes and stored at -80^{o}C before being used for experiments.

Before electrophoresis protein was quantified using the method described by Bradford[68] in order to quantify and standardize the amount of protein loaded from

each sample onto the well. Each dosing and nuclear extraction process was carried out three times (on different days) on each cell line in order to gain three sets of samples and achieve an overall "N" number of 3 for analysis and measure intra-experimental assay variability.

2.2.5 Acrylamide gel preparation

Gels were cast using the gel casting equipment and reagents from Bio-Rad. 7.5% acrylamide gels were needed in order to separate the proteins out enough for analysis. These gels were made up by altering the protocol provided by Bio-Rad for making 10% gels and reducing the volumes of all the reagents and making up to the same volume with distilled water. The table demonstrates this below:

	Running gel (7.5%)		**Stacking gel (4%)**
Protogel (Acrylamide)	2.5	Protogel (Acrylamide)	0.7
Resolving buffer	2.6	Resolving buffer	1.2
Distilled water	4.9	Distilled water	3.0
TEMED	10µl	TEMED	5µl
APS	100µl	APS	25µl

Table 2.3 Protocol for preparation of Acrylamide gel

2.2.6 Running a reducing gel to separate nuclear proteins from extract

5µg of each sample was aliquoted into a newly labelled eppendorf tubes. Reducing agent and sample buffer where mixed together (3:7) in a separate eppendorf and 5µl was added to each sample. Samples where then placed on a heat block (85°C) for 5 minutes. Afterwards samples where incubated on ice for 10 minutes. Hand-cast gels were inserted into the gel holder within the electrophoresis chamber and samples were loaded into each of the wells left to right in increasing concentration. Tris glycine buffer was poured into the chamber as a cooling blanket. Samples were loaded onto the gel from left to right in increasing concentrations using a pipette and a protein ladder (Bio-Rad Kaleidoscope) was added onto the farthest left hand side of the gel. The protein ladder allows the molecular weight of the protein to be estimated and identification of the desired protein (i.e. p65 & Actin). 90V was applied for 10 minutes and then increased to 150V for 45 minutes.

2.2.7 Immunoblotting for p65 subunit of NFκB

The gel was carefully removed and then sandwiched between pre-soaked nitrocellulose membrane and filter paper and inserted into a transfer chamber. The transfer chamber was filled with 1x transfer buffer (100ml 10x buffer consisting of glycine and Tris base, 200ml methanol and 700ml of distilled water). A current of 80V was supplied for 1 hour. Sufficient transfer was detected using ponceau red stain. Membranes where then washed four times for 5 minutes with 0.1%/1x Tween, Tris & buffered saline (TTBS) while being agitated. Afterwards they were placed into 10% analytical grade non-fat milk (Bio-Rad) for 45 minutes while being agitated. Membranes where then cut at the 50kDa marker (using the Bio-Rad Kaleidoscope ladder) with a scalpel in order to incubate each section with the appropriate antibody. As p65 has a molecular weight 65KDa the >50kDa section was incubated primarily with mouse monoclonal anti-p65 antibody made up in 2% milk to a concentration of 1:1000; while the lower section was incubated primarily with mouse monoclonal anti-β actin made up to a dilution of 1:160000 in 2% milk. Both were incubated for 1 hour while constantly being agitated. Membranes were then washed 4 times for 5 minutes with 0.1%/1x TTBS. Both membranes were then incubated with the secondary antibody (goat derived mouse monoclonal) against IgG. The p65 membrane was incubated at a concentration of 1:5000 made up in 2% milk while the β-actin membrane is exposed to a secondary antibody dilution of 1:10000.

The secondary antibody was linked to horseradish peroxidise with the ability to cleave chemiluminescent reagents generating a detectable signal.

2.2.8 Chemiluminescence and Development of actin and p65

Proteoqwest™ reagents were mixed up in a bijou. Excess reagents were washed off. Membranes were then fixed to a development cassette and developed onto an X- ray film in a dark room. Exposure times where optimised until an acceptable signal strength and film quality was obtained for densitometry. Films where then soaked in fixing and developing solutions while in the dark room.

2.2.9 Densitometry and interpretation of p65:actin ratios

Films were scanned onto a computer and using subtraction analysis on visionworks®, values for densities of p65 and actin bands were calculated. This

allowed a p65:actin ratio to be calculated were increases in density of p65 corresponded with increasing values. Data was interpreted on Microsoft excel ® and curves constructed using GraphPad Prism 5 ®.

2.3 Results

2.3.1 Detection of p65 nuclear translocation in THP1 cells dosed with LPS

The nuclear extract of the THP1 cells dosed with LPS was collected after 1 hour to quantify (with densitometry) the translocation of p65 from the cytoplasm to the nucleus after stimulation of the cells with LPS. It was found that increasing the concentrations of LPS stimulated translocation of p65 from the cytoplasm to the nucleus in a dose-response relationship. An increase in basal p65 density (Mean 0.214 SD 0.0238) was seen at doses as small as 0.1ng/ml (Mean 0.519 SD 0.0641). This indicates that p65 is a reliable marker of TLR activation and subsequent down – stream signalling leading to NFκB "classical" pathway activation. Furthermore activation of this pathway after 1 hour of cellular exposure to LPS demonstrates the acute nature of potential cytokine production and response to low doses reflects the sensitive nature of these human monocytes to insult. *Figure 2.2* displays the densitometry results of each replicate of the experiment. *Figure 2.3* displays the means of the replicates. The trend is clear; it shows there is a gradual increase in the p65: Actin ratio with increasing dose of LPS, indicating an increase in the nuclear p65. There was a significant difference between all doses and controls ($p<0.05$). This similar trend was also seen between individual doses.

Coefficient of variation is defined as the standard deviation of a set of data divided by the mean. Here it was used to assess inter experimental variation. The overall range of variation was 11.5-27.62%. This shows that there is a high level of inter-experimental variability between day to day assays. *Figure 2.4* shows this graphically.

(A)

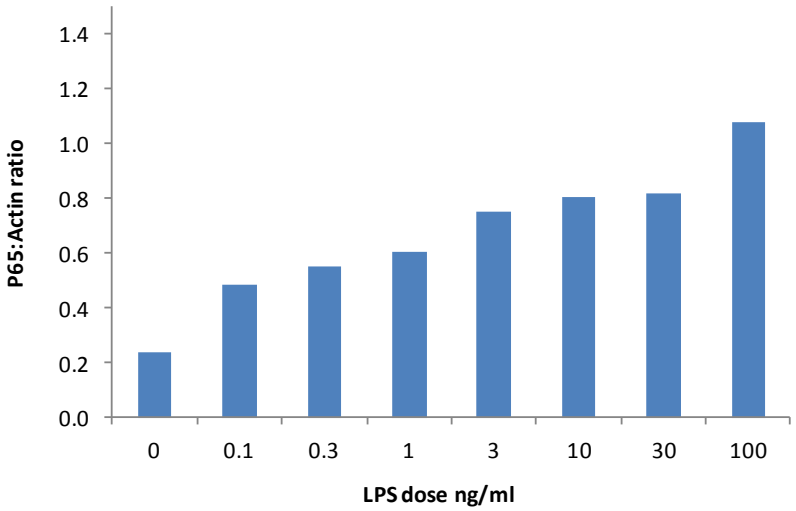

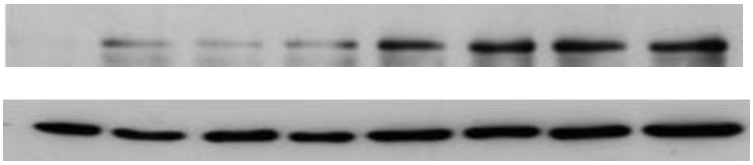

LPS dose ng/ml:	0	0.1	0.3	1	3	10	30	100

(B)

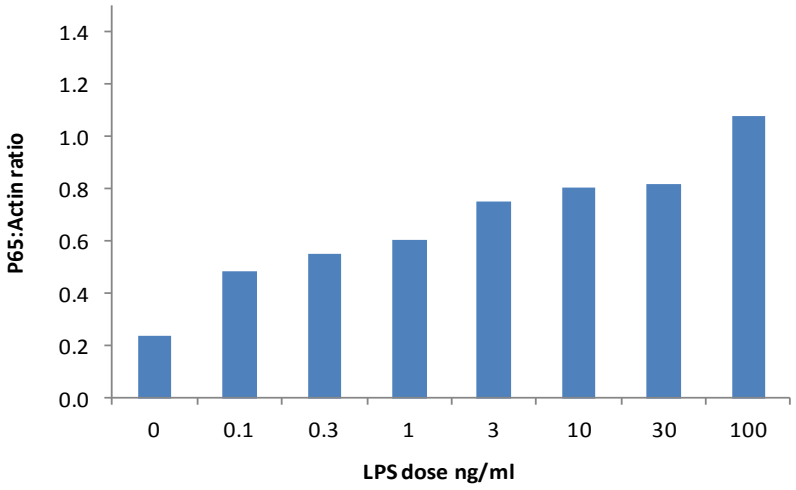

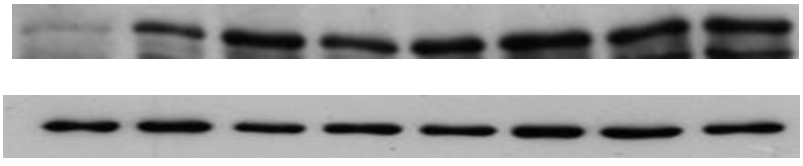

LPS dose ng/ml:	0	0.1	0.3	1	3	10	30	100

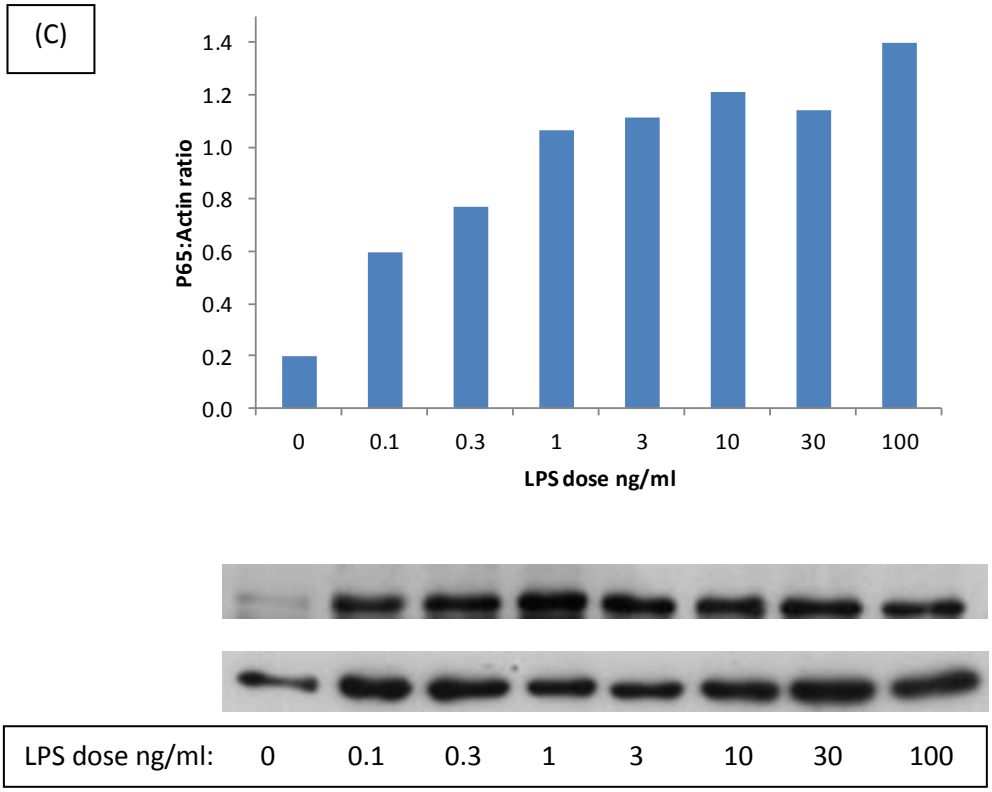

Figure 2.2: Results of densitometry on developed films of Immunoblots of THP1 nuclear extract from cells dosed with varying concentrations of LPS. All bar charts are displayed with P65:Actin ratio on the Y axis and LPS dose (ng/ml) on the X axis. Underneath are pictures of p65 1 minute films on top along with 10 second actin films on the bottom. A-C are repeats of the same method done on three sets of different nuclear extracts carried out on dosing experiments done on different days (N=3). Immunoblots were carried out on the same day.

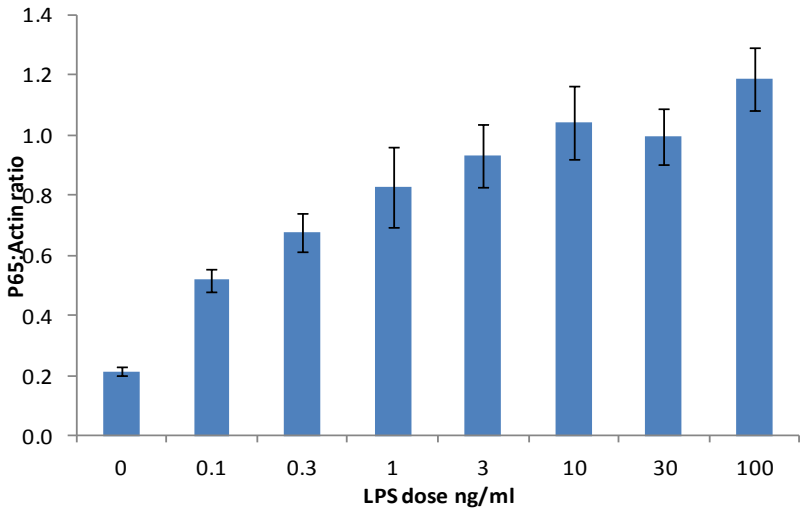

Figure 2.3: Results of densitometry on developed films of Immunoblots of THP1 nuclear extract from cells dosed with carrying concentrations of LPS. Bar charts are displayed with P65: Actin ratio mean (N=3) on the Y axis and LPS dose (ng/ml) on the X axis. Means are plotted with standard error of the means (SEM).

(A)

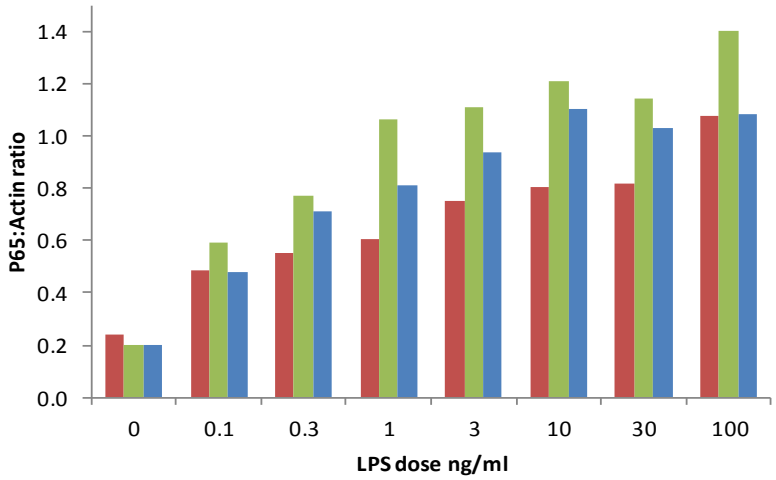

(B)

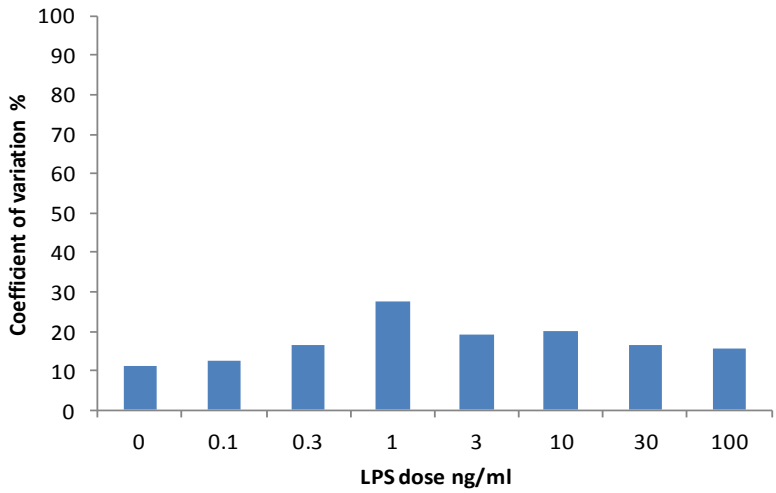

Figure 2.4: Results of densitometry on developed films of Immunoblots of THP1 nuclear extract from cells dosed with carrying concentrations of LPS.(A) is a combination of all the replicates (N=3 in Blue, Red & Green) with P65:Actin ratio on the Y axis and LPS dose (ng/ml) on the X axis. The bar chart shows the variability between each set of results and (B) shows the % coefficient of variation (X axis) between each replicate dose. This was done by dividing the standard deviation by the mean. The range of variation was 11.5-27.62%.

2.3.2 Detection of p65 nuclear translocation in RAW 264.7 cells dosed with LPS

The nuclear extract of the RAW 264.7 cells dosed with LPS was collected after 1 hour to quantify (with densitometry) the translocation of p65 from the cytoplasm to the nucleus after stimulation of the cells with LPS. It was found that increasing the concentrations of LPS stimulated translocation of p65 from the cytoplasm to the nucleus. An increase in basal p65 density (Mean 0.17 SD 0.025) was only seen when a dose of 3ng/ml (Mean 0.387 SD 0.078) was used (which is much higher in comparison to 0.1ng/ml used for THP1 cells) this indicates again that p65 is a reliable marker of TLR activation and subsequent down-stream signalling leading to NFκB "classical" pathway activation. However in this particular cell line much higher concentrations of LPS were required in order to stimulate the cells and a maximal response was seen between 100-300 ng/ml (Mean 0.647, SD 0.046 and Mean 0.7, SD 0.11 respectively). Higher LPS concentrations lead to a mean decrease in mean nuclear p65 density, probably indicating that these higher doses are potentially cytotoxic. *Figure 2.5* displays the densitometry results of each replicate of the experiment. *Figure 2.6* displays the means of the replicates. The trend is clear, it shows there is a gradual increase in the p65: Actin ratio with increasing dose of LPS, indicating an increase in the nuclear p65. There was a significant difference between all doses and controls ($p<0.05$). This similar trend was also seen between individual doses.

Coefficient of variation is defined as the standard deviation of a set of data divided by the mean. Here it was used to assess inter experimental variation. The overall range of variation was 7-28.7%. This shows that there is a high level of inter-experimental variability between day to day assays. *Figure 2.7* shows this graphically.

(A)

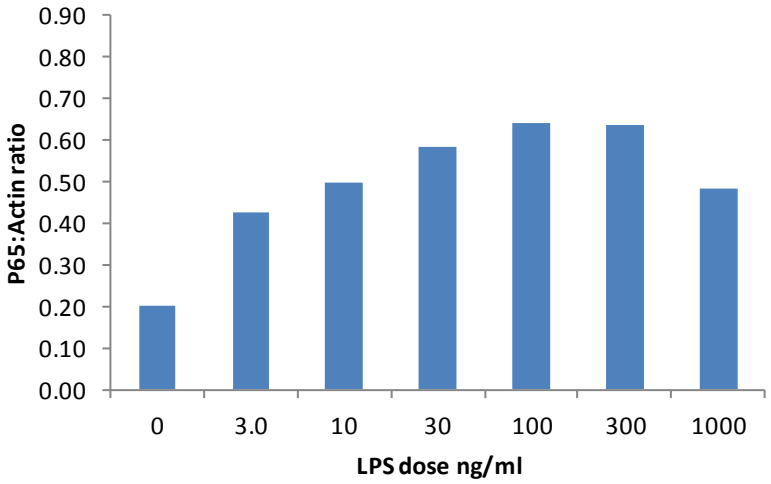

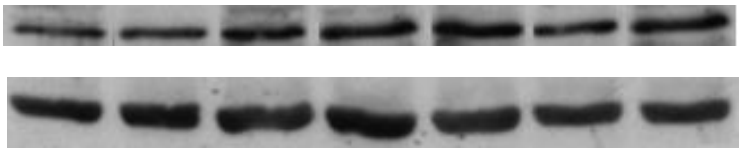

LPS dose ng/ml: 0 3.0 10 30 100 300 1000

(B)

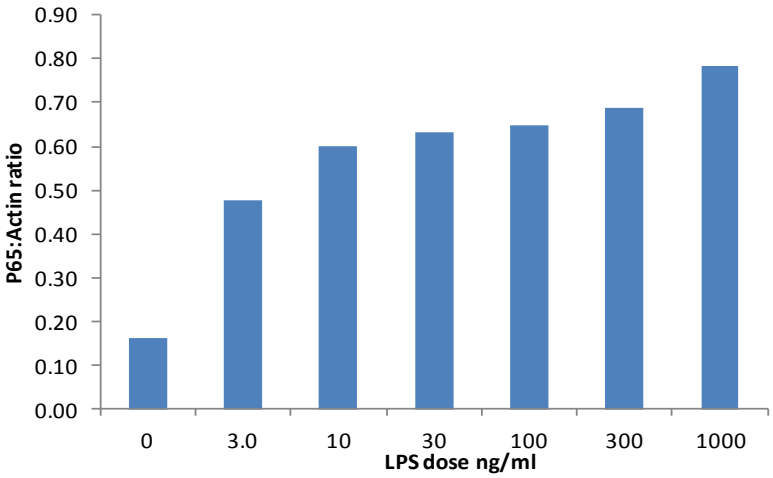

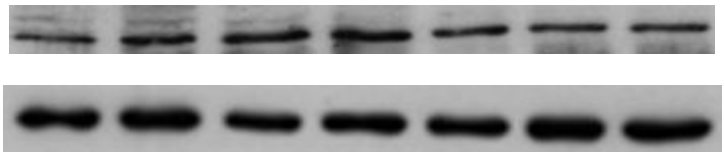

LPS dose ng/ml: 0 3.0 10 30 100 300 1000

(C)

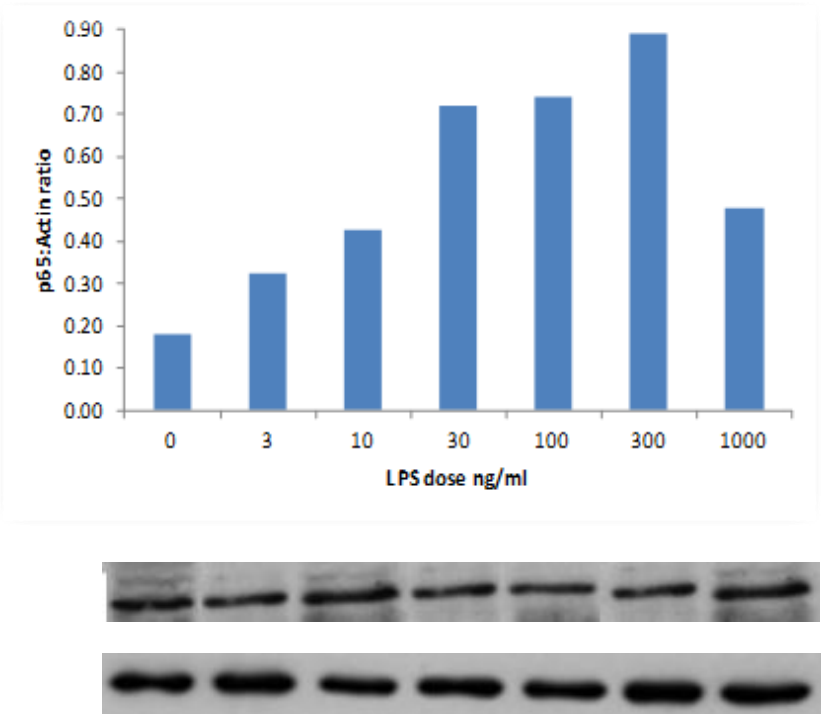

LPS dose ng/ml:	0	3.0	10	30	100	300	1000

Figure 2.5: Results of densitometry on developed films of Immunoblots of RAW 264.7 nuclear extract from cells dosed with varying concentrations of LPS. All bar charts are displayed with P65:Actin ratio on the Y axis and LPS dose (ng/ml) on the X axis. Underneath are pictures of p65 1 minute films on top along with 10 second actin films on the bottom. A-C are repeats of the same method done on three sets of different nuclear extracts carried out on dosing experiments done on different days (N=3). Immuno blots were carried out on the same day.

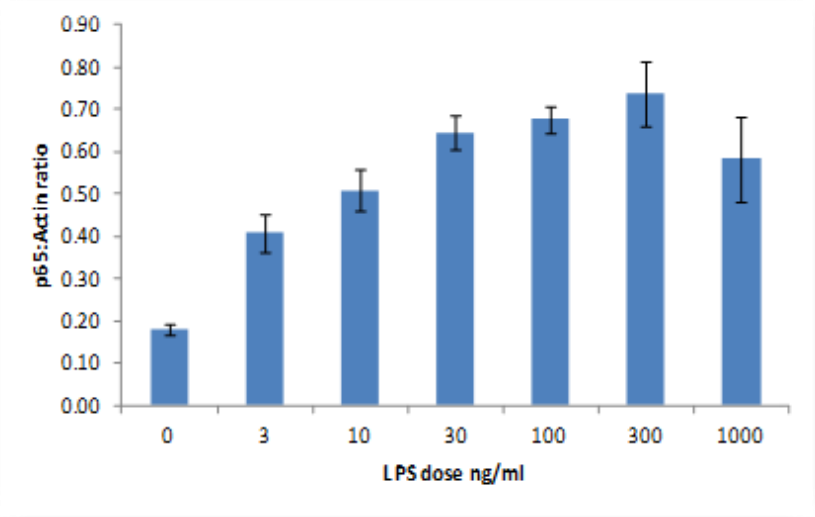

Figure 2.6: Results of densitometry on developed films of Immunoblots of RAW 264.7 nuclear extract from cells dosed with carrying concentrations of LPS. Bar charts are displayed with P65: Actin ratio mean (N=3) on the Y axis and LPS dose (ng/ml) on the X axis. Means are plotted with SEM.

(A)

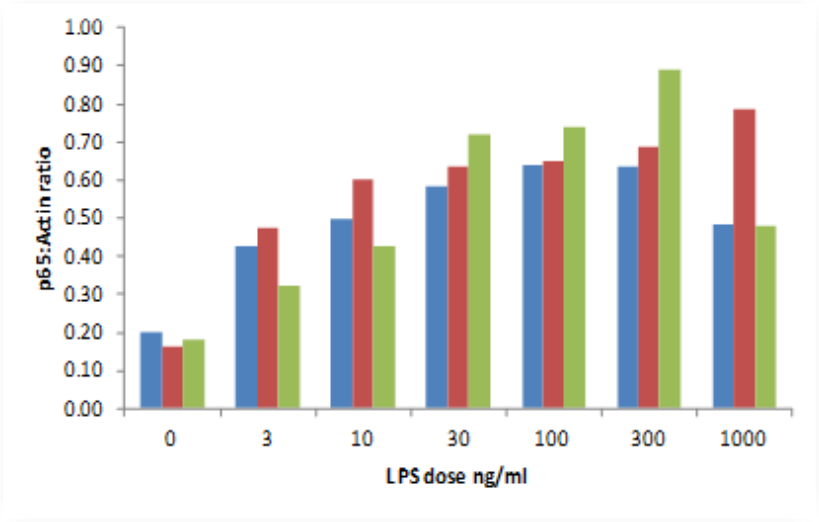

(B)

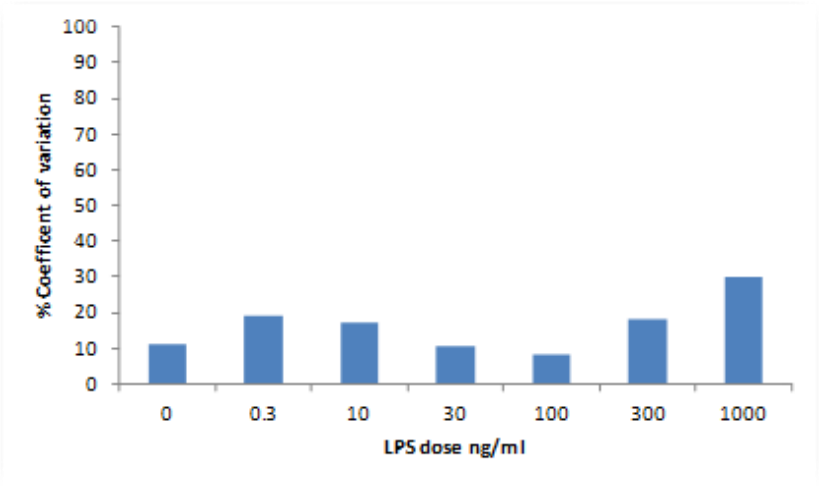

Figure 2.7: Results of densitometry on developed films of Immunoblots of RAW 264.7 nuclear extract from cells dosed with varying concentrations of LPS.(A) is a combination of all the replicates (N=3 in Blue, Red & Green) with P65:Actin ratio on the Y axis and LPS dose (ng/ml) on the X axis. The bar chart shows the variability between each set of results and (B) shows the % coefficient of variation (X axis) between each replicate dose. This was done by dividing the standard deviation by the mean. The range of variation was 7-28.7%.

2.3.3 Comparison of p65 nuclear translocation in THP1 and RAW 264.7 cells dosed with LPS

THP1 monocytes did not only respond to lower doses such as 0.1ng/ml, they also showed a greater increase in nuclear p65. Similar numbers of cells where used in each experiment $5x10^6$ in 7 mls of THP1 cells and $5x10^6$ in 5mls of RAW 264.7 cells). This could either mean that the individual monocyte cell type is more sensitive to LPS than the macrophage or there is a species variation (murine versus human) between sensitivities to LPS. *Figure 2.8* demonstrates graphically the visible differences in response to similar doses of LPS in the two cell lines. This effect could also be explained by the nature of the cell culture. THP1 cells are suspension cells cell meaning they multiply while suspended in the media, whereas the RAW 264.7 cells are semi adherent meaning they can adhere to the side of cell culture flasks and multiply. This adherence could potentially reduce the available surface area that the RAW 264.7 macrophage exposes be stimulated by LPS and subsequent activation of the inflammatory pathway.

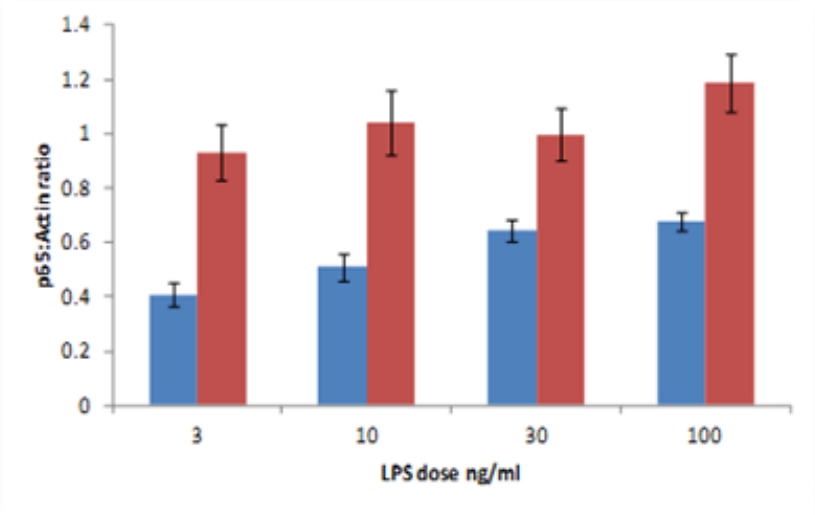

Figure 2.8: Results of densitometry on developed films of Immunoblots of THP1 (Red) and RAW 264.7 (Blue). Comparison of similar doses in the two cell lines shows higher responses in the THP-1 cell line versus RAW 264.7 at respective doses.

2.3.4 Dose-Response relationship and Comparison of p65 nuclear translocation in THP1 and RAW 264.7 cells dosed with LPS

Dose-response relationship describes the change in effects to an organism that a varying level of a stressor makes, defined within a certain period of time [69]. In this case the organisms are the cell lines; THP1 and RAW 254.7 and the stressor is LPS. Analysis of fold increase in nuclear p65 from basal levels allows for an observation of the threshold and range of LPS that the cell lines can respond to and also identifies the relationship and relative sensitivities of the cells to changes in dose. Figure 2.9 (A) is the dose response curve for fold increase in p65: Actin density against dose and (B) is the same but for the RAW 264.7 cell line. Fold increase was calculated by dividing the basal level of p65 into all the p65 response seen at each dose. The X axis is calculated by log [LPS]; the doses where first converted into pg/ml in order to allow for even spacing on the graph. GraphPad Prism 5 ® was used to calculate the curves and this software uses the four parameter logistic non-linear regression model for curve fitting.

Comparison of the curves suggest that THP1 cells respond to lower doses of LPS than RAW 264.7 cells and lower doses produce a greater fold increase in the nuclear p65 density indicating that they are more sensitive to lower concentrations cells. The Hill slope for RAW 264.7 cells was 1.5 whereas for THP1 cells it was between 0.7, this suggest that although higher concentration of LPS were required in order to cause an effect in the RAW 264.7 cells, the effect was greater and more potent than that seen in the THP1 cell line. RAW 264.7 cells appear to be more sensitive to changes in concentration of LPS but overall THP1 cells have a higher p65 fold increase compared to RAW 264.7 cells.

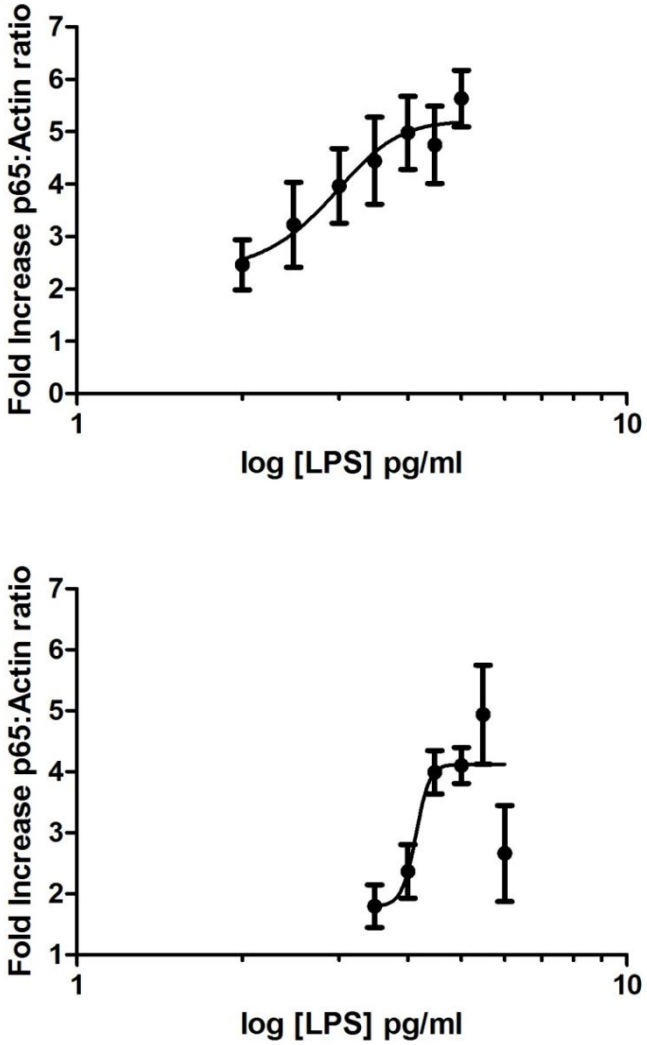

Figure 2.9: Dose-response curves for (A) THP1 and (B) RAW 254.7 cell lines dosed with varying concentrations of LPS. X axis are the log values of the concentrations with fold increase in the p65: Actin ratio on the Y axis. Fold increase was calculated by dividing the mean basal p65 response into all other mean doses. Means are plotted with SEM.

2.4 Discussion

NFκB translocation is an important event in the inflammatory response for transcription and production of new cytokines including TNF-α, which is not stored in the cell but made *de novo*. In these experiments, p65 detection through immunoblotting was demonstrated to be a valuable, reliable way of detecting activation of the NFκB pathway in cells dosed with LPS. Gradual dosing showed that increasing the dose of LPS resulted in a greater translocation of the p65 subunit of NFκB from the cytoplasm to the nucleus of the cell, in both human and murine cells. However it appeared that the murine cells required a higher dose of LPS than human cells and therefore demonstrated resilience to endotoxin.

2.4.1 Species variation in response to LPS

The different dose-response to LPS in human and murine cells has been reported before; with RAW 264.7 cells requiring higher doses of LPS in order to elicit similar responses to those seen in THP1 cells[70]. TLR 4 is an important receptor expressed on most myeloid cell derivatives, that allow them to detect and respond to LPS [71]. *In vitro* studies have shown that human macrophages up-regulate and increase their activation of TLR 4 on stimulation with LPS[72], whereas murine cells appear to down-regulate TLR 4 transcripts under similar conditions [73]. This fundamental variation in expression pattern could explain the higher levels of p65 translocation in human but not murine cells seen in this chapter, as TLR 4 activation is the important first step in the phosphorylation of IκB and subsequent release of the p65-p50 NFκB heterodimer as part of the classical pathway (see *figure 1.1*).

Lymphocyte antigen 6 (or MD-2) an extracellular protein and ligand of the TLR 4 is important in LPS binding to this receptor r[74]. *Hajjar et al* [70] demonstrated that the human TLR4-MD-2 complex is more sensitive in humans than in mice and has the ability to recognize acetylation of the LPS molecule allowing it to generate a more specific inflammatory response. Bacteria can undergo acetylation of their LPS in the cell wall in response to environmental change. Pseudomonas aeurginosa is a prime example in cystic fibrosis patients where it can modify its LPS structure within the airway in order to avoid being killed by the innate immune system[75]. On challenging THP-1 cells and RAW 264.7 cells with this acetylated LPS and normal (less acetylated) E coli LPS, *Hajjar et al* [70] showed that murine cells produced a similar response with both types of LPS but human cells were able to differentiate and alter

their immune response producing higher levels of NFκB activation and cytokine release in response to E coli compared to the more acetylated LPS. This show that even at molecular level humans can modulate their innate immune system in response to pathogens in a more specific way than rodents.

Warren et al [76] suggested that the differences in resilience to LPS between species, with humans towards one end and rodents towards the other end of a spectrum, may not be due to an intrinsic cellular process, but rather may be related to mechanisms involving and perhaps regulated by serum proteins. This was demonstrated by the ability of isolated mouse serum to suppress the LPS induced TNF-α production in macrophages to a greater extent than human serum.

2.4.2 Immune cell response to LPS

Upon differentiation to macrophages monocytes lose their ability to multiply and their immune functions and their antibacterial properties become enhanced. The monocyte cell itself has been shown to be less sensitive to LPS than the macrophage in vivo [77] and this was shown by accumulation of NFκB in the cytoplasm of differentiated THP1 cells in comparison to non-differentiated cells. *Takashiba et al*[77] concluded that this accumulation was a priming event in making the macrophage more sensitive to LPS stimulation and resulted in a more rapid NFκB translocation and overall higher nuclear content. Therefore you would have expected to see higher levels of p65 translocation in a primed highly sensitive macrophage compared to a monocyte. The results within this chapter demonstrated less nuclear translocation of p65 in the murine macrophage in comparison to the human monocyte, but these results can be explained by the overpowering resilience and species variation[70, 76] to LPS.

2.4.3 Translational implications

The results from this chapter demonstrate that immunoblotting p65 is a reliable, detectable and reproducible way of measuring activation of the "classical" NFκB pathway in murine and human cell lines dosed with LPS. It also demonstrated the dose-response relationship of NFκB pathway activation with LPS; where increasing doses of LPS resulted in a higher accumulation of p65 in the nucleus of the cells.

Furthermore, comparison of the human and murine cell lines allowed the significant, fundamental molecular differences between the initiating steps in an inflammatory

process to be demonstrated. These results, in line with the literature[60, 66] highlight the pitfalls in using murine cell lines, which have been shown to have more primitive responses[60], compared to human alternatives in the study of inflammation. This can also be seen on an *in vivo* level with most wild type mice being highly resilient to LPS challenge. The dose of LPS used in most *in vivo* studies, 1–25 mg/kg, has a significant mortality rate [78]. This dose is much greater than the 2–4 ng/kg dose of LPS needed to elicit a similar response of cytokines in humans[79]. Therefore the so called "translational disconnect" that exists between in vivo and human sepsis appears to begin at a molecular level and is further augmented by the use of stimuli that do not efficiently recapitulate the environment of human sepsis *in vivo*.

Additionally while immortalized cell lines often originate from a well-known, described tissue type, frequently they have undergone mutations to become immortal. This will alter the internal physiology of the cell and needs to be taken into consideration when analysing results and translating to clinical medicine.

2.4.4 limitations & future work

One hour was chosen as a time point as activation of the p65 pathway is known to take a short time[80]. A major limitation of this study was that it only looked at a single time point. In future work it is hoped to look at a time course in order to ascertain whether or not high doses reflect the maximum activation of the pathway. Also further analysis is needed in order to investigate how the activation of the pathway translates to cytokine production.

Chapter 3:

Comparative histopathological analysis of two murine models of sepsis

Contents

3. Comparative histopathological analysis of two murine models of sepsis

3.1 Introduction

Doi et al[81] stated in their review on animal models of sepsis that murine sepsis should mimic the pace and severity of human sepsis; reproduce key haemodynamic and immunologic stages and mimic histology findings in the key organs lung, liver, spleen, kidney. Failure of models to do this has led to a reduction in preclinical efficacy of therapeutic treatments and a failure of translation. This is most notable in the case of the development of monoclonal antibodies against TNF-α, which improved survival in endotoxaemic mice, but failed to have a similar translational effect in humans[9].

3.1.1 LPS model of endotoxaemia

Endotoxaemia is defined as the presence of endotoxin in the blood. LPS a bacterial endotoxin from Gram negative bacteria is a widely used in models of murine sepsis and endotoxaemia by inducing "sterile inflammation". In experimental animals, a bolus injection of LPS will induce a sharp, but transient increase in pro-inflammatory cytokines such as TNF-α, IL-1, and IL-6[8], whereas in human sepsis the host response is triggered by live bacteria, giving detectable cytokine levels that are significantly lower, but sustained over a longer period of time. Despite the disparities LPS is widely used in research because models are relatively straightforward, produce the greatest homogeneity among all *in vivo* models of sepsis and are, thus, relatively easy to replicate[82].

LPS has become widely superseded by the development of surgical techniques for the induction of peritonitis. The two most common procedures used now are CLP and CASP. These methods produce a so called "polymicrobial" sepsis and not a "sterile inflammation". *Remick et al*[8, 47] found that although the mortality and the morbidity of the two models (LPS versus CLP) was similar, the inflammatory responses evoked are distinctly different[47]. In their study LPS induced substantially higher levels of cytokines than CLP and these peaked around 8 hours and then began to decline, cytokine levels in the CLP model were continuing to increase at the 8 hour time point and often exceeded the LPS induced values at this time. *Remick et al*[83, 84] therefore demonstrated that CLP was more successful in recapitulating this gradual increase in cytokines similar to human sepsis; however, *Maeir et al*[46] found

that CASP was a superior model to CLP, as mice undergoing CLP often developed intra-abdominal abscesses which changed the focus of their peritonitis and sepsis[46].

Although most research has been aimed at highlighting the difference between cytokine levels in each model, not a lot of research has gone into the significance of these cytokine levels with regards to organ damage and organ damage during sepsis, seeing whether or not it is similar to the human disease. Often, damage during sepsis is not from primary bacterial particles or LPS, but due to an over active immune response and production of cytokines[62].

3.1.2 Faecal peritonitis model of sepsis

The major problems with both these models along with those highlighted in section (see *1.3*) appear to be reproducibility and variability. It was often hard to control the size of the ligations and punctures and severity would differ from experiment to experiment. *Gonnert et al*[48] seemed to overcome this with a more robust polymicrobial model using a standardised polymicrobial inoculation model. They produced a batch of stool that was able to reproduce a clinically significant, quantifiable and reproducible model of sepsis in rodents. The stool was inoculated into the peritoneum of mice and induced a cytokine response similar to that of human sepsis (reflected by the rises and kinetics of IL-6 and IL-10). Microbiological analysis showed that the stool contained Escherichia coli (E coli) and Bacteroides species (Bacteroides spp), important Gram negative organisms that are known causatives of sepsis in humans[85]. The stool preparation was stored at -80^{o}C and over time (3 years) the bacterial content of the stool remained consistent. The translatability of the model was also tested by the administration of antibiotics and fluid resuscitation, these are common treatments in human sepsis and administration of antibiotics had similar effects on survival as did the fluid recovery mimicking effectively the responses that would be achieved in ICU patients. Follow up of the mice two weeks after also gave researchers the opportunity to study the chronic inflammatory changes, in particular the liver, which still contained marked levels of activated immune cells.

3.1.3 Pathology of organ damage in sepsis

Organ dysfunction is a common complication in human and experimental sepsis. These dysfunctions are attributed to the huge increase in systemic cytokine and mediator release which results in immune dysregulation, hormonal alterations, metabolic changes, mitochondrial dysfunction, micro- vascular dysfunction, epithelial dysfunction and coagulation activation[58] (see *1.3*). However, in sepsis models, organ dysfunction varies depending on the type of insult and model used.

Dear et al[86] demonstrated that acute renal failure (ARF) and liver dysfunction induced by polymicrobial sepsis through CLP had significant pathophysiological differences to ARF and liver dysfunction induced by administration of LPS. LPS is dependent on TLR 4 activation for *de novo* production and release of TNF-α, However, *Dear et al*[86] showed that polymicrobial CLP has the potential to activate multiple different receptors and is not dependent on TLR 4. Subsequent rises in TNF-α seen with LPS treatment lead to renal cell apoptosis and as CLP mice showed lower levels of serum TNF-α, they showed an absence of renal cell apoptosis. The conclusion was that polymicrobial sepsis induced by CLP more accurately reflects human sepsis than administration of LPS. In humans and polymicrobial sepsis, severity is not dependent on TLR 4[87], this could be a significant contributing factor for reduced efficacy of therapies based on TNF-α inhibition. Post-mortem analysis has also shown that despite a large renal dysfunction in septic patients, often no apoptosis is detected in routine haematoxylin and eosin (H&E) staining sections[88]. Although apoptosis is not the mechanism for renal dysfunction in the CLP model, significant levels have been noted in the liver and spleen during human and LPS induced experimental sepsis[88, 89]. Apoptosis in the spleen is reported to be significant in sepsis mortality and can occur via TNF-α independent pathways[86]. The discrepancies between mode of cell death and cellular level organ dysfunction, highlight the need for an in depth histopathological analysis of individual tissues from the LPS model and comparison with the newer more clinically relevant faecal inoculation model, to see which are consistent with changes observed in human tissue.

3.1.4 Liver damage during sepsis

In patients with sepsis and SIRS, the liver plays a significant role as a source of inflammatory mediators. The liver is pivotal in modulating the systemic response to severe infection, because it contains the highest portion of macrophages (Kupffer cells) in the body; these Kupffer cells can effectively clear the endotoxin and bacteria that initiate the systemic inflammatory response. However, in sepsis, the over-zealous inflammatory response often becomes counter-intuitive as the liver itself begins to become damaged. In experimental modelling, LPS causes a significant increase in TNF-α which induce secondary hepatocyte apoptosis and has no primary hepatotoxic effect[90].

Detailed liver studies by *Koskinas et al* [91] in patients with sepsis showed that the main histological changes were hepatitis and steatosis in the majority of patients dying from sepsis. Liver biopsies showed portal inflammatory infiltration in 73.3%, centrilobular heaptocyte necrosis in 80%, lobular inflammation in 66.7% and hepatocellular apoptosis in 66.6% of patients. This apoptotic/necrotic pattern in the liver has also been observed in a further histopathological analysis of a similar group of patients[88]. In experimental models, *Gonnert et al*[48] reported leukocyte–endothelium interactions (i.e. leukocyte rolling and adhesion) within the liver 15 hours after the septic insult. Interestingly, they did not report any apoptosis or necrosis at this time, although they reported undetectable levels of TNF-α at 5 hours, concluding that levels must have normalized before serum was taken off for detection[48]. Follow up of the mice showed a pattern of persistent immune cell infiltration (i.e. neutrophils, prominent macrophages and irregularly shaped lymphocytes) and altered architecture. In experimental modelling, TNF-α induced hepatocyte apoptosis is an early, general, and possibly causal event during experimental liver failure triggered by inflammatory stimuli such as LPS[92]. Understanding acute changes in the liver may provide information on the discrepancies between models and show whether or not at cellular level, LPS or faecal inoculation involves changes similar to human sepsis.

3.1.5 Adipose tissue and sepsis

Adipose tissue has become regarded as a significantly active endocrine organ that has the potential to play a major role in the inflammatory process through expression of a diverse set of receptors, proteins, hormones and the secretion of a large family of proteins called adipokines[93]. In humans, adipose tissue is situated in the sub-cutis beneath the skin and around organs as visceral fat. Adiponectin is a protein exclusively secreted from adipose tissue that modulates a number of metabolic processes, including glucose regulation and fatty acid catabolism[94]. Plasma adiponectin declines before the onset of obesity and insulin resistance in non-human primates, suggesting that hypoadiponaectinemia contributes to the pathogenesis of these conditions and the so called "metabolic syndrome"[95]. Levels of the hormone are inversely correlated with body fat percentage in adults[96].

Three receptors for adiponectin exist but the most abundant are AdipoR1 & R2. The activation of AdipoR1 & R2 results in increased hepatic and skeletal muscle fatty acid oxidation, increased skeletal muscle lactate production, reduced hepatic gluconeogenesis, increased cellular glucose uptake and inhibition of inflammation and oxidative stress. Several studies have highlighted the ability of adiponectin to modulate the inflammatory response. *In vitro* adiponectin decreases the production of TNF-α and IL-6 in LPS stimulated human macrophages[97]. In rats with induced polymicrobial sepsis through CLP, plasma adiponectin levels negatively correlated with plasma LPS and TNF-α levels [98]. *Teoh et al*[99] concluded that adiponectin homeostasis serves to limit leukocyte infiltration, chemotaxis, and endothelial activation. Furthermore, adiponectin deficiency has been shown to exacerbate hepatic injury during CLP and this is hypothesised to be a result of inhibition of TNF-α release (demonstrated in obese KK-Ay mice)[100]. The pathological implications indicate that adiponectin deficiency leads to enhanced hepatic steatosis[101], a known mechanism for hepatic injury in sepsis[89].

Adipose tissue recruitment and activation is, therefore, an important stage in human sepsis as adiponectin has been shown to play a significant role in modulating the inflammatory process[97, 98, 100-102]. By analysing adipose tissues and a diverse set of organs in various mice models of sepsis, a difference in endothelial activation and leukocyte recruitment into tissues might help elicit further, which models are mimicking the septic process in humans most effectively.

3.1.6 Skeletal muscle and sepsis

Maintenance of skeletal muscle function is important in sepsis in order to effectively ventilate and maintain respiratory capacity. Studies have shown that the proteolytic activity of the proteasome is higher in skeletal muscle from patients with sepsis and multiple organ failure compared with healthy controls and that both respiratory and leg muscles are affected similarly[98]. This mechanism has been attributed to increased transcription of the ubiquitin-proteasome pathway proteins[83].

Skeletal muscle has also been shown to be an important site of adiponectin activity during sepsis. *Delaigle et al*[84] found that adiponectin is up-regulated *in vivo* and *in vitro* in human and rodent myotubes in response to inflammatory stimuli, concluding that it's over expression may be a local anti-inflammatory protection and a way to supply extra energy during inflammation. This was further reinforced by *Wei et al*[103] who found that induction of adiponectin into skeletal muscle in response to an inflammatory infiltration appears to be a crucial mechanism to counteract excessive inflammatory damage, oxidative stress, and subsequent apoptosis. These mechanisms highlight the protective role of adiponectin in the maintenance of muscle function and inadvertently respiration.

The subtle inflammatory infiltrations and recruitment of leukocytes appears to be significant in human sepsis and should be equally important in experimental sepsis, along with trying to mimic the criteria stated by *Doi et al*[81]

3.1.7 Aims of this chapter

Recreating an effective model of experimental sepsis similar to that of humans is proving difficult. However, more recent models are moving closer to mimicking key immunological, endothelial and cytokine alterations along with levels of organ dysfunctions. These models are superseding and replacing the LPS model of endotoxaemia favouring a "polymicrobial" approach instead. Analysis of cytokines has already shown that a bolus of LPS will induce a sharp non sustained rise in key cytokines, whereas newer surgical models favour a more sustained gradual incline [57]. The aim of the experiments of this chapter is to investigate how these cytokine differences will correspond with acute changes, and inflammatory infiltration of organs (in particular the liver). This will be carried out by looking at how the LPS model differs from the newer faecal peritoneal inoculation model proposed by *Gonnert et al*[48]. At the same time it will allow for analysis of differences in recruitment of other tissue namely fat and skeletal muscle which have shown to be key players in human inflammation and sepsis[104, 105]. Detailed histopathological analysis of the LPS model will also allow for discrepancies and "endotoxaemia" phenomenon to be highlighted that may not be representative of normal human sepsis. APAP will also be included as positive control at a dose where organ damage will be expected. This will also provide information about how mechanisms of organ damage in drug toxicity differ from those with inflammation. 6 hours was chosen as a time point for culling as it allowed enough time for serum cytokine levels to elevate high enough so acute , early, changes in tissue can be observed. This will also allow for a direct comparison with tissue from the same time point provided by our collaborators. The hypothesis is restated below:

"LPS induces histopathological changes different from faecal inoculation: Histopathological analysis of tissues from mice dosed IP with LPS or faecal suspension will show differing levels of tissue recruitment and damage of various tissues compared to controls and those dosed with acetaminophen."

3.2 Materials and Methods

3.2.1 Materials

Tissue from the faecal peritonitis murine model of sepsis was kindly donated by Jana Lemm, Department of Anesthesiology and Intensive Care Research Unit: Molecular Mechanisms of Organ Failure Research Center, Lobeda Erlanger Allee 101, Friedrich-Schiller-University, D-07747 Jena, Germany. Samples were collected from C57/BL6 mice at necropsy and included liver, gastrocnemius muscle, epididymal, peri-renal and sub-cutaneous fat. Samples were fixed in 4% paraformaldehyde (PFA) and embedded in paraffin cassettes before being shipped to the UK. Mice used in the LPS dosing experiment were 23 male C57BL/6 mice (25-30g) obtained from Charles-River (Margate, UK). LPS used in dosing was obtained by phenol extraction from Escherichia coli 0111:B4 (SIGMA, Aldrich L2630). Acetaminophen and sodium chloride for saline (SIGMA, Aldrich A7085, S7653) along with LPS where all in powder form and were reconstituted in distilled water before administration.

3.2.3 Intra-peritoneal inoculation of faeces into C57/BL/6 mice

11 male C57BL/6 mice (25-30g) received an intraperitoneal injection (right upper quadrant) for induction of sepsis, 1.75 mL/kg body weight stool suspension, diluted (1:4) in saline, was injected i.p. into the right lower quadrant of the abdomen with a 21-gauge cannula as described by *Gonnert et al*[48]. 11 control animals were injected in a similar manner with normal saline. All animals also received 25 µl per gram body weight normal saline subcutaneously to compensate for fluid losses. Mice were then euthanized at 6 hours using carbon dioxide suffocation and a standard protocol for removal of organs was followed. Samples from the liver, epididymal, peri-renal and sub-cutaneous fat depots along with muscle gastrocnemius were either frozen or fixed in 4% paraformaldahyde (PFA) before being embedded in paraffin cassettes. Frozen samples where then transported securely to the UK on dry ice. Fixed samples were shipped at room temperature.

3.2.2 Animal housing and preparation

23 male C57/BL/6 (25-30g) were ordered from the biomedical services unit and allowed to acclimatize for one week prior to the experiment. Animals were treated in accordance with guidelines set out by the home office (project licence 40/3143) with regards to the handling and experimentation of animals. Throughout the experiment animals had free access to food and water and were kept in cages.

3.2.3 Dosing regimen of C57/BL6 mice with LPS, APAP & saline

Animals were weighed, marked and divided into three groups and given one of the following treatments intra-peritoneally (right upper quadrant): 25mg/Kg LPS (a dose known to induce lethal endotoxaemia), Saline (an equivalent amount to that used in LPS dosing) or 350mg/Kg of acetyl-para-aminophenol (APAP) and culled using carbon dioxide suffocation at 6 hours (allowing results to be comparable with our collaborators experiments). Animals were dosed based on weight and the schedule is summarised in the table below:

Animal numbers	**Total number**	**Intervention**	**Dose**	**Dose based on average weight of 30g**	**Cull**
1-11	11	LPS	25mg/Kg	0.75mg	6 hours
12-17	6	No intervention	No intervention	No intervention	6 hours
18-23	6	acetaminophen	350mg/Kg	10.5mg	6 hours

Table 3.1: Table showing the dosing regimen and number of animals in each group

APAP dosed mice were included as a positive control to ensure that dosing was done correctly, but also to compare if necrosis and apoptosis patterns along with organ damage differs to that caused by inflammation. All animals were given sub-cutaneous saline to compensate for fluid volume of 25 µl per gram body weight.

3.2.4 Culling and sample collection

Animals were euthanized by carbon dioxide at 6 hours. Blood was removed and spun to isolate the serum (which was frozen at -80°C). Tissue samples removed included the liver, epididymal, peri-nephritic and sub-cutaneous fat (small deposits from the back) along with muscle gastrocnemius (similar to the samples sent from our collaborators). Heart, lungs, spleen, thymus, bone marrow, brain & intrascapular brown adipose tissue were also removed for an in-depth analysis of LPS changes at the cellular level. Aliquots of the organs were frozen and stored at -80°C, while microscopic samples were treated as described below.

3.2.5 Tissue fixation, slide preparation and interpretation

Tissue was fixed in 4% PFA before being cut into an appropriate size and placed in a cassette and tissue processor overnight to remove water and replace it with paraffin wax. Within the processor tissues are dehydrated using increasing concentrations of ethanol and excess ethanol was removed using xylene. Finally molten paraffin wax replaces the xylene and the tissue is embedded into moulds before sectioning. Basic staining (Haematoxylin & eosin) was carried out for a general histopathological assessment of the tissue. Periodic acid-schiff (PAS) was also done where appropriate.

2.3 Results

A detailed description of the histopathological findings of all organs/tissues from each animal is provided in *Appendix 1*. Animals are indexed by their case number and this is given along with the study number, intervention and a description of the major histological findings from each individual tissue.

2.3.1 Histological findings in the liver

Livers from control animals did not exhibit any histological abnormalities. There was presence of diffuse hepatocellular glycogen accumulation, represented by a diffuse cloudy cytoplasmic vacuolation in HE stained sections (*figure* 3.1) and the presence of granular Periodic acid Schiff (PAS)-positive material after the PAS reaction (data not shown).

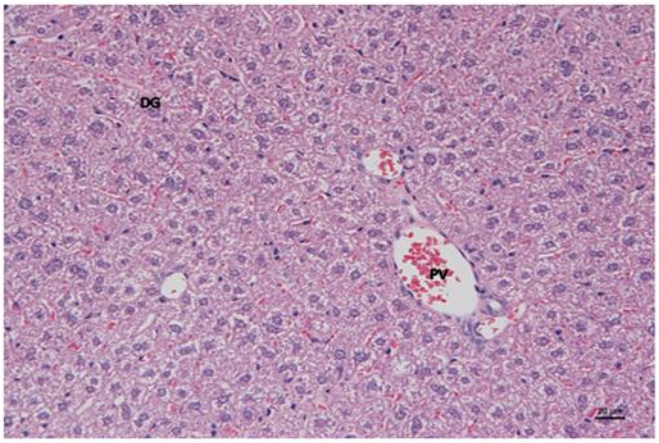

Figure 3.1. C57Bl6 mouse at 6 hours post intraperitoneal inoculation of saline (control animal; case No 12L-1405). Liver. No histological abnormality is recognised. Hepatocytes exhibited diffuse cloudy cytoplasmic vacuolation, consistent with glycogen accumulation. PV: portal vein. HE stain.

Animals that had been intraperitoneally inoculated with faecal suspension exhibited an acute suppurative perihepatitis, represented by a variably thick layer of neutrophils attached to the liver surface. These were mixed with amorphous granular eosinophilic material (faecal matter) and occasional bacterial colonies from the suspension. This was underlain by a thin sub-serosal layer of neutrophils (*figure* 3.2 A, B). In addition, a few to several neutrophils were found in the lumen of central veins and portal veins (*figure* 3.2 C). Large numbers of neutrophils in the blood vessels indicate a release of neutrophils from storage pools (i.e. bone marrow) and a neutrophilia – a finding consistent with systemic inflammation. Rarely, individual neutrophils were also seen in the sinusoids immediately adjacent to the central veins. The PAS reaction highlighted diffuse hepatocellular glycogen accumulation, which was most pronounced in centrilobular areas.

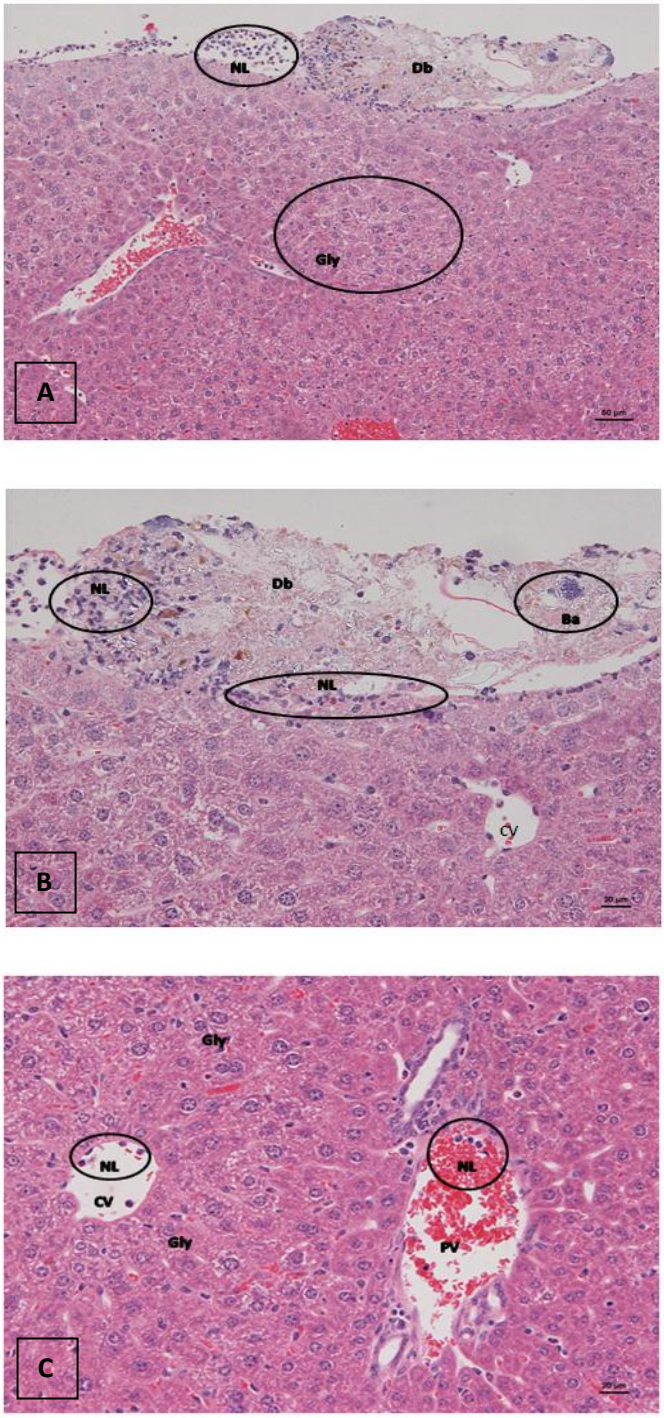

Figure 3.2: C57BL/6 mouse at 6 hours post intraperitoneal inoculation of faeces (1.75 mL/kg) (case No 12L-1393). Liver. (A) Liver parenchyma with capsule, exhibiting focal serosal attachment of neutrophils and cellular debris (perihepatitis). Underlying the infiltrate is a thin layer of subserosal neutrophils (arrow). (B) Closer view of the perihepatitis, showing debris (Db) and bacterial colonies (Ba) from the faecal suspension. (C) Liver parenchyma with neutrophils in the lumen of central veins (CV) and portal veins (PV). Hepatocytes exhibit cloudy cytoplasmic vacuolation consistent with diffuse glycogen accumulation. HE stain.

LPS-treated animals did not show any evidence of perihepatitis. However, they exhibited more intense leukocyte recruitment into the parenchyma, as represented by the presence of increased numbers of disseminated neutrophils between hepatic cords (*figure 3.3* A&B). Neutrophils were also present in the lumen of central veins and portal veins, in similar amounts to those observed in the mice that had undergone faecal peritoneal inoculation. In addition, diffuse glycogen loss was observed. This was represented by a loss of hepatocellular cytoplasmic vacuolation and the absence of PAS positive material within hepatocytes (*Figure 3.3* B).

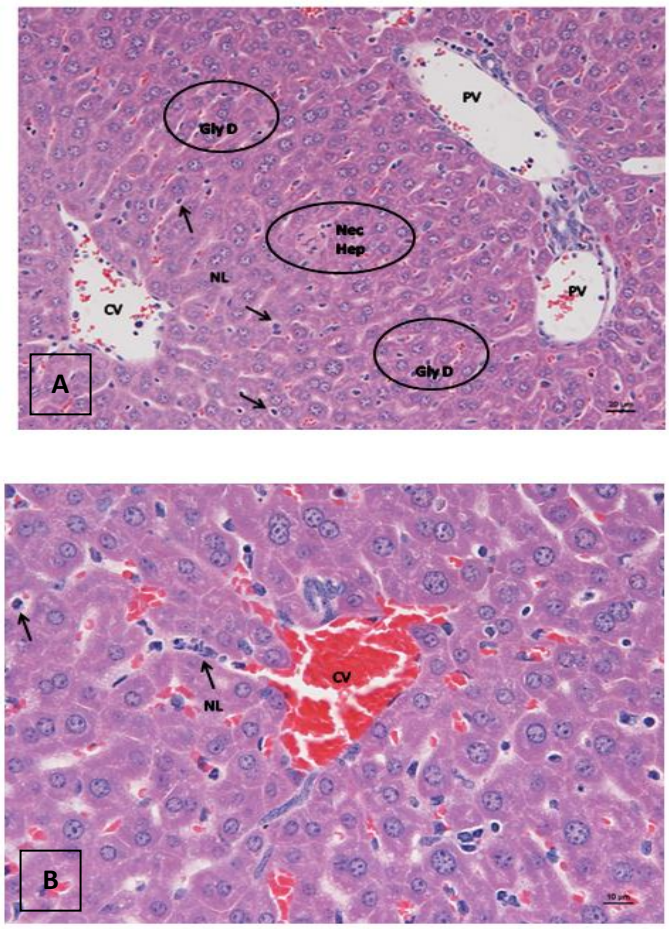

Figure 3.3: C57BL/6 mouse at 6 hours post intraperitoneal inoculation of LPS (25mg/kg) (case No 12L-1402). Liver. (A) Small random neutrophil aggregates are seen in the parenchyma. Isolated individual necrotic hepatocytes (Nec Hep) are seen. There are several neutrophils in the lumen of central veins (CV) and portal veins (PV). (B) Closer view of the liver parenchyma, highlighting the increased amount of neutrophils between hepatic cords. Hepatocytes do not exhibit cytoplasmic vacuolation, consistent with a diffuse loss of glycogen. HE stain.

APAP treatment of mice was associated with a variable degree of centrilobular hepatocyte loss with the presence of small numbers of degenerate/necrotic hepatocytes and/or a variable degree of hydropic degeneration of centrilobular hepatocytes. Diffuse loss of hepatocellular glycogen was observed. There was no distinct evidence of neutrophil recruitment, i.e. there was no increase in neutrophils within veins or hepatic cords (*figure 3.4*)

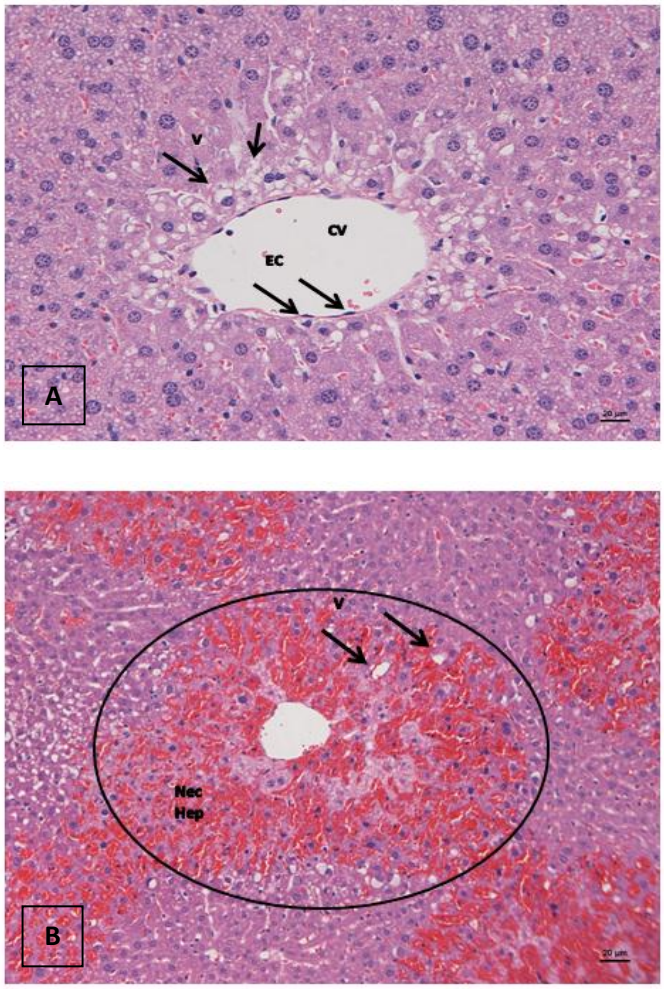

Figure 3.4: C57BL/6 mouse at 6 hours post intraperitoneal inoculation of APAP (350mg/kg). Liver. (A) Case No 12L-1411, without significant centrilobular cell loss. There is evidence of hydropic degeneration of centrilobular hepatocytes (1-2 cell layers), represented by swelling of hepatocytes and delineated cytoplasmic vacuoles (arrows, V). Scattered centrilobular apoptotic/necrotic hepatocytes and a few neutrophils are seen. Endothelial cells (arrows, EC) within the central veins (CV) appear activated. Hepatocytes do not exhibit cytoplasmic vacuolation, consistent with a diffuse loss of glycogen. (B) Case No 12L-1412. No glycogen (NG). There is marked centrilobular hepatocyte loss (grade II[106]) and hydropic swelling and degeneration of remaining hepatocytes (encircled). Blood fills the areas of hepatocyte loss. HE stain.

2.3.2 Histological findings in Adipose tissue and skeletal muscle

Mice treated with LPS and faecal inoculation showed variable evidence of neutrophil recruitment, represented by the presence of veins in which neutropihls were found in the lumen and rolling along (attached to) endothelial cells (*figure* 3.5). This was more frequent in mice that had been inoculated with the faecal suspension, indicating an early onset of systemic neutrophil recruitment into these tissues in these animals. The latter also showed some degree of serosal inflammation at the surface of the perirenal adipose tissue, consistent with peritonitis (see also perihepatitis above *figure* 3.2).

In LPS treated animals, the skeletal muscle (M gastrocnemius) did not exhibit any pathological changes. Mice that had been inoculated with faecal suspension often exhibited variable amounts of neutrophils with the lumen of veins (*figure* 3.6).

In APAP treated mice and in control mice, adipose tissue and gastrocnemius muscle did not exhibit any pathological changes. Occasionally, veins in the subcutis contained a few neutrophils and there was a focal inflammatory cell infiltration, but this was considered as a local reaction.

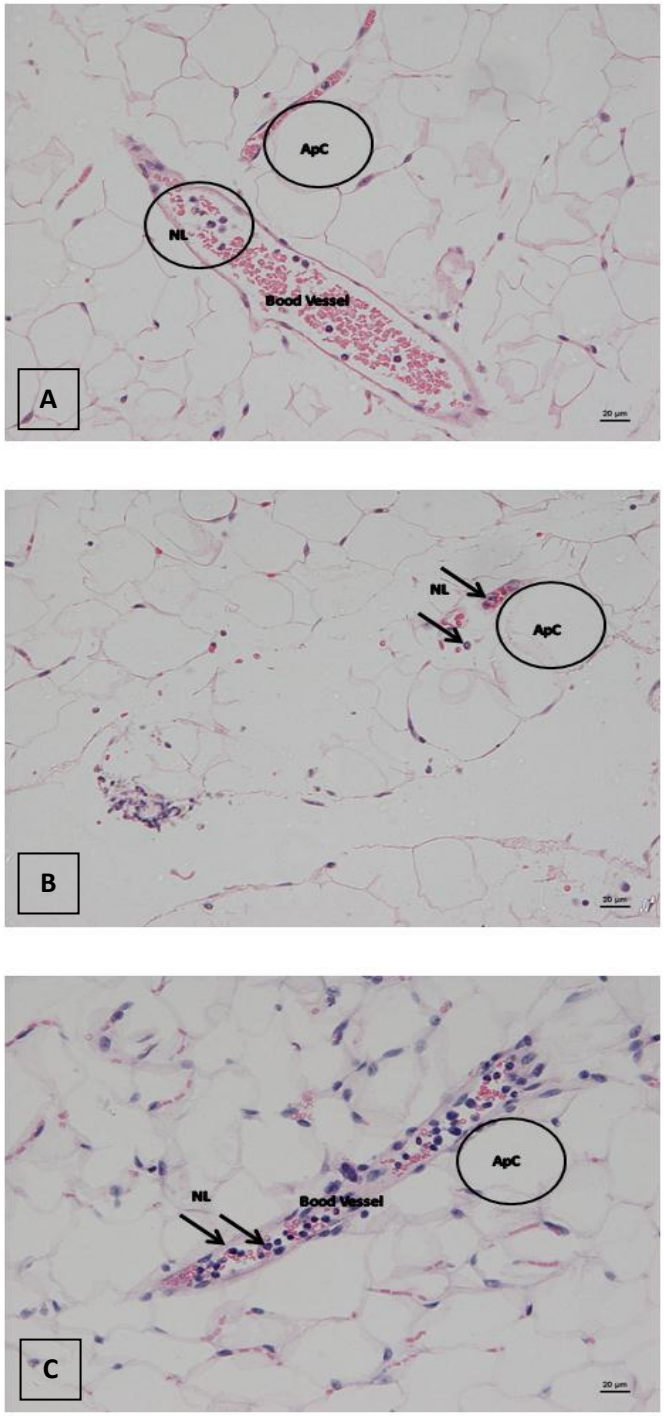

Figure 3.5: C57BL/6 mouse at 6 hours post intraperitoneal inoculation of faeces (1.75 mL/kg) (case No 12L-1393). A,B Case No 12L-1093. (A) Epididymal adipose tissue. Embedded between adipocytes (ApC) are veins that exhibit several neutrophils in the lumen. (B) Peri-renal fat with focal serosal neutrophil infiltration with admixed bacteria (peritonitis) and veins containing neutrophils in the lumen. (C) Case No 12L-401. Epididymal adipose tissue. Vein packed with neutrophils. HE stain.

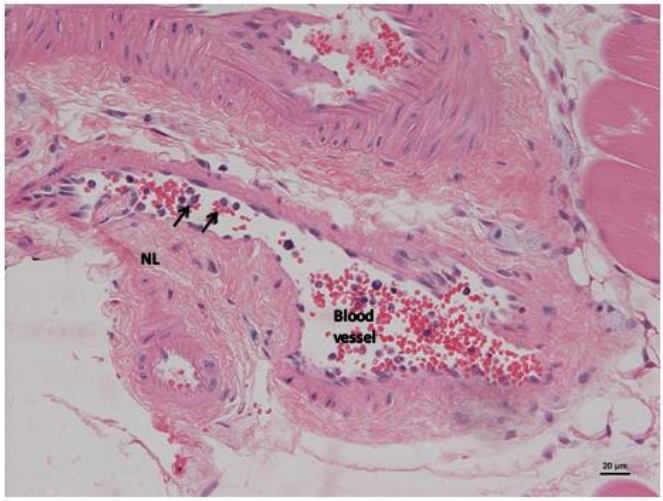

Figure 3.6: C57BL/6 mouse at 6 hours post intraperitoneal inoculation of faeces (1.75 mL/kg) (case No 12L-1093). Muscle gastrocnemius. Larger artery with several neutrophils in the lumen. HE stain.

2.3.3 Histological Findings in Other Tissues of mice inoculated with LPS and APAP

There was no additional tissue available from mice dosed intra-peritoneally with the feacal suspension. However, in animals that had been treated with LPS and APAP, other tissues were examined in order to identify any pathological changes consistent with a systemic inflammatory response and any associated other changes.

In lungs, control animals did not show any pathological changes and only rare neutrophils were seen within vessel lumina (*figure* 3.7). In LPS treated animals, several neutrophils were generally present in the lumen of veins and arteries (*figure* 3.8 (A)). There was also evidence of neutrophil rolling along the endothelium which occasionally appeared activated (*figure* 3.8 B&C). Occasionally, vessels were completely packed with neutrophils.

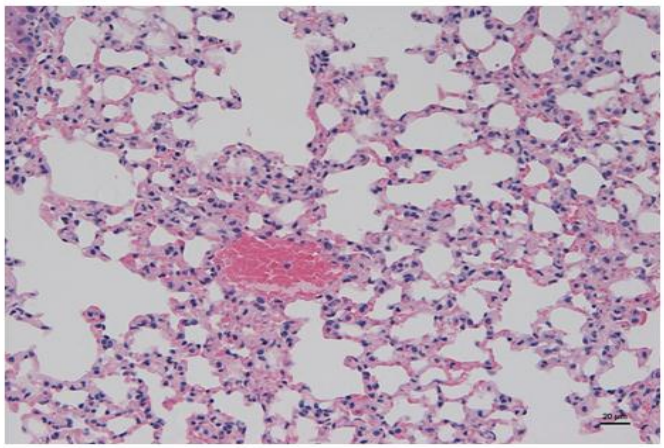

Figure 3.7: C57BL/6 mouse at 6 hours post intraperitoneal inoculation of saline (control animal; case No 12L-1405). Lung. No histological abnormality is recognised. Blood vessels do not exhibit neutropils in the lumen. HE stain.

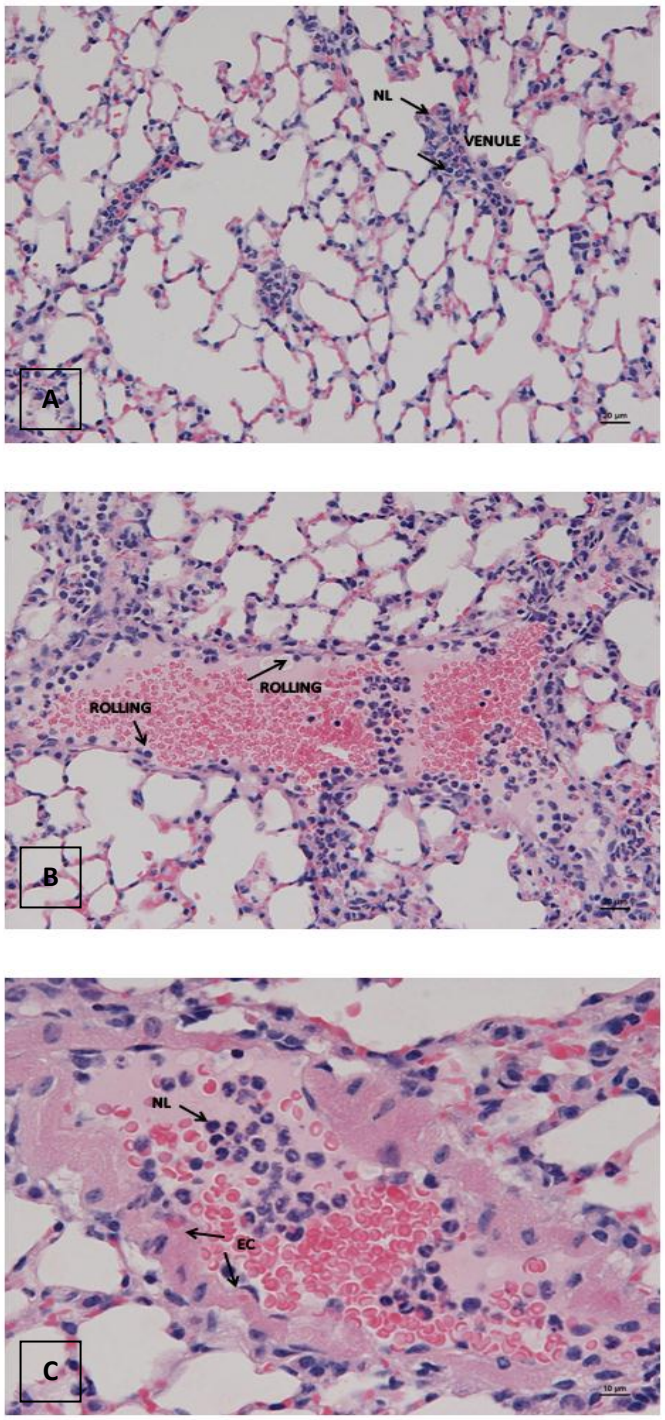

Figure 3.8: C57BL/6 mouse at 6 hours post intraperitoneal inoculation of LPS (25mg/kg) (case No 12L-401). Lung. (A) Small venules and larger veins are found packed with neutropihls. (B) Neutrophils are found rolling along the endothelium indicating recruitment into the tissue. (C) Some endothelial cells (EC) appear activated (arrows) and there are number neutrophils in the lumen of an artery, some of which are seen rolling along the endothelium. HE stain.

The Spleen and thymus were also examined in order to assess the potential effect of LPS and APAP treatment on the lymphocyte populations.

In LPS treated animals, the spleen exhibited larger follicles than in control animals, and they contained larger numbers of apoptotic cells. *Figure* 3.9 (A) Control animal; (C) LPS treated animal control. The latter were also numerous in the red pulp which otherwise exhibited a generally low cellularity and often several variably sized aggregates of neutrophils. After APAP treatment, spleens showed a large number of apoptotic lymphocytes, both in red pulp and follicles. However, there was no evidence of substantial cell loss in the red pulp and follicles generally appeared small (no evidence of activation) (*Figure* 3.10 (C)).

The thymus of control animals did not show any evidence of involution and only scattered apoptotic lymphocytes (*Figure* 3.10A). The latter were numerous in the thymus of LPS and APAP treated animals, in particular in the cortex (*Figure* 3.10 B&C).

The bone marrow was normocellular in all animals, but in LPS and APAP treated animals, a few apoptotic cells were observed.

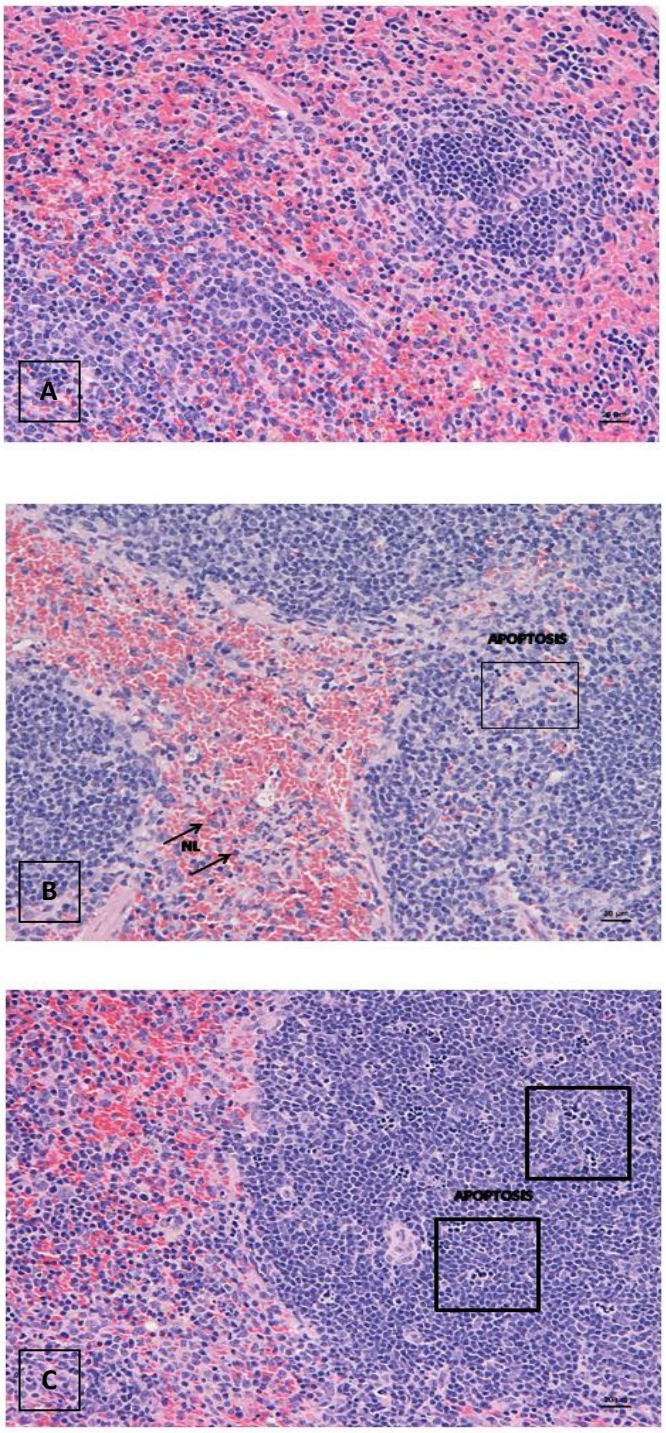

Figure 3.9: C57BL/6 mice at 6 hours post intraperitoneal inoculation. Spleen. (A) Inoculation with saline (control animal; case No 12L-1405). Follicles are small and do not exhibit numerous apoptotic cells. The red pulp exhibits high cellularity. (B) Inoculation with LPS (25mg/kg) (Case No -12L-1394). Moderately sized follicles with several apoptotic cells. The red pulp exhibits a low cellularity and numerous apoptotic cells as well as some neutrophil aggregates. (C) Inoculation with APAP (350mg/kg) (case No 12L-1411). Follicles are relatively small, but exhibit numerous apoptotic cells. The latter are also seen in the cell rich red pulp . HE stain.

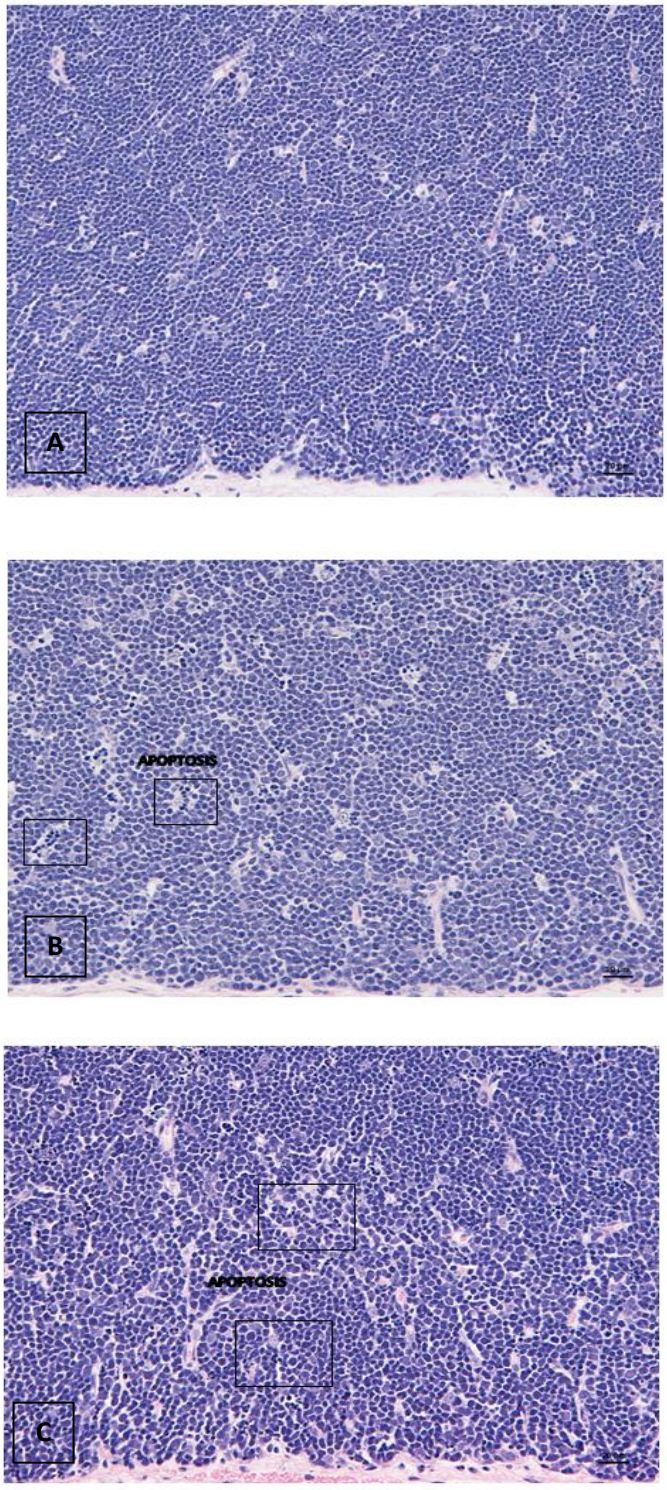

Figure 3.10: C57BL/6 mice at 6 hours post intraperitoneal inoculation. Thymus. (A) Inoculation with saline (control animal; case No 12L-1405). The cortex exhibits occasional individual apoptotic lymphocytes. (B) Inoculation with LPS (25mg/kg) (case No. 12L-1393). Numerous disseminated apoptotic lymphocytes are seen, in particular within the cortex. (C) Inoculation with APAP (350mg/kg) (case No. 12L-1411).Numerous apoptotic cells are seen, in particular within the cortex. HE stain.

2.3.4 Summary

The major differences between the two models of murine sepsis (LPS versus faecal peritoneal inoculation) are summarised below:

- After faecal peritoneal inoculation, animals develop an acute suppurative peritonitis. This is not seen after LPS treatment.
- Both models showed evidence of systemic neutrophil recruitment into tissues. This was more intense after LPS treatment.
- Faecal peritoneal inoculation resulted in more substantial evidence of neutrophil recruitment into fat and skeletal muscle.

The histopathological analysis of further tissues from LPS treated animals confirmed the lungs as a significant tissue of neutrophil recruitment and thereby a good indicator of the systemic inflammatory response in mice, with numerous neutrophils in the vessel lumen and rolling along the activated endothelium.

Both LPS and APAP treated animals showed a significant increase in apoptotic lymphocytes in the spleen and thymus, a finding known to be associated with rises in TNF-α (particularly in an LPS model of sepsis).

2.4 Discussion

Remick et al[8, 47] compared the cytokine profile in the murine LPS model of sepsis with that of the CLP model and found that the CLP model exhibited a profile that is more similar to the one in human sepsis than the LPS model (gradual rising and sustained cytokine response) [8]. *Gonnert et al*[48] found a similar response in their faecal inoculation model. The analysis of tissues from the faecal inoculation model and the LPS model in the present study showed that the differences in the cytokine pattern are not reflected by significant differences in the acute histological changes in key tissues. In both models, treated animals displayed acute changes consistent with an early systemic inflammatory response. This was more pronounced in LPS treated mice, which showed more intense features of neutrophil recruitment into tissues such as the liver and in particular the lungs. This is most likely due to the greater increase of TNF-α and other cytokines (which are known to cause neutrophil aggregation in the liver vasculature [101]) seen in the LPS model [8]. This similarity indicates that despite differences in cytokine increases and profiles in both models, activation of neutrophils and endothelial cells and thereby recruitment of neutrophils into tissues isn't as pronounced.

Parenchymal cell death was not seen in any organ (heart, lungs, liver, kidneys, brain) in either model and it is known that TNF-α in the LPS model peaks beyond 6 hours [8] and in the faecal model levels normalise before 5 hours[48], suggesting levels are never high enough to induce cell death, but can merely initiate the systemic inflammation. *Gonnert et al*[48] noted that significant adherence and rolling of neutrophils is only seen from 15 hours onwards, at which time detectable levels of cell death were not observed either. Principle histopathological changes are similar (i.e. neutrophilia and tissue recruitment) so the dichotomy between models must exist beyond 6 hours, i.e. acute changes are similar. The use of APAP mice as "positive controls" allowed for methodological anomalies with dosing to be ruled out as a contributing factor. APAP is known to cause significant release of TNF-α and IL-1 from [100] which contribute to hepatocyte necrosis along with direct drug toxicity[101]. However negligible neutrophil recruitment observed in this study demonstrated that hepatocyte necrosis in this study was a direct result of drug toxicity as opposed to immune mediated damage.

In the context of human sepsis classification, LPS mice did not meet the ACCP/SCCM [1] defined sepsis criteria:

"Whenever SIRS is the result of a confirmed infectious process it is sepsis"

LPS mice showed no evidence of peritonitis from injection of LPS, whereas faecal inoculated mice resulted in an acute suppurative peritonitis induced by the bacteria from the inoculum. This shows that the latter model reflects the pathogenesis of bacterial sepsis of any origin much better than the LPS model which can be considered as a model of "end stage sepsis" when substantial generalised endotoxaemia has occurred.

2.4.1 Neutrophil recruitment into tissues

Neutrophils are known to be the common first leukocyte to increase in number and infiltrate tissues during the inflammatory process induced by bacteria[33]. They migrate into tissues through the process of chemotaxis, attracted by chemokines such as IL-8. Chemotaxis is directed movement of cells up a chemical a gradient [105]. The classical emigration cascade comprises the elements of capture, rolling, activation and adhesion[83]. Neutrophil capture and rolling can be mediated by endothelial cells through P-selectin binding PSGL-1, activation may occur through a chemokine (i.e. IL-8) and adhesion requires intercellular adhesion molecule-1 (ICAM-1), binding β2 integrins on the neutrophil [98]. Rapid cessation of neutrophil emigration which occurs remarkably early in the evolution of the acute inflammatory response represents one of the earliest events in the resolution process [107]. However, in sepsis models and particularly the LPS model, neutrophils often back up blood vessels and over recruitment and impaired neutrophil apoptosis leads to their persistence in tissues. Flooding the blood with cytokines and chemoattractants in sepsis causes inappropriate neutrophil activation associated with a paradoxical inability to recruit neutrophils to the site of infection [98]. The recruitment and beginnings of infiltration of neutrophils into the tissues in both models was at 6 hours, reflecting the acute nature of the inflammatory response.

It could be suggested that the differences in both models used were reflected by a difference in endothelial activation. The faecal model had a tendency to show greater numbers of neutrophils in other secondary tissues such as adipose tissue and skeletal muscle. Using gene knock-out mice, *Andonegui et al*[108] were able to show that

endothelium-derived TLR 4 was more important than leukocyte derived TLR 4 in LPS-induced neutrophil sequestration into the lungs. Low doses of LPS (0.5 mg/kg) induced a dramatic increase in neutrophil sequestration into the lungs of Leukocyte TLR 4–/– mice over the first 4 hours and by contrast, endothelial TLR 4–/– mice showed very little increase in neutrophil sequestration in the lungs, suggesting that endothelial rather than leukocyte TLR 4 was important and further highlighting the significant role of endothelial activation in inflammation and sepsis [108]. Considering the histopathological results of the present study, perhaps the key to understanding the difference between the models lies in the level, extent and tissue pattern of endothelial activation in each, where the more gradual rising sustained level of cytokines seen by *Gonnert et al*[48], favours a wider, more diffuse systemic response and recruitment of leukocytes into tissues.

2.4.2 Lymphoid organs and inflammation

Lymphoid organs are known to be vulnerable to apoptosis in human patients with sepsis[88]. We observed significant lymphocyte apoptosis in spleen and thymus of LPS and APAP treated mice. This finding is known to be associated with rises in TNF-α (particularly in the LPS model of sepsis), however these changes would only be expected at levels of TNF-α that would also affect the liver and other organs, where no significant cell death was detected. *Zhang et al* [109] demonstrated that apoptosis in the thymus of mice injected with LPS was mainly mediated by adrenal hormones, since adrenalectomy completely inhibited the appearance of apoptosis in mice. In contrast, the use of anti-TNF-α antibody only partially inhibited the lymphocyte apoptosis, indicating that although contributing it is not the significant cause of apoptosis in this species. Similarly, in the LPS and APAP treated animals in the present experiments, the apparent lack of parenchymal organ damage would suggest that TNF-α levels were not high enough to cause the latter damage, but probably contribute towards the apoptosis seen in spleen and thymus. Nonetheless, it is largely other mechanisms (such as adrenal hormones) that are governing it. TNF-α independent pathways of thymic apoptosis have been previously described in mice undergoing CLP [110]. Furthermore, apoptosis in the spleen has been shown to be an important pathogenic step in HMGB1 sepsis related lethality[111]. The LPS and APAP treated mice had similar levels of lymphoid apoptosis, and in the case of the APAP treated animals alongside toxic liver damage; accordingly, it is debatable as to

whether or not TNF-α is inducing apoptosis on its own or whether similar adrenal mechanisms are triggered after APAP treatment. Without definitive quantification of serum cytokine levels and assessment of adrenal hormones, this cannot be concluded.

Ayala et al[104] demonstrated a differential induction of apoptosis in polymicrobial sepsis. The thymus was often affected a lot earlier than the bone marrow (detectable changes were at 4 hours and 24 hours respectively). It was concluded that different from thymic cells, cells in the bone marrow are not affected directly by glucocorticoids or TNF-α, to the same extent, released during sepsis. This is consistent with our results where the degree of apoptosis in thymus and spleen was far higher than that in the bone marrow.

2.4.3 APAP and drug toxicity

The initial morphological changes in the liver following APAP overdose include glycogen loss and vacuolisation of centrilobular hepatocytes, and single-cell necrosis of hepatocytes, pyknotic nuclei and eosinophilic cytoplasm [96]. In the present study, the presence of hepatocyte necrosis was detected at 6 hours. It has been shown that TNF-α and IL-l play an important role in modulating APAP induced liver injury. Altering the actions of either of these cytokines by increasing or decreasing their levels by specific modulators can suppress or enhance the severity of these effects[100]. This highlights that, like the LPS model of sepsis, TNF-α plays a crucial role in mediating organ damage.

2.4.4 Summary & further research

In *chapter 1* the important mechanisms and cell signalling pathways behind the inflammatory response were studied. The results demonstrated that there was a key species variation in response to LPS. In this chapter, comparative analysis of two well characterised murine models of sepsis (LPS and faecal peritoneal inoculation) has shown further that difficulty in recapitulating a similar environment of human sepsis in rodents widens the gap that the translational bridge must cross. This makes it difficult to accurately assess whether or not treatments developed *in vivo* will be efficacious in humans. Both models showed a similar level of changes consistent with an acute systemic inflammatory response at 6 hours post treatment, which suggests that despite the known differences in cytokine profiles between these two models, the dichotomy must exist and represent themselves later in histological changes. The initiating steps are fairly similar (i.e. neutrophilia and recruitment into

tissues), but it may be the maintenance and resolution of these events later on in the course of the disease that differ. The faecal inoculation model is known to cause persistent inflammatory changes weeks later from the insult (persistent neutrophil & macrophage infiltration along with abnormal lymphocytes[48]), whereas similar changes are not seen with LPS dosing.

This chapter also highlighted the importance of cellular necrosis and apoptosis in the septic process. In the general introduction a novel biomarker of this (caspase cleaved and uncleaved CK18) was identified and results and discussion in this chapter have identified its potential application in a clinical setting. Similarly HMGB1 (a late pro-inflammatory cytokine), would indicate a prolonged inflammatory process and in combination with CK18 may give an invaluable insight into the internal environment and status of damage within this group of patients.

Chapter 4:

Analysis of novel biomarkers of sepsis in human serum

Contents

4. Analysis of novel biomarkers of sepsis in human serum

4.1 Introduction

Translational medicine is the progression of turning appropriate discoveries about processes and physiology, into therapeutic interventions that can treat patients effectively. Solid evidence has to support clinical decision making and treatments. *Chapter 2 & 3* have looked at the benefits and drawbacks of *in vitro* and *in vivo* techniques in the study of inflammation and sepsis, and highlighted the significance of species variation in response to inflammatory insults, early histological changes associated with sepsis and identified niches for the use of potential novel biomarkers in clinical medicine.

HMGB1 a late pro-inflammatory cytokine and product of NFκB signalling It is an ubiquitously expressed protein that has recently been discovered as a marker of inflammation in humans and an important therapeutic target for sepsis in endotoxaemic mice [34] (see *General introduction 1.2.4*). CK18 has also been identified as a novel way of measuring apoptosis (caspase cleaved CK18) and necrosis (full length CK18), known important processes in sepsis and indicators of severity of illness [88] (see *section 1.4*).These novel biomarkers will be investigated to see whether or not they are useful indicators of outcome and prognosis in patients with sepsis admitted to ICU. Furthermore pre-study analysis has highlighted their use in another sub-group of patients.

4.1.1 Liver disease and sepsis

Liver disease is a significant problem in the UK; with non-relenting high mortality rates and an increasing association with increasing age [112] . Although it has a varied aetiology the majority of patients develop it secondary to alcohol and this is also a major contributing factor to the worsening progression of other liver diseases (i.e. Hepatitis C) [113]. Their presentation to the ICU is varied and provides physicians and anaesthetists with questionable problems about management, and difficulties in prognosis. Alcoholic liver disease (ALD) in particular is showing an increase in admission and mortality[114] . Not only does liver disease as a primary presentation cause these problems, but also when it presents as an underlying process in patients with other primary complaints i.e. sepsis [115].

The pathogenesis of ALD has been attributed to altered Kupffer cell activity, oxidative stress and innate immune responses caused by gut derived endotoxin in response to ethanol consumption[116]. With this better understanding treatments for it are becoming more efficacious and the emphasis should now lie on the earlier detection and better understanding of liver damage, in order to prevent a critical admission to the ICU with decompensated failure.

In the review by *Berry et al* [117], they identified that the most worrying complications of ALD that result in ICU admission are "variceal bleeding", "hepatorenal syndrome" and "Acute on chronic liver failure". However, although mortality has somewhat decreased with these conditions, with the instigation of newer more evidence-based treatments, mortality still remains high [118] . *Berry et al* [117] conclude that better understanding and identification is needed in order to be able to treat these patients as survival is not improving

4.1.2 Pre-study retrospective analysis

An audit was carried out at the Royal Liverpool University Hospital to assess the incidence of different aetiologies of liver disease in patients admitted to the critical care unit. Patients admitted between January 2008 and July 2011, were included and various admission parameters for each patient were recorded including haematological, electrolyte, liver function and clotting values. These were recorded along with APACHE II scores, length of stay, and evidence of diagnostic imaging (i.e. ultrasound), ventilator and organ support and overall hospital mortality.

4.1.4 Results

ALD patients were found to have lower blood sodium levels (Mean 135.56; CI 133.41-137.71. P = 0.004) and were hypocalcaemic (1.93; CI 1.88-1.99), and had more severe derangements in various liver function tests (P < 0.001) and clotting studies (P < 0.001), see *table 4.1* and *4.2* below. ALD patients also had significantly longer ITU stays (P <0.001) and higher mortality rates (45.45% ALD versus 13.2% NALD) which is in keeping with the literature [118].

Liver function test		Alcoholic liver disease (N=66)		Non-Alcoholic liver disease (N=53)		
	Normal value	Mean	Confidence interval	Mean	Confidence interval	P value
GGT	<75iu/L	127.12	92.92; 161.32	67.36	32.64; 102.07	<0.001
ALP	30-150iu/L	101.52	86.7; 116.33	75.21	59.28; 91.13	=0.001
ALT	3-35iu/L	82.33	44.88; 119.78	197.6	17.06; 378.15	=0.184
Albumin	36-52 g/L	82.17	58.55; 105.78	22.69	9.3; 36.09	<0.001
Bilirubin	3-17mmol/L	24.39	22.55; 26.24	33.74	31.75; 35.72	<0.001

Table 4.1: Table showing the admitting Liver function tests (LFTs) of patients admitted to ICU with a primary liver complaint. Patients were divided into two groups depending on whether or not that had presence of ALD.

Clotting studies		Alcoholic liver disease (N=66)	Non-Alcoholic liver disease (N=53)		
Confidence interval	Mean	Confidence interval	Mean	Confidence interval	P value
PT	17.22	14.23; 20.21	21.89	19.76; 24.03	<0.001
APTT	34.54	29.23; 39.86	43.74	40.12; 47.36	<0.001
INR	2.22	0.89; 1.26	1.35	1.21; 1.49	<0.001
Fibrinogen	2.43	2.18; 2.68	1.74	1.44; 2.05	<0.001
Platelets	1.08	150.19; 193.8	103.83	87.66 120.01	<0.001

Table 4.2: Table showing the admitting Clotting studies (LFTs) of patients admitted to ICU with a primary liver complaint. Patients were divided into two groups depending on whether or not that had presence of ALD.

4.1.3 Receiver operated characteristic curve analysis

This analysis allows a test to be evaluated for its usefulness in distinguishing between positive and negative results. It uses the sensitivity and specificity of an investigation in order to generate a curve, where the area underneath represents the efficacy or discriminatory value of that test [119]. Receiver operated curve (ROC) analysis revealed that current biochemical markers (ALT, PT, GGT, Albumin) are not sensitive and specific enough in detecting failure associated with ALD, when using fatality as the measured outcome. Pro-thrombin time yielded the best area under the curve with 80.4% in ALD versus 71.7% in NALD, see *figure 4.1 A & B.* None of the markers was discriminatory for determining type of liver damage.

4.1.4 Conclusions of the pre-study analysis

The results suggest that currently used markers of liver disease are neither sensitive nor specific enough, particularly in critically ill patients suffering from failure secondary to ALD. More research is needed to develop novel biomarkers to better prognosticate outcome. Aetiology of acute-on-chronic liver failure plays a major role in determining outcome, and subgroups of liver patients should be analysed individually.

4.1.5 Applications of HMGB1 and CK18

HMGB1 and CK18 have shown to be serum based markers released depending on the type of damage (necrotic versus apoptotic) and differ in acute liver damage of different origin[38, 39, 55]. ALD has been shown to have two main routes of liver failure either decomposition or acute on chronic failure (AoCF) i.e. patients with ALD who develop a sepsis[117]. Comparing these patients with patients with no ALD and sepsis alone will give an understanding about the mechanistic differences in the pathologies of liver damage in these diseases (i.e. hepatocyte damage) and whether or not serum biomarkers (HMGB1 and CK18) can be used in a novel way to represent these differences. Inflammation is an important process in the development of cirrhosis and sepsis[11, 88, 116], so serum biomarker HMGB1 should be found in the serum of these patients. Necrosis and apoptosis are important cellular processes that have been shown to be significant in sepsis both in human[88, 91] and animal models (see *chapter 3*), indicating that cleaved and uncleaved CK18 could have an application along with HMGB1 in this group of patients.

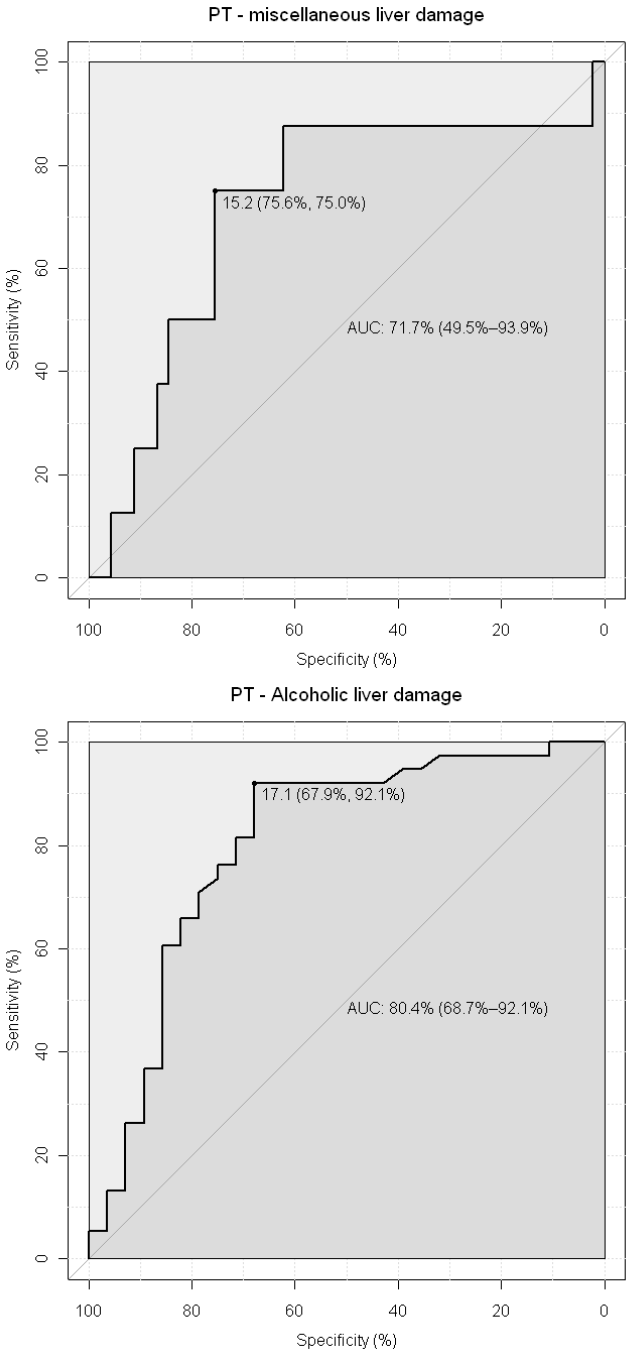

Figure 4.1: graphs showing receiver operated characteristic (ROC) curve analysis for admitting pro-thrombin time in patients admitted to ICU with a primary liver complaint and using fatality as outcome. Patients were divided into groups depending on whether or not they had ALD (bottom B) or no ALD (top A)

4.1.6 Aims of the chapter

Pre-study analysis has shown that there is a need for novel biomarkers in a defined group of patients in ICU. These biomarkers could potentially help better discriminate between types of liver damage and sepsis severity in these patients and help better prognosticate and predict outcome. The study has also shown that no individual biomarker is completely sensitive or specific enough, and that perhaps the way forward is the development of biomarker combinations, or adding new biomarkers to ones that are already widely used. The hypothesis is stated below:

"Serum levels of sepsis biomarkers HMGB1 and CK18 vary with the underlying liver condition: Serum HMGB-1 and CK18 levels differ in patients with sepsis depending on their underlying liver condition. Two groups of critically ill patients will be compared: 1. Patients with sepsis and no history of liver disease 2. Patients with sepsis and known liver disease. Results will be compared to healthy volunteers (controls) and patients admitted to ICU patients without sepsis or underlying liver disease. ."

4.2 Materials and Methods

4.2.1 Materials

HMGB1 ELISA plates for the detection of the protein in human serum were obtained from Innovation beyond limits (IBL) international (ST51011). M30 Apoptosense® ELISA for the detection of epithelial apoptosis and caspase cleaved K18 was bought from PEVIVA along with the M65 Epideath® ELISA for the detection of epithelial cell death and full length K18. The revelation® software and MRX plate reader where from Dynex technologies. Patient samples where kindly donated by Professor Cheng-Hock Toh. The Department of clinical infection, microbiology and immunology, University of Liverpool.

4.2.3 Statistics used in the analysis of results

Statistics and figures were done using StatsDirect® and Microsoft excel®.

For analysis of the differences of serum biomarkers (HMGB1 and cleaved and uncleaved CK18) between patients admitted to ICU and healthy controls, a Mann-Whitney U test was used. This test was also used to test for differences between serum concentrations of HMGB1 and CK18 between defined patient groups. The data was non-normally distributed, indicating the need for use of a non-parametric test. Furthermore, the Mann-Whitney U test is useful for assessing whether one of two samples of independent observations tends to have larger values than the other (i.e. whether one group of patients has a higher serum concentration of serum biomarker than the other). Values of <0.05 are considered statistically significant.

For comparison of cleaved and uncleaved CK18 with a patient group the Kruskall-Wallis test was used as again the data was non-normally distributed but coming from the same sample. The test compares the medians of two or more samples to determine if the samples have come from different populations.

4.2.3 Patient recruitment and basic characteristics

Patient serum was recruited from patients admitted to ICU between 2008-2012. All patients gave consent and collection was in line with the Local and National research ethics (L/NREC) guidelines. Serum will be analysed from patients in each of the following groups:

Patients with;

- Alcoholic liver disease
- Sepsis with no liver dysfunction
- Sepsis with liver dysfunction
- Alcoholic liver disease with co-morbid sepsis

Patients were included and excluded based on the following criteria:

Inclusion Criteria:

- Patients that fell into one of the specified groups identified above and who were admitted to the intensive care unit at the Royal Liverpool University Hospital.
- Patients with Sepsis who met the SIRS criteria set out by the ACCP/SCCM[1]
- Patients with Alcoholic liver disease who had significantly deranged liver function and had a Child-Pugh score of A or more (Child-Pugh scoring[120])
- Patients with sepsis induced liver dysfunction who met the SIRS criteria and who had significant deranged liver function.
- Patients with Alcoholic liver disease (Child-Pugh of A or more) who had evidence of sepsis and met the SIRS criteria. An example of this type of patient, would be an alcoholic liver disease patient (liver function twice that of the normal value) admitted to ICU with spontaneous bacterial peritonitis and decompensated liver failure.

Exclusion criteria

- Patients under the age of 18 or over the age of 90.
- Patients who had co-morbid HIV/ hepatitis A, B, C or other significant liver/system chronic infectious states.
- Patients who had Liver failure secondary to causes other than sepsis or alcohol excess.

The serum was initially collected for another study but patients had given consent for serum to be kept and allowed for use in further research. It was stored at -80°C and thawed completely before being aliquoted for each experiment. The number of days used in these analysis was three (1=admitting, 2=second & 3=discharge or last samples taken). Basic patient characteristics are summarised below (*table 4.3*). Patients where matched based on age, sex, APACHE II and their medical records, so that patients in each group where comparable and to remove as much as possible confounding variables. All the ALD patients had a child-pugh score of (B-C). The scoring system is given in table 12.

Patient group	N	Age mean & (range)	Sex ratio (M:F)	APACE II mean & (range)	Length of stay mean & (range)	ICU mortality %
ALD	4	49.5 (38-62)	1:1	17.25 (8-24)	16 (2-20)	25%
ALD & Sepsis	3	60 (60-62)	2:1	15.5 (11-20)	17 (8-17)	66%
Sepsis	4	58 (41-85)	3:1	21 (17-32)	4.5 (3-4)	50%
No ALD no Sepsis	4	58 (52-61)	1:1	21.3(9-22)	3 (2-4)	0%
Healthy controls	5	48.3 (40-59)	2:3	N/A	N/A	N/A

Table 4.3: Basic characteristics of patients in defined groups and healthy controls.

Score	**1 points**	**2 points**	**3 points**
bilirubin (micromol/l)	<34	34-50	>50
albumin (g/l)	>35	28-35	<28
PT (seconds prolonged)	<4	4-6	>6
encephalopathy	none	mild	marked
Ascites	none	mild	marked

Table 4.4: Child-Pugh scoring system for cirrhosis severity[120]

Score:

- 5-6 points = Grade A
- 7-9 points = Grade B
- 10-15 points = Grade C

4.2.4 Enzyme linked immunosorbant assay (ELISA) for the quantitative determination of total HMGB1 in patient serum

The test procedure provided with the plate and reagents (IBL international) was followed. 100µl of dilutent buffer was pipetted into each well of the plate using a multichannel pipette. Then 10µl of each serum sample, standard or positive control was put into respective wells and the plate was gently agitated for 30 seconds. The plate was then covered and incubated overnight at 37°C. The plate was then washed 5 times in diluted wash buffer and excess solution was removed by tapping the plate on the lab bench. The plate was then incubated for 2 hours at 25°C with 100µl of enzyme conjugate in each well. Afterwards the plate was washed again 5 times and tapped on the lab bench to remove excess solution. 100µl of Enzyme conjugate was pipetted into each freshly washed and dried well and covered in foil and incubated at 25°C for 2 hours. The wash steps where repeated like before. 100µl of colour solution was pipette into each well and incubated at room temperature in the dark for 30 minutes before 100µl of stop solution was added. The plate was left for 5 minutes before being read on a plate reader using the Revelation® software using a preset program.

4.2.5 M30 Apoptosense® ELISA for the quantitative determination of cleaved CK-18 in patient serum

The test procedure provided with the plate and reagents (PEVIVA) was followed and is summarised in *figure 4.2*.

4.2.6 M65 Epideath® ELISA for the quantitative determination of full length CK-18 in patient serum

The test procedure provided with the plate and reagents (PEVIVA) was followed and is summarised in *figure 4.3*.

4.2.7 Optimization

Both ELISAs where initially carried out using neat samples. However, many of the concentrations measured fell off the standard curve as they were too high. A 1:10 dilution was done by mixing 5µl of sample with 45µl of standard A (which contained no protein) in a freshly labelled Eppendorf tube. Samples were then vortexed and then 25µl was loaded onto each well.

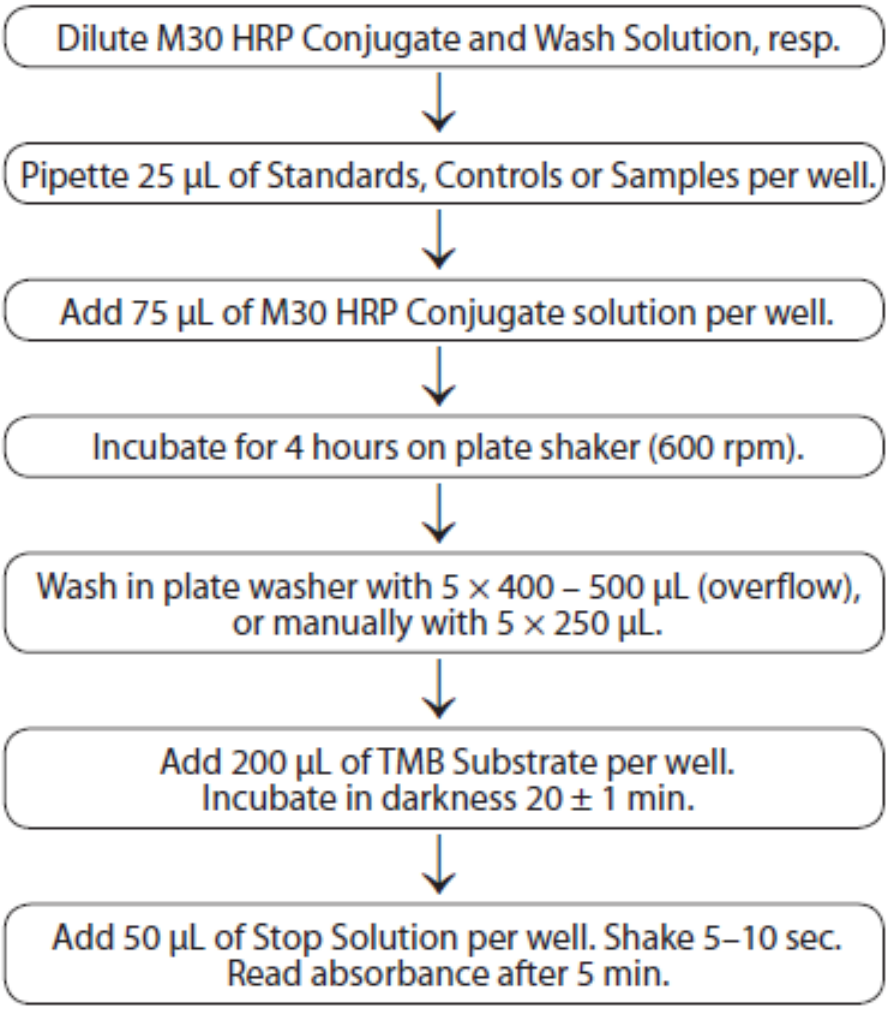

Figure 4.2: Flowchart taken from protocol provided by PEVIVA summarising the protocol for the M30 Apoptosense® ELISA for the detection of caspase cleaved CK18.

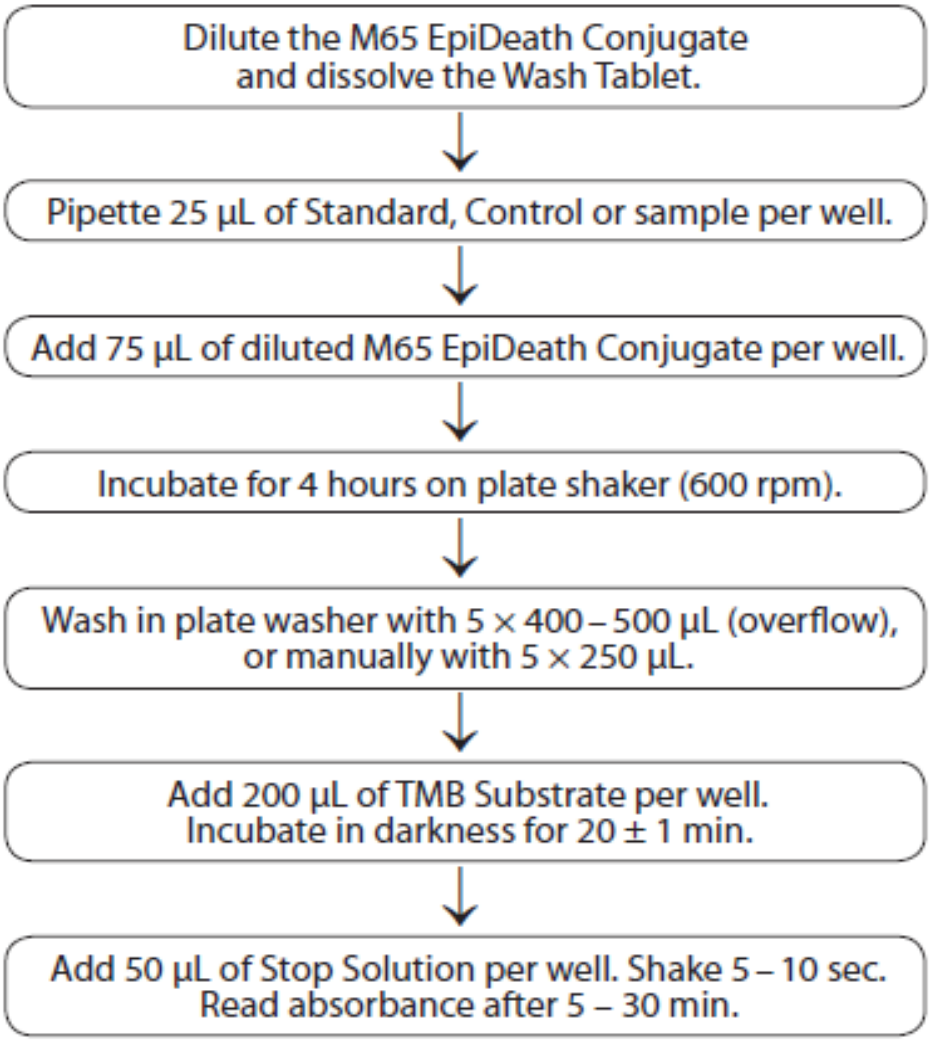

Figure 4.3: Flowchart taken from protocol provided by PEVIVA summarising the protocol for the M65 Epideath® ELISA for the detection of full length CK18.

4.3 Results

4.3.1 Serum total HMGB1 and CK-18 cleaved and uncleaved in the serum of healthy controls

Five healthy controls (characteristics defined in *table 4.3*) were recruited and a single serum sample was taken in order to detect serum total HMGB1 and cleaved and uncleaved CK18. *Table 4.5-4.7* provides this information along with the ICU admitting day levels of the defined patient groups. Mann Whitney U testing showed that there was a significant difference ($p<0.05$) between healthy controls and patients admitted to ICU.

	Day	N	Range	Mean	SD	Mann Whitney U test (compared with healthy controls)
Healthy controls	1	4	0.8-2.2	1.576	0.59	
ALD	1	4	2.91-15.33	7.14	4.63	0.0286
ALD & Sepsis	1	3	10.64-11.84	11.17	0.61	0.0286
Sepsis	1	4	6.79-33.27	17.60	4.21	0.0286
No ALD no sepsis	1	4	7.27-21.99	13.70	6.12	0.0286

Table 4.5: Serum total HMGB1 (ng/ml) in healthy controls compared with ICU admitting day of defined patients groups. Mann Whitney U test was done in order to look for statistical differences. A levels <0.05 was significant. Means are given with the range, standard deviation (SD) and P value. Statistical differences were detected between all patient groups and healthy controls.

	Day	N	Range	Mean	SD	Mann Whitney U test (compared with healthy controls)
Healthy controls	1	4	332-427	384.4	37.86	
ALD	1	4	849.72-2316.63	1538.01	665.58	0.0159
ALD & Sepsis	1	3	911.07-1305.81	781.883	599.0604	0.5714
Sepsis	1	4	920.19-1468.01	1199.78	249.065	0.0159
No ALD no sepsis	1	4	1210.5-2712.7	1664.705	712.606	0.0159

Table 4.6: serum cleaved CK18 (U/L) in healthy controls compared with ICU admitting day of defined patients groups. Mann Whitney U test was done in order to look for statistical differences. A levels <0.05 was significant. Means are given with the range, standard deviation (SD) and P value. Statistical differences were detected between all patient groups and healthy controls.

	Day	N	Range	Mean	SD	Mann Whitney U test (compared with healthy controls)
Healthy controls	1	4	76-289	154	90.00	
ALD	1	4	1567.18-6910.37	3111.224	1990.263	0.043
ALD & Sepsis	1	3	911.07-1305.81	1850.092	524.5204	0.043
Sepsis	1	4	896.9-2382.84-	1347.121	667.1293	0.043
No ALD no sepsis	1	4	289.871-8097.00	2687.94	268.7	0.043

Table 4.7: serum uncleaved CK18 (U/L) in healthy controls compared with ICU admitting day of defined patients groups. Mann Whitney U test was done in order to look for statistical differences. A levels <0.05 was significant. Means are given with the range, standard deviation (SD) and P value. Statistical differences were detected between all patient groups and healthy controls.

4.3.2 Serum total HMGB1 (ng/ml) and CK-18 (U/L) cleaved and uncleaved in the serum of patients with ALD

Serum total HMGB1 (ng/ml) was measure in patients with ALD and no sepsis (N=4) over their stay in ICU. Samples included admitting (1), second (2) and last day (3). Patients had a significantly elevated (p=0.0286) total HMGB1 on their admitting day (Mean 7.14 ng/ml SD 4.63) compared with healthy controls. An elevation of HMGB1 between day 1 and 2 was associated with worsening liver function tests (LFTs) and increase in serum urea and creatinine on those days. A rise in serum total HMGB1 between days 2 to 3 were associated with a fatal outcome in one of the patients (4.503ng/ml to 9.478ng/ml). However, a higher concentration on any other day did not indicate a poorer outcome as one patient almost doubled between days 1 to 2, but had a good outcome (15.33ng/ml to 29. 865ng/ml). See *Figure 4.4 (A)* for a line graph of the mean serum total HMGB1 values in those days in patients with decompensated ALD.

The same samples where measured for serum cleaved and uncleaved CK18 (U/L). Patients showed a significant increase on admitting values for cleaved (Mean 1538.01 U/L SD 665.58) and uncleaved (Mean 3111.224 U/L SD 1990.263) CK18 (p=0.0159 & 0.043 respectively) compared to healthy controls. Patients in this group showed visibly higher levels of uncleaved CK18 compared to cleaved CK18 (*figure 4.4* (B)), indicating higher levels of necrosis. However, these differences were not significant *(*see *table 4.8*). Three out of the four patients were admitted with variceal haemorrhage while the fourth was admitted with worsening liver function tests and alcohol withdraw.

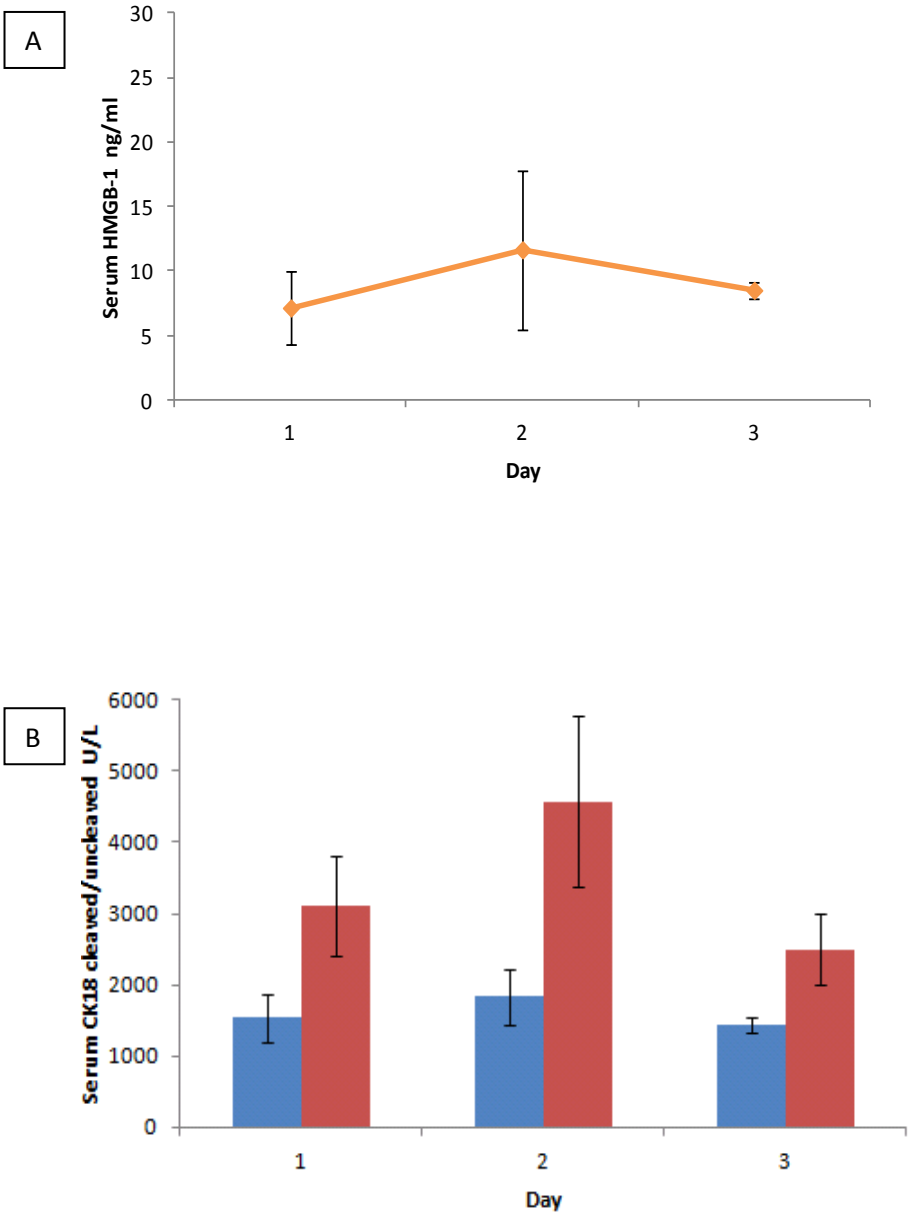

Figure 4.4: (A) Line graph showing the mean (N=4) serum total HMGB1 (ng/ml) in the admitting, second and discharge day of patients with decompensated alcoholic liver disease (ALD). Means are plotted with Standard error of the mean (SEM). Trend demonstrates an increase in serum total HMGB1 between days 1 and 2 and a fall on discharge day. X axis is the serum concentration of HMGB1 and Y axis is Day. (B) Bar chart showing the Mean (N=4) serum cleaved/uncleaved CK18 (U/L) in the admitting, second and last day of patients with decompensated ALD. Means are plotted with SEM. X axis is serum concentration of cleaved/uncleaved CK18 and Y axis day. Blue = cleaved CK18 & Red= uncleaved CK18. Graph shows a substantial difference between cleaved and uncleaved CK18 in this patient group and the general trend is a rise between days 1 and 2, with a fall on last day.

	Day	N	CK18 (U/L)	Range	Mean	SD	Kruskall Wallis for cleaved versus uncleaved CK18 (U/L)
Decompensated ALD (N=4)	1	4	Cleaved	849.72-2316.63	1538.008	665.5797	0.0894
			Uncleaved	1567.18-6910.37	3111.224	1990.263	
	2	4	Cleaved	920.67-2016.50	1833.43	795.0031	0.0894
			Uncleaved	10701.627-11610.94	4577.693	3384.91	
	3	3	Cleaved	1295.16-1674.18	1437.41	206.433	0.4386
			Uncleaved	981.686-4100.74	2501.34	1210.182	

Table 4.8: Serum cleaved and uncleaved CK18 (U/L) in the ICU admitting, second and last days of patients with decompensated ALD. Mean values are given with the range and standard deviation (SD). Kuskall Wallis test was used to test for a significant difference between levels of cleaved and uncleaved in CK18 in each individual patient. There was no significant difference detected between values.

4.3.3 Serum total HMGB1 (ng/ml) and CK-18 (U/L) cleaved and uncleaved in the serum of patients with ALD & sepsis

Serum total HMGB1 (ng/ml) was measured in patients with ALD and sepsis (N=3) over their stay in ICU. Samples included admitting (1), second (2) and last day (3). Patients had a significant elevated (p=0.0286) total HMGB1 on their admitting day (Mean 11.14ng/ml SD 0.61) compared with healthy controls. An elevation of HMGB1 between day 1 and 2 was associated with worsening liver function tests (LFTs) and increase in serum urea and creatinine on those days, although the elevation of HMGB1 did not reflect the magnitude of increase in these routine chemistries (LFTS and serum urea and creatinine doubled while there was only a mild increase in total HMGB1). A fall in serum total HMGB1 between days 2 and 3 was associated with a poorer outcome in two patients (i.e. 7.836ng/ml to 6.1ng/ml and 15.181ng/ml to 10.442ng/ml). See *Figure 4.5 (A)* for a line graph of the mean HMGB1 in those days in patients with ALD and sepsis.

The same samples were measured for serum cleaved and uncleaved CK18. Patients showed a visible increases on admitting values for cleaved (Mean 781.883 U/L SD 599.0604) and uncleaved (Mean 1850.092 U/L SD 524.5204) CK18 (p=0.5714 & 0.043 respectively) compared to healthy controls. Patients in this group showed visibly higher levels of uncleaved CK18 compared to cleaved CK18 (*figure 4.5* (B)), indicating higher levels of necrosis. The difference is only significant on the admitting day (p=0.0389) (*see table 4.9*).

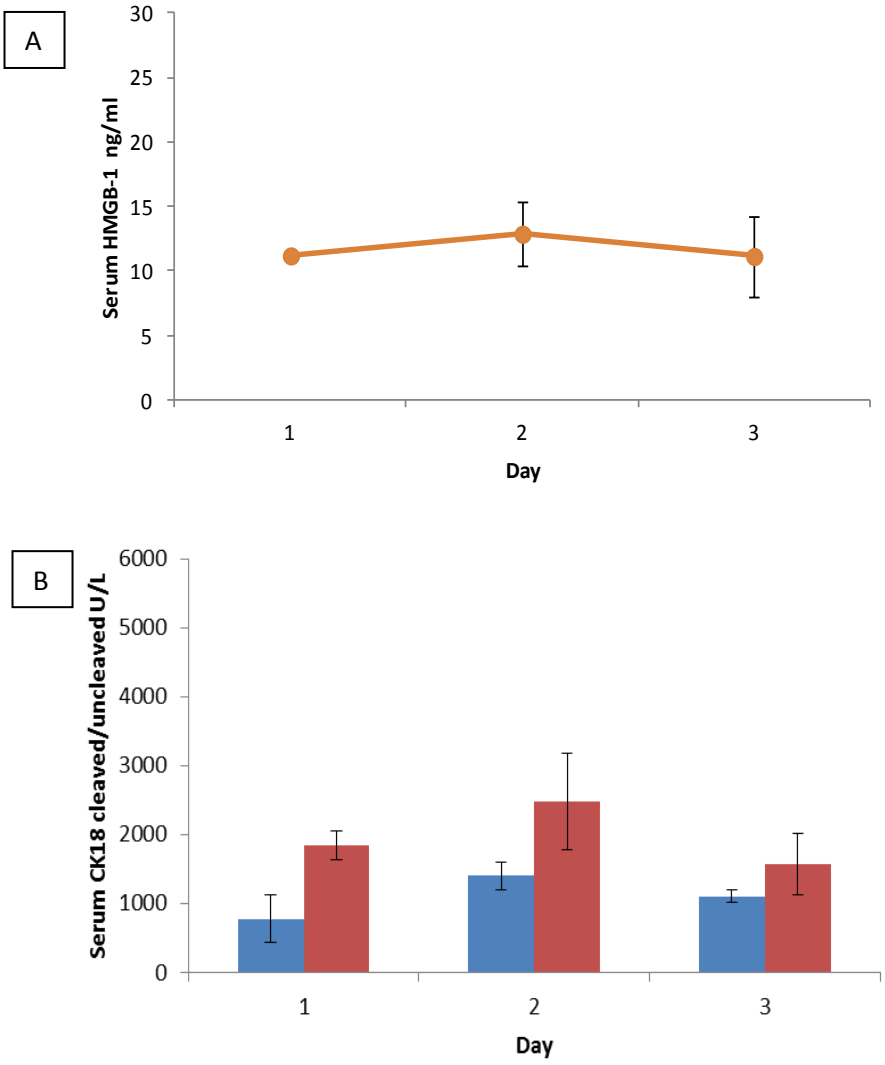

Figure 4.5: (A) Line graph showing the mean (N=3) Serum total HMGB1 (ng/ml) in the admitting, second and last days of patients with ALD & sepsis. Means are plotted with Standard error of the mean (SEM). X axis is the serum concentration of HMGB1 (ng/ml) and Y axis is Day. Trend demonstrates slight increase in serum total HMGB1 (ng/ml) between day 1 and 2 and fall on the last day. (B) Bar chart showing the Mean (N=3) serum cleaved/uncleaved CK18 in the admitting, second and last days of patients with ALD & sepsis. Means are plotted with SEM. X axis is serum concentration of cleaved/uncleaved CK18 and Y axis day. Blue = cleaved CK18 & Red= uncleaved CK18. There appears to be visibly higher levels of uncleaved CK18 (U/L) compared to cleaved on all three days.

	Day	N	CK18 (U/L)	Range	Mean	SD	Kruskall Wallis for cleaved versus uncleaved CK18 (U/L)
ALD & sepsis (N=3)	1	3	Cleaved	911.07-1305.81	781.883	599.0604	0.0389
			Uncleaved	1390.12-2518.993	1848.76	524.5204	
	2	3	Cleaved	1040.01-1747.35	1402.813	354.0236	0.3017
			Uncleaved	1040.746-5399.037	2477.43	1701.286	
	3	3	Cleaved	1004-1284.41	1102.793	157.4872	0.6056
			Uncleaved	399.977-3490.914	1569.71	1285.104	

Table 4.9: serum cleaved and uncleaved CK18 in the ICU admitting day of patients with ALD & sepsis. Mean values are given with the range and standard deviation (SD). Kuskall Wallis test was used to test for a significant difference between levels of cleaved and uncleaved in CK18 in each individual patient. No significant differences between CK18 (U/L) were detected apart from the admitting day.

4.3.5 Comparative analysis of serum total HMGB1 (ng/ml) and serum cleaved/uncleaved CK18 (U/L) in patients decompensated ALD versus patients with ALD and sepsis

Serum total HMGB1 was measured in patients with decompensated ALD (N=4) and patients with ALD and sepsis (N=3) over their stay in ICU. Samples included admitting (1), second (2) and last day (3). Patients with ALD and sepsis had higher admitting levels of total HMGB1 (11.17ng/ml SD 0.61) compared with patients with decompensated ALD (Mean 7.14ng/ml SD 4.63) .This was a similar pattern for all other measured days (*figure 4.6*). This is an expected observation as HMGB1 levels are known to increase with sepsis, however, the difference between levels were not significant (*table 4.10).*

Patients with decompensated ALD were found to have both higher levels of cleaved and considerably higher levels of uncleaved CK18 than patients admitted with ALD and sepsis (*figure 4.7 A & B*). This indicates that the levels of apoptosis and more importantly necrosis are higher in the patient group. Although these values are not significant (*table 4.11*), they are approaching a significant level suggesting that perhaps the sample size is too small.

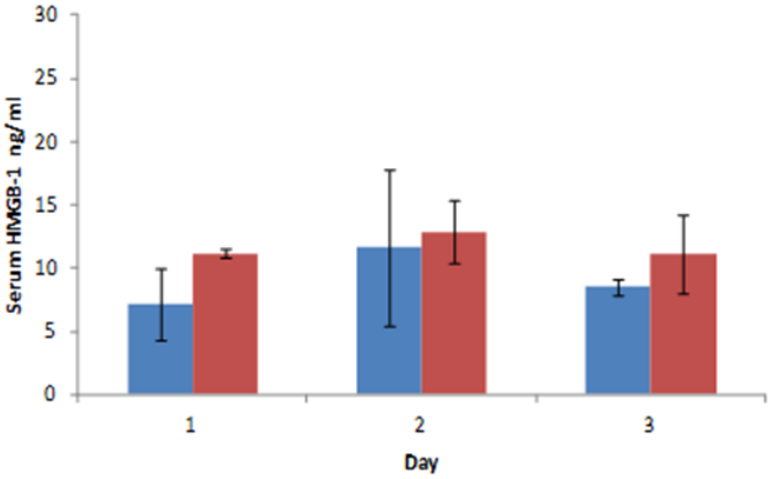

Figure 4.6: Bar chart showing the Mean serum total HMGB1 (ng/ml) in patients with decompensated ALD (N=4, Blue) and patients with ALD and sepsis (N=3, Red). Means of admitting, second and last days are plotted with SEM. X axis is the serum total HMGB1(ng/ml) and Y axis is the day. Trend shows that there is a mean increase in HMGB1 in both patient groups between day 1 and 2 and a fall from day 2 to 3. Patients with ALD and sepsis have visibly higher levels of serum total HMGB1 on all days.

	Day	N	Range	Mean	SD	Mann Whitney U test	
ALD No sepsis	1	4	3.30-15.33	7.14	5.28	Day 1	0.4
	2	4	3.99-29.87	11.65	11.65		
	3	3	7.05-9.48	8.50	8.50	Day 2	0.63
ALD & sepsis(N=4)	1	3	10.64-11.84	11.174333	0.61		
	2	3	7.84-15.56	12.86	4.35	Day 3	0.7
	3	3	6.1-16.85	11.13	5.41		

Table 4.10: Table showing significance testing, using the Mann-Whitney U test, on serum total HMGB1 (ng/ml) in patients with decompensated ALD versus patients with ALD and sepsis. Mean values are given with the range and standard deviation (SD). There are no significant differences.

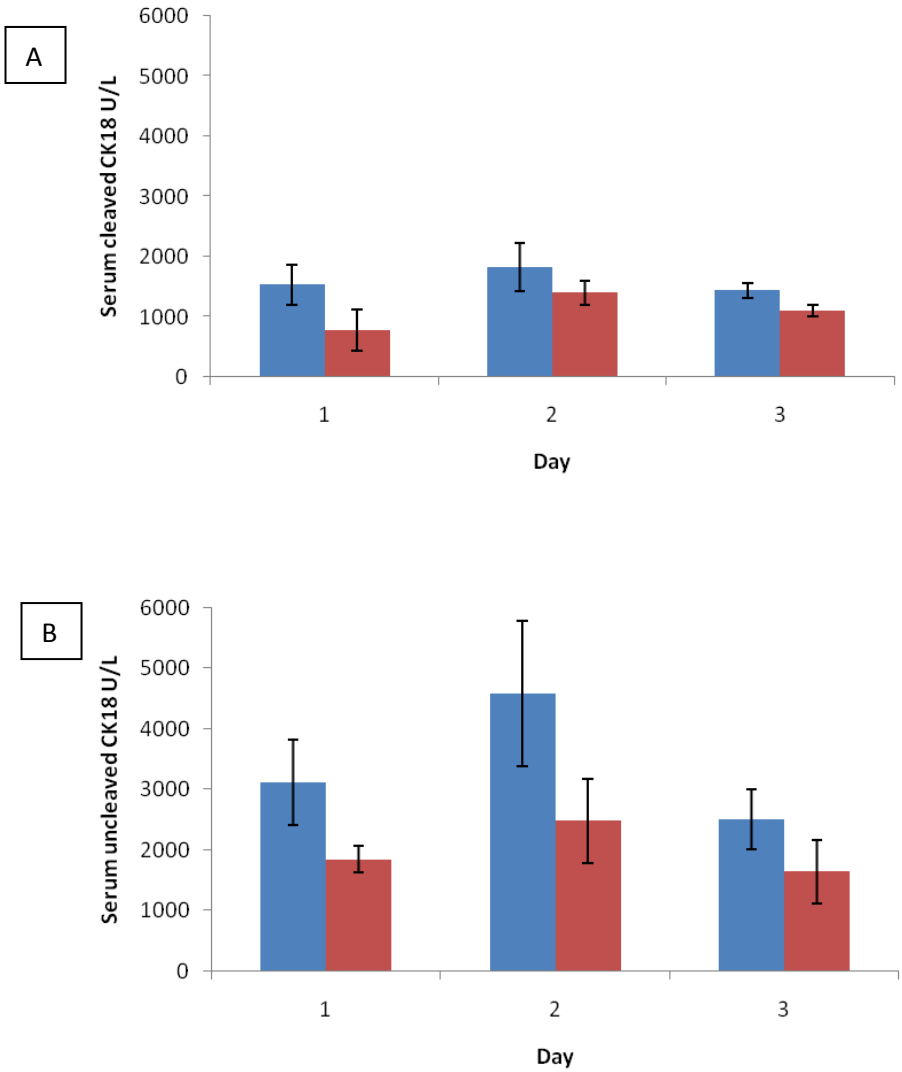

Figure 4.7: Top (A) Bar chart showing the mean serum cleaved CK18 (U/L) in patients with decompensated ALD (N=4, Blue) and patients with ALD and sepsis (N=3, Red). Patients with decompensated ALD have mildly higher levels than patients with ALD and sepsis. Bottom (B) Bar chart showing the Mean serum uncleaved CK18 in patients with decompensated ALD (blue) and ALD & sepsis (red) Patients with decompensated ALD have visibly higher levels of uncleaved CK18 than patients with ALD & sepsis. Means of admitting, second and discharge days to ICU are plotted with SEM. X axis is cleaved/uncleaved CK18 in U/L and Y axis is the day.

	Day	N	CK18 (U/L)	Range	Mean	SD	Mann Whitney U (ALD no sepsis versus ALD & sepsis)	
ALD No sepsis (N=4)	1	4	Cleaved	849.72-2316.63	1538.008	665.5797	Day 1	C= 0.4
			Uncleaved	1567.18 - 6910.37	3111.224	1990.263		
	2	4	Cleaved	920.67-2016.50	1833.43	795.0031		UC= 0.1
			Uncleaved	10701.627-11610.94	4577.693	3384.91		
	3	3	Cleaved	1295.16 - 1674.18	1437.41	206.433	Day 2	C= 0.4
			Uncleaved	981.686 - 4100.74	2501.34	1210.182		
ALD & sepsis (N=3)	1	3	Cleaved	911.07-1305.81	781.883	599.0604		UC= 0.18
			Uncleaved	1390.12 - 2518.993	1848.76	524.5204		
	2	3	Cleaved	1040.01 - 1747.35	1402.813	354.0236	Day 3	C= 0.63
			Uncleaved	1040.746-5399.037	2477.43	1701.286		
	3	3	Cleaved	1004-1284.41	1102.793	157.4872		UC= 0.18
			Uncleaved	399.977 - 3490.914	1569.71	1285.104		

Table 4.11: Table showing results of Mann Whitney U testing on serum cleaved versus uncleaved CK18 in patients with decompensated ALD versus patients with ALD and sepsis. Mean values are given with the range and standard deviation (SD). There are no significant differences.

4.3.6 Serum total HMGB1 (ng/ml) and CK-18 (U/L) cleaved and uncleaved in the serum of patients with Sepsis

Serum total HMGB1 (ng/ml) was measured in patients with sepsis (N=4) over their stay in ICU. Samples included admitting (1), second (2) and last day (3). Patients had an elevated HMGB1 (Mean 17.60 ng/ml SD 4.21) on their admitting day (p=0.0286) compared with healthy controls. A rise was seen in all patients between day 1 to 2 and this was associated with worsening LFTs and serum urea and creatinine. All patients exhibited a decline between day 2 and discharge day. (*Figure 4.8 (A)*). The overall ICU % mortality rate in this group of patients was 50%.

The same samples where measured for serum cleaved and uncleaved CK18 (U/L). Patients showed visible increases on admitting values for cleaved (Mean 1199.78 U/L SD 249.065) and uncleaved (Mean 1347.121 U/L SD 667.1293) CK18 compared to healthy controls (p=0.0159 & 0.0143 respectively). There was a visible increase in uncleaved CK18 between day 1 to 2 but this was not significant (*figure 4.9 (B)*). There were no significant differences between values for cleaved and uncleaved CK18 on any day. See *table 4.12.*

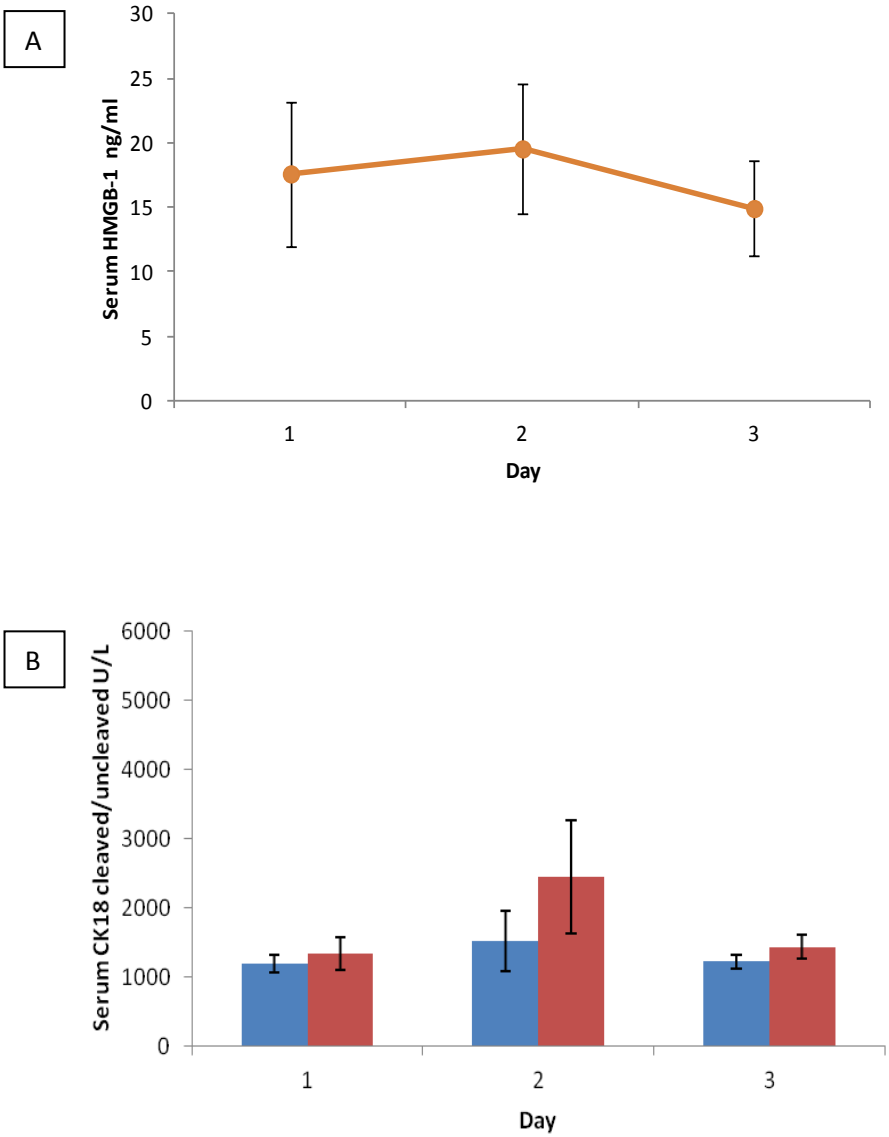

Figure 4.9: Top (A) Line graph showing the mean (N=4) serum total HMGB1 (ng/ml) in the admitting, second and discharge day of patients with sepsis. Means are plotted with Standard error of the mean (SEM). X axis is the serum concentration of HMGB1 (ng/ml) and Y axis is Day. Trend shows an increase in HMGB1 between days 1 and 2 and a fall on the last day. Bottom (B) Bar chart showing the Mean (N=4) serum cleaved/uncleaved CK18 (U/L) in the admitting, second and last day of patients with sepsis. Means are plotted with SEM. X axis is serum concentration of cleaved/uncleaved CK18 (U/L) and Y axis day. Blue = cleaved CK18 & Red= uncleaved CK18. Patients have higher levels of uncleaved CK18 compared to cleaved CK18, particularly on day 2. Same trend is observed with an increase in both markers between day 1 and 2 and a fall on day 3.

	Day	N	CK18 (U/L)	Range	Mean	SD	Kruskall Wallis cleaved versus uncleaved
Sepsis (N=4)	1	4	Cleaved	1071.45-1468.01	1199.78	249.0648	0.73
			Uncleaved	896.9-2382.84-	1347.121	667.1293	
	2	4	Cleaved	1029.64-2813.48	1523.713	862.4694	0.49
			Uncleaved	449.86-5143.977	2441.738	2304.678	
	3	4	Cleaved	947.95-1459.27	1224.095	213.7419	0.39
			Uncleaved	1035.562-1661.198	1439.501	479.1486	

Table 4.12: serum cleaved and uncleaved CK18 in the admitting, second and last day of patients admitted to ICU with sepsis (N=4). Mean values are given with the range and standard deviation (SD). The Kuskall Wallis test was used to test for a significant difference between levels of cleaved and uncleaved in CK18 in each individual patient. No significant differences were observed.

4.3.7 Serum total HMGB1 (ng/ml) and CK-18 (U/L) cleaved and uncleaved in the serum of patients without Sepsis or ALD

Serum total HMGB1 (ng/ml) was measured in patients without sepsis or ALD (N=4) over their stay in ICU. Patients were admitted for various reasons including cardiac arrest, pulmonary embolism & diabetic ketoacidosis (DKA). Samples included admitting (1), second (2) and last day (3). Patients had a significant elevated total HMGB1 (Mean 13.70ng/ml SD 6.12) on their admitting day compared to healthy controls (p=0.0286). They maintained a relatively similar HMGB1 level between days 1 to 2. (*Figure 4.10 (A)*)

Serum cleaved and uncleaved CK18 (U/L) was measured in this same patient cohort over their stay in ICU. Patients showed a visible increases on admitting values for cleaved (Mean 1664.705 U/L) SD 712.606) and uncleaved (Mean 2687.94 U/L SD 268.7) CK18 compared to healthy controls (p=0.0159 & 0.043 respectively). There was a visible decrease in uncleaved CK18 between day 1 to 2 but this was not significant (*figure 4.10 (B)*). There were no significant differences between values for cleaved and uncleaved CK18 on any day. See *table 4.13*.

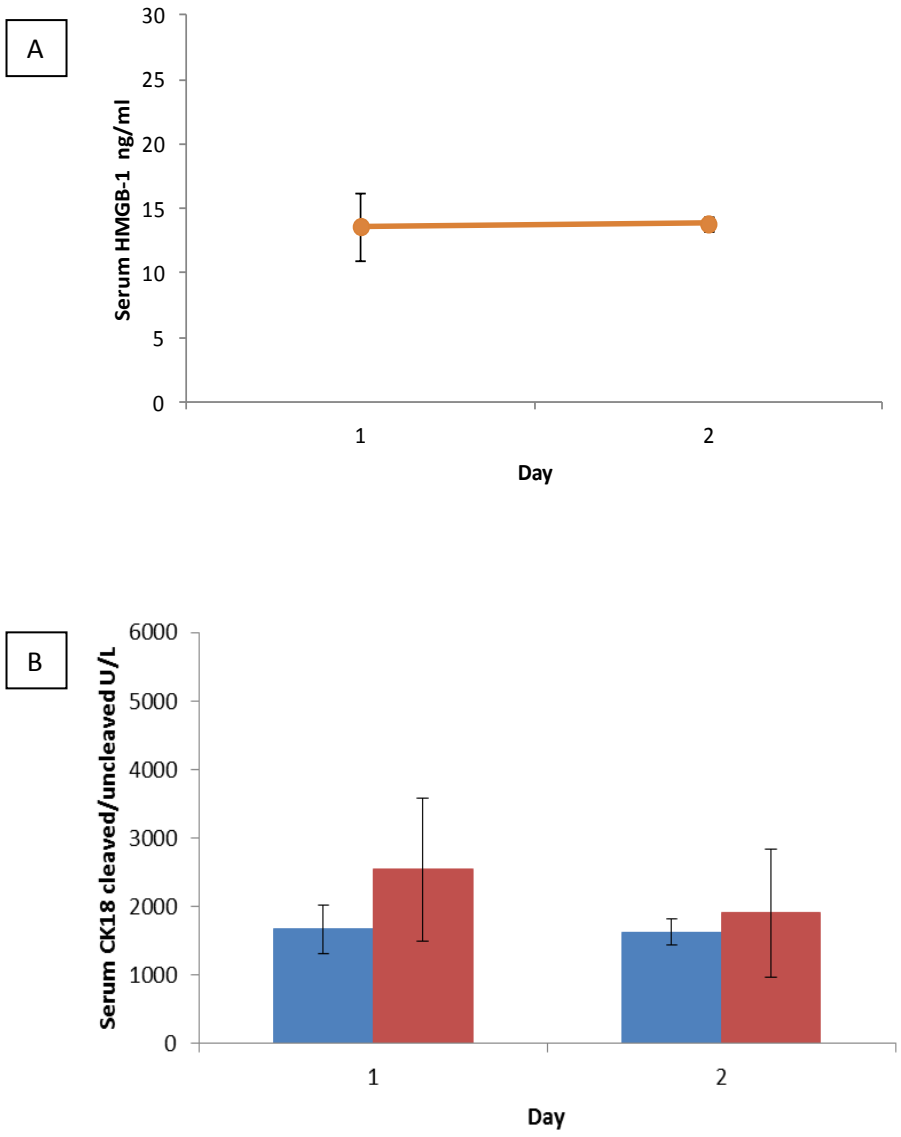

Figure 4.10: Top (A) Line graph showing the mean (N=4) serum total HMGB1 (ng/ml) in the admitting, second and last day of patients without ALD or sepsis. Means are plotted with Standard error of the mean (SEM). X axis is the serum concentration of total HMGB1 (ng/ml) and Y axis is Day. Trend shows relatively similary serum total HMGB1 between days 1 and 2 (B) Bar chart showing the Mean (N=4) serum cleaved/uncleaved CK18 (U/L) in the admitting, second and last day of patients without ALD or sepsis. Means are plotted with SEM. A axis is serum concentration of cleaved/uncleaved CK18 (U/L) and Y axis day. Blue = cleaved CK18 & Red= uncleaved CK18. These patients exhibited higher levels of admitting uncleaved CK18 than cleaved. Both levels fell between day 1 and 2.

	Day	N	CK18 (U/L)	Range	Mean	SD	Kruskall Wallis cleaved versus uncleaved
Sepsis (N=4)	1	4	Cleaved	1210.5-2712.7	1664.705	748.69	0.73
			Uncleaved	340.282-2600.419	2537.459	356.30	
	2	4	Cleaved	1223.2-1945.36	1626.11	184.14	0.60
			Uncleaved	332.244-6426.202	1906.852	934.41	

Table 4.13: serum cleaved and uncleaved CK18 (U/L) in the admitting, second and last day of patients admitted to ICU with no ALD or sepsis (N=4). Mean values are given with the range and standard deviation (SD). Kuskall Wallis testing was used to test for a significant difference between levels of cleaved and uncleaved in CK18 in each individual patient. No significant differences were detected.

4.3.8 Comparative analysis of serum total HMGB1 (ng/ml) and serum cleaved/uncleaved CK18 (U/L) in patients with sepsis versus patients with no ALD and no sepsis.

Serum total HMGB1 (ng/ml) was measured in patients with sepsis (N=4) and patients with no ALD or sepsis (N=4) over their stay in ICU. Samples included admitting (1), second (2) and last day (3). Patients with sepsis had higher admitting levels of total HMGB1 (Mean 17.60ng/ml SD 4.21) compared with patients with no ALD or sepsis (Mean 13.70ng/ml SD 6.12) .This was a similar pattern for all other measured days (*figure 4.11*). This is an expected observation as HMGB1 levels are known to increase with sepsis, however, the difference between levels were not significant (*table 4.10).*

Both patient groups showed fairly similar levels of cleaved and uncleaved CK18 with no significant differences (*figure 1.12 A & B*).

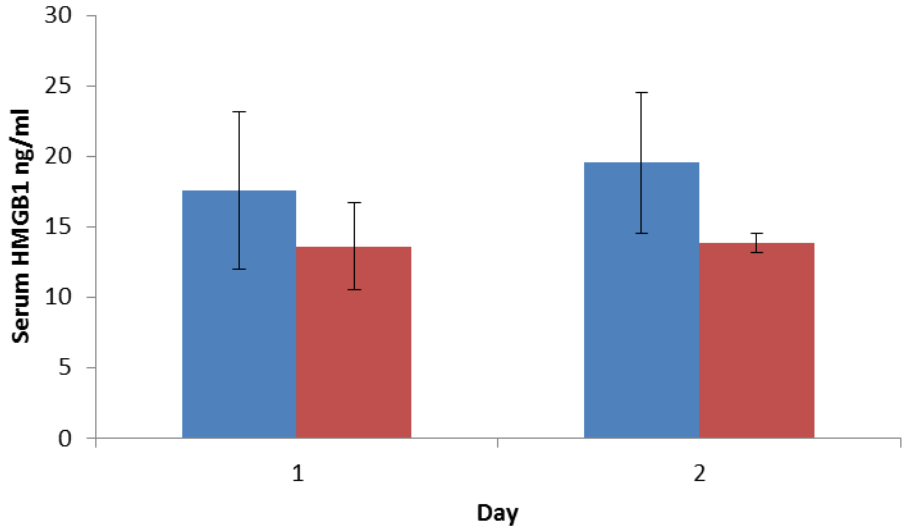

Figure 4.11: Bar chart showing the mean (N=4) serum total HMGB1(ng/ml) in the admitting, second and discharge day of patients with sepsis (Blue) versus patients without ALD or sepsis (Red). Means are plotted with Standard error of the mean (SEM). X axis is the serum concentration of HMGB1 (ng/ml) and Y axis is Day. Patients with sepsis had higher levels of HMGB1 on both days, with an increase between days 1 and 2.

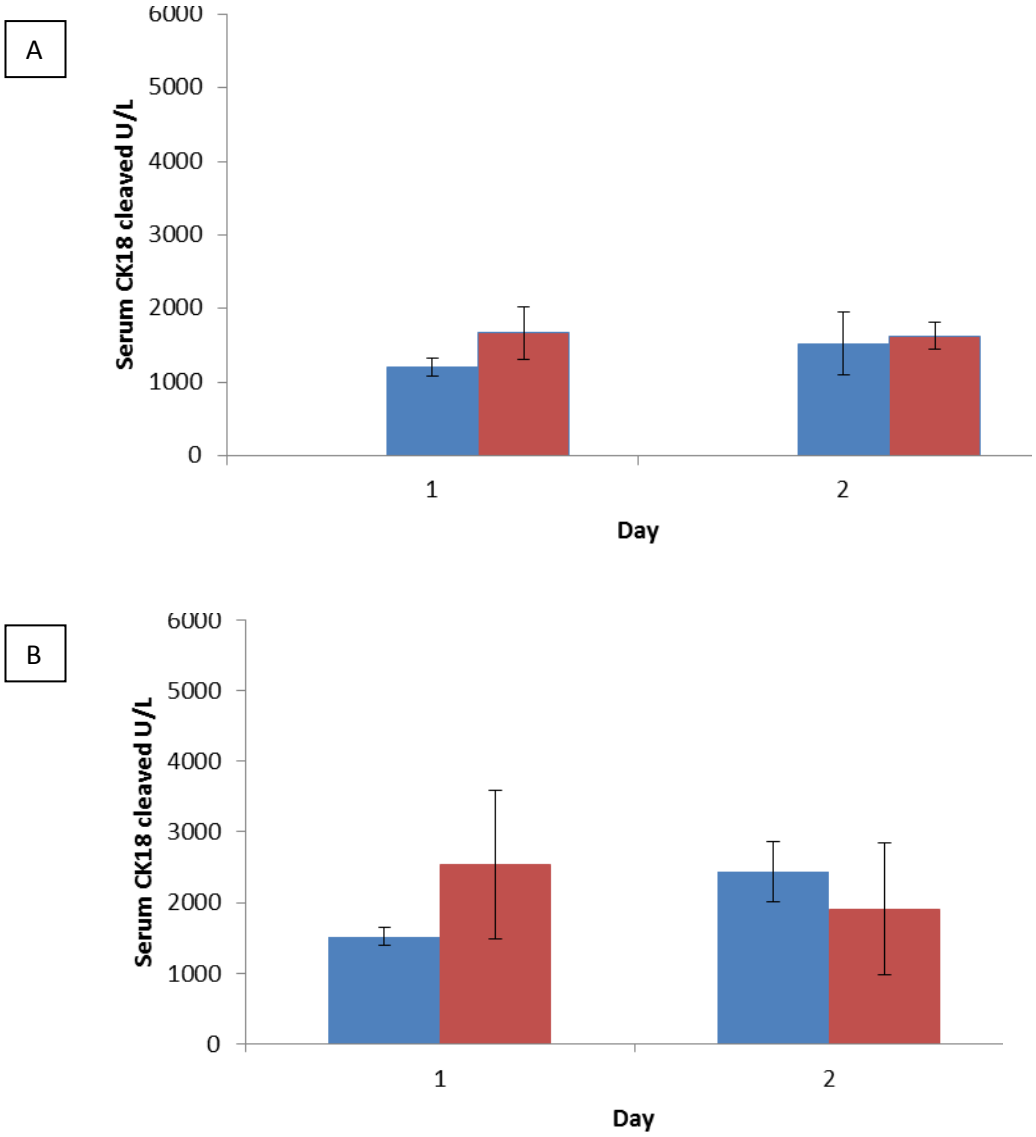

Figure 4.12: Top (A) Bar chart showing the mean serum cleaved CK18 (U/L) in patients with sepsis (N=4, Blue) and patients with no ALD or sepsis (N=4, Red). Patients exhibited fairly similar levels of serum cleaved CK18. Bottom (B) Bar chart showing the Mean serum uncleaved CK18 in patients with sepsis (N=4, Blue) and patients with no ALD or sepsis (N=4, Red). Again similar levels of uncleaved CK18 with patients without sepsis or ALD exhibiting a fall between day 1 and 2 and the opposite being observed in patients with sepsis. Means of admitting, second and discharge days to ICU are plotted with SEM. X axis is cleaved/uncleaved CK18 (U/L) and Y axis is the day.

4.3.9 Comparative analysis of serum total HMGB1 (ng/ml) and serum cleaved/uncleaved CK18 (U/L) in patients with ALD and sepsis versus patients with sepsis.

Serum total HMGB1 (ng/ml) was measured in patients with ALD and sepsis (N=3) and patients with sepsis (N=4) over their stay in ICU. Samples included admitting (1), second (2) and last day (3). Patients with sepsis had higher admitting levels of total HMGB1 (Mean 17.60ng/ml SD 4.21) compared with patients with ALD and sepsis(Mean 11.17ng/ml SD 0.61) .This was a similar pattern for all other measured days (*figure 4.11*). The difference between levels was not significant (*table 4.10).* Serum total HMGB1 levels of patients with ALD and sepsis were also lower than patients with no ALD and no Sepsis on both days.

Both patient groups showed fairly similar levels of cleaved and uncleaved CK18 with no significant differences (*figure 1.12 A & B*) (*table 4.14*)

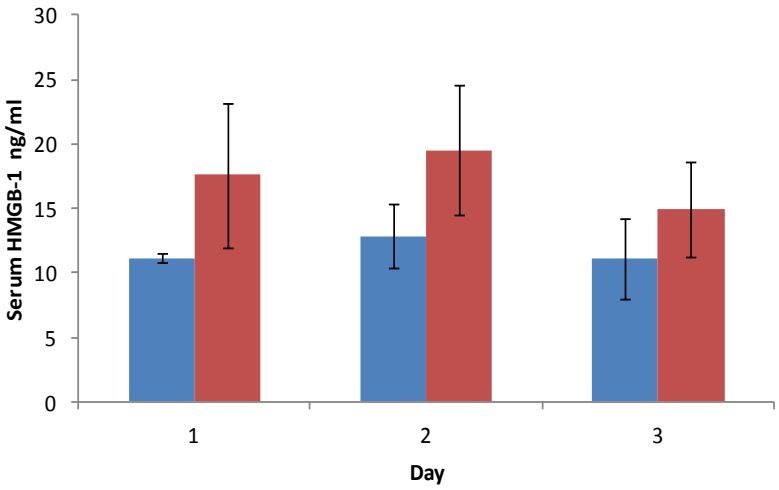

Figure 4.13: Bar chart showing the mean serum total HMGB1 (ng/ml) in the admitting, second and discharge day of patients with ALD and sepsis (N=3,Blue) versus patients with sepsis (N=4,Red). Means are plotted with Standard error of the mean (SEM). X axis is the serum concentration of HMGB1 (ng/ml) and Y axis is Day. Patients with sepsis had visibly higher concentrations of serum total HMGB1 than patients with ALD and sepsis on all days.

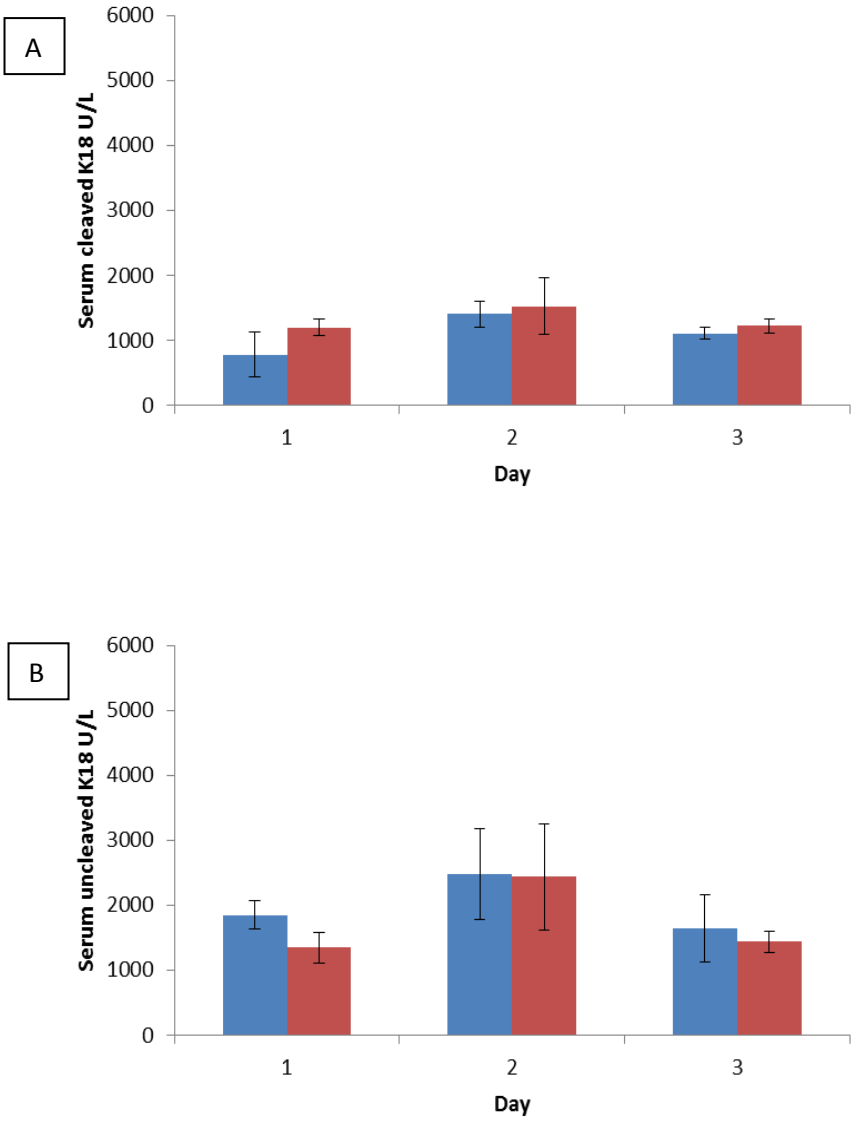

Figure 4.14: Top (A) Bar chart showing the mean serum cleaved CK18 in patients with ALD and sepsis (N=3, Blue) and patients with sepsis (N=4, Red). Patients in both groups exhibited comparable concentrations of cleaved CK18 in all days. Bottom (B) Bar chart showing the Mean serum uncleaved CK18 in patients with ALD and sepsis (N=3, Blue) and patients with sepsis (N=4, Red). Again comparable concentrations of uncleaved CK18 were observed in both patient groups. Means of admitting, second and discharge days to ICU are plotted with SEM. X axis is the serum total cleaved/uncleaved CK18 in ng/ml and Y axis is the day.

	Day	N	CK18 (U/L)	Range	Mean	SD	Mann Whitney U (sepsis versus ALD & sepsis)	
Sepsis (N=4)	1	3	Cleaved	1071.45-1468.01	1199.78	249.0648	Day 1	C=0.2284
			Uncleaved	896.9-2382.84-	1347.121	667.1293		
	2	3	Cleaved	1029.64-2813.48	1523.713	862.4694		UC=0.662
			Uncleaved	449.86-5143.977	2441.738	2304.678		
	3	3	Cleaved	947.95-1459.27	1224.095	213.7419	Day 2	C=0.22884
			Uncleaved	1035.562-1661.198	1439.501	479.1486		
ALD & sepsis(N=3)	1	3	Cleaved	911.07-1305.81	781.883	599.0604		UC=0.94
			Uncleaved	1390.12-2518.993	1848.76	524.5204		
	2	3	Cleaved	1040.01-1747.35	1402.813	354.0236	Day 3	C=0.2284
			Uncleaved	1040.746-5399.037	2477.43	1701.286		
	3	3	Cleaved	1004-1284.41	1102.793	157.4872		UC=0.226
			Uncleaved	399.977-3490.914	1569.71	1285.104		

Table 4.14: *Table showing significance testing, using the Mann-Whitney U test, on serum cleaved and uncleaved CK18 (U/L) in patients with sepsis versus patients with ALD and sepsis. Mean values are given with the range and standard deviation (SD). No significant differences were observed.*

4.3.10 Comparison of Routine biochemistry and relationship with novel biomarkers

Routine clinical chemistry was collected on patients with ALD and sepsis and patients with sepsis alone to look for significant differences. Alanine transaminase (ALT) is a gold standard marker of liver dysfunction; normal levels are between 10-40U/L[121]. Pro-thrombin time (PT) was identified by the pre-study analysis to be the most sensitive and specific test in this sub group of patients (patients with ALD). Normal range is a PT of 10-14 seconds. ALD and sepsis patients had higher ALT values and more prolonged PT times than patients with sepsis alone. However patients with Sepsis alone had higher levels of HMGB1 than patients with ALD and sepsis. This analysis shows that patients with more deranged liver function have lower concentrations of serum total HMGB1. Cleaved and uncleaved CK18 were similar between patient groups, despite the derangement seen in ALT and PT and relative differences between HMGB1.

These differences in routine biochemistry aren't significant, but confirms, that sample size is contributing to significance levels, as these differences where significant in the pre-study cohort (sample size was 119). (*Table 4.15 & 4.16)*

	Day	N	Range	Mean	SD	Mann Whitney U test	
ALD & Sepsis	1	3	24-88	54.67	32.1	Day 1	0.2284
	2	3	13-74	45.3	30.7		
	3	3	31-102	69.67	35.0	Day 2	0.662
Sepsis	1	4	26-31	36.25	17.32		
	2	4	18-62	33.5	20.5	Day 3	0.8
	3	3	18-78	44.25	29.5		

Table 4.15: Table showing mean values of ALT, given with the range and standard deviation (SD) in patients with ALD and sepsis versus patients with sepsis. Mann Whitney U testing was done to test for significant differences.

	Day	N	Range	Mean	SD	Mann Whitney U test	
ALD & Sepsis	1	3	14.9-25.1	21.2	5.5	Day 1	0.8
	2	3	15-21.1	18.13	3.0		
	3	3	15.1-29.9	21.9	7.5	Day 2	0.4
Sepsis	1	4	16.3-21.8	16.3	3.5		
	2	4	14.1-28.7	18.1	6.1	Day 3	0.2
	3	3	11.9-16.2	14.1	1.7		

Table 4.16: Table showing mean values of Pro-thrombin time (PT), given with the range and standard deviation (SD) in patients with ALD and sepsis versus patients with sepsis. Mann Whitney U testing was done to test for significant differences.

4.3.11 Summary

HMGB1 is significantly elevated in all patients admitted to ICU compared to healthy controls ($P<0.05$). However it appears to be non-specific for sepsis, as even those patients who were admitted without sepsis had elevated admitting levels similar to sepsis patients (i.e. mean admitting serum total HMGB1 in sepsis patients 17.60ng/ml, mean admitting serum total HMGB1 in non-sepsis and non ALD patients 13.70ng/ml).

Patients with ALD as a group had lower levels of HMGB1 when compared to other patients admitted to ICU. Comparison between patients with decompensated ALD and ALD with sepsis showed that there was a mild elevation on all days that wasn't significant. However, ALD and sepsis patients had lower levels of HMGB1 on all three days when compared to patients with sepsis alone. This indicates that patients with ALD potentially have an impaired ability to produce HMGB1.

Higher concentrations of uncleaved CK18 (U/L) were observed in the serum of patients with decompensated ALD compared to cleaved levels, suggesting that these patients are undergoing significant hepatocyte loss through necrosis more than apoptosis. This is probably related to their presenting complaint (i.e. variceal haemorrhage). This difference is not statistically significant, but approaching a significant level (i.e. $p=0.089$), suggesting that perhaps sample sizes aren't large enough. Patients with ALD and Sepsis and patients with sepsis alone also had higher concentrations of uncleaved as opposed to cleaved CK18 (U/L) indicating that either necrosis is the mode by which cells are being lost or apoptosis is impaired in some way with these patients.

Correlation with routine chemistry shows that although other routine tests (i.e. ALT & PT) are significantly elevated in patients with ALD and sepsis compared to patients with sepsis alone, novel biomarker HMGB1 is the opposite. Lack of significant differences between clinical chemistry of patients with ALD and sepsis and patients with sepsis alone also highlights the significance of samples size. Where significant differences existed during the pre-study analysis where sample size was much larger.

4.4 Discussion

4.4.1 HMGB1 in sepsis

HMGB1's structure and pro-inflammatory characteristics are discussed in the *section 1.2.4.* Research has shown that HMGB1 release is largely divided into two pathways, either active secretion by monocytes as a pro-inflammatory cytokine or passive release from apoptotic and necrotic cells [122]. It has recently been demonstrated in RAW 264.7 macrophages that magnesium sulphate ($MgSo^4$) inhibits the translocation of HMGB1 from the nucleus to the cytoplasm via inhibition of the NF-κB signalling pathway[123].

Studies have already shown that HMGB1 levels are significantly increased in patients with severe sepsis[29]. Research has thus far been unable to ascertain whether or not this is related to disease severity and outcome. *Cullberg et al*[124] found that lower levels of HMGB1 were detected in patients with a poorer outcome compared to those that survived and levels in those that did survive remained elevated even after other cytokine levels had normalised. Persistent immune cell infiltration and chronic inflammation has also been noted in experimental sepsis were *Gonnert et al*[48] found persistence of inflammatory infiltration in the liver weeks after insult. This persistence has been noted in other human studies[125], but its significance has not been quantified. Further studies have found that HMGB1 levels did not differ in survivors and non survivors of severe sepsis.[126] This mixed picture was observed in patient analysis in this chapter.

Apoptosis occurs in a wide range of cells in patients with sepsis and shock. The lymphoid organs and columnar epithelial cells of the gastrointestinal tract have been shown to be particularly vulnerable[88] Apoptosis induces macrophages to release HMGB1 *in vivo* and administering anti-HMGB1 antibodies protect against organ damage but not apoptosis in the spleen[127]. In *chapter 3* splenic apoptosis was found in an LPS model of murine sepsis and concluded to be a result of pathways involving adrenal corticosteroid hormone release, potentially explaining failure of anti-HMGB1 antibodies to protect against lymphocyte apoptosis in *Qin et al*[127]. They also concluded that HMGB1 production is downstream of apoptosis on the final common pathway to organ damage in severe sepsis.

In the present study HMGB1 levels were elevated in patients who had no evidence of sepsis or an inflammatory process. The consensus by the ACCP/SCCM[1] explains that a SIRS (i.e. inflammation) can occur as a result of non-infectious insults. It has been shown that HMGB1 release is an early event after traumatic injury in humans[128].

4.4.2 HMGB1 and cirrhosis

In this study patients with ALD and sepsis had a tendency to have more deranged ALT and PT (*table 4.15* & *4.16*), however, their HMGB1 values were consistently lower than patients with sepsis. This indicates that there is a potential inherent disability in a patient with ALD's ability to secrete HMGB1. This was further confirmed by the lower levels of HMGB1 seen in patients with a decompensation of ALD, compared to patients admitted to ICU with no ALD or sepsis (see *figure 4.4 & 4.10*).

Cirrhosis is known to be caused by a chronic inflammatory process[116]. It has been shown that HMGB1 serum levels are significantly higher in patients with low fibrosis compared to those with high fibrosis in patients with hepatitis B virus (HBV). This study concluded that HMGB1 is a non-invasive, repeatable, and convenient marker for distinguishing advanced fibrosis from low fibrosis in chronic HBV patients[129]. In the present analysis, patients had Child-Pugh[120] scores of B/C (see *table 4.4*) indicating a high level of cirrhosis. So this is a probable explanation for the lower concentrations of HMGB1 seen in these patients. Clinical impact of this is reflected where patients with cirrhosis are found to have an increased susceptibility to bacterial infection[130]. With respect to HMGB1 levels detected in cirrhotic patients in this study, it could be due to an inability to mount an effective inflammatory response. Furthermore, HMGB1, although not a specific marker of liver function, has been shown to be important in the pathogenesis of acute liver failure. *In vivo* use of anti-HMGB1 antibodies to neutralize HMGB1's effects resulted in suppression of hepatic enzymes and plasma inflammatory cytokines, along with a marked improvement in histological findings and survival[131].

Acute episodes of chronic hepatitis B (CHB) represent the "acute on chronic liver failure" (AOCF) much like ALD patients with a sepsis. It has been shown that during an acute episode of CHB, an excessive immune response is triggered, and a huge

amount of HMGB1 can be detected in the blood. This systemic increase of HMGB1 causes an amplified systemic inflammation and further aggravates liver injury[132].

4.4.3 CK18, Apoptosis and Necrosis

All cells, including hepatocytes, require oxygen for their metabolism, most importantly for ATP generation. A restriction in oxygen supply results in damage to the cell and can lead to apoptosis or necrosis. Patients with decompensated ALD showed higher concentrations of uncleaved compared to cleaved CK18 in this analysis (see *figure 4.4*). Three of the four patients were admitted with variceal haemorrhage (a common reason for admission of cirrhotic patients[117]). During episodes patients haemorrhage a significant amount of blood, leading to reduced blood flow and perfusion of organs, which can lead to hypoxia and necrosis, and therefore an increased concentration of uncleaved CK18. *Nanji et al*[133] stated that reduced oxygen levels through hypoxia is a cause of hepatocyte necrosis. Similarly, alcohol consumption can influence several other factors believed to be involved in hepatocyte necrosis, including depletion of the energy-storing molecule ATP, oxidative stress, and release of endotoxins. Conversely, they stated that hepatocyte apoptosis was influenced by alcohol consumption through alterations to enzyme cytochrome P450 system, small molecules (i.e., cytokines) involved in cell communication, oxidative stress, and changes in iron metabolism.

While lymphocyte apoptosis contributes to immunosuppression in sepsis, recent evidence suggests that necrosis of hepatocytes predominates in septic patients with liver dysfunction and correlates with poor survival[134]. *Hofer et al*[135] found that serum total CK18 concentrations were significantly elevated in patient's not surviving sepsis. Further analysis showed no differences of the biomarkers between survivors and non-survivors when liver function was retained. Importantly, however, significantly higher levels of uncleaved CK18 were observed in the non-surviving group with decreased liver function. They concluded that, unlike apoptosis, hepatocyte necrosis is an early predictor of disease outcome in septic patients with liver dysfunction. Furthermore, the loss of parenchymal cells due to necrosis may be the primary mode of cell death in these patients. The current analysis showed that all patients with sepsis with and without ALD had visibly elevated levels of uncleaved compared to cleaved CK18 (*figure 4.14* A&B). These levels were similar between patient groups (ALD & sepsis and patients with sepsis alone) despite patients with

ALD and sepsis having higher concentrations of serum ALT and prolonged PT (*table 4.15 & 4.16*). Post-mortem analysis of patients dying from severe sepsis showed significant levels of apoptosis and lobular necrosis in the liver parenchyma[91].

It's difficult to define the mechanisms contributing to the increase of uncleaved CK18 in patients with sepsis, as apoptosis is known to be impaired. Meaning, those elevations look could look exacerbated and augmented by a reduction in apoptosis.

4.4.5 Summary and further research

In the present study, HMGB1 and cleaved/uncleaved CK18 have been identified as markers of sepsis in the defined patient groups. They were significantly elevated in patients admitted to ICU compared with healthy controls. Analysis of HMGB1 was shown to be elevated in patients with sepsis and having an underlying liver disease seems to impair its release (as reflected by lower serum levels in ALD and ALD & sepsis patients). This is probably due to the chronic inflammatory process related to cirrhosis[129].

Uncleaved CK18 was also found to be a reliable marker of necrosis in these patients, and in keeping with the literature, highlighted the significant, emerging role that necrosis has to play in patients with sepsis. Furthermore, in patients with decompensated ALD (particularly those with variceal haemorrhage) uncleaved CK18 was elevated, indicating a possible use as a marker of severity in these patients.

In future work *Bonferroni* correction of the P values should be carried out to correct for multiple testing, furthermore, these preliminary results require validation in larger patient cohorts in order to increase statistical power. As discussed, HMGB1 can exist as acetylated and oxidised sub forms depending on mode of cell death. Further investigation may show visible differences in concentrations between patient groups and may reflect a further difference in concentrations of sub forms. Cleaved and particularly uncleaved CK18, are proving in the literature, to be reliable markers of hepatocyte necrosis (patients with elevated LFTs had significantly higher levels of uncleaved CK18 and poorer outcome[135]). This is reflected partially in the current study and further work could help quantify and clarify the significance of necrosis and apoptosis in patients with sepsis.

Chapter 5:

General discussion

Contents

5 General discussion

Sepsis is a significant problem in the United Kingdom. Diagnosis, management and prognosis are proving difficult for clinicians. This is further exacerbated by the lack of sensitive and specific biomarkers for the disease, and complications related with it (i.e. organ dysfunction). The lack of biomarkers and efficacious therapeutic intervention is a result of inadequate understanding of this disconnect between murine and human sepsis on a molecular level and *in vivo*.

5.1 Understanding in vitro pathways of inflammation and their limitations

By comparing two different immune cells from murine (RAW 264.7) and human donors (THP1), responses to LPS and the inflammatory signalling pathway could be compared through the detection of the p65 subunit of NFκB, a common pathway for the production of *de novo* cytokines such as TNF-α. The differences in response to LPS on a molecular level explain why there is an apparent disconnect between murine and human sepsis on an *in vivo* level (see *Chapter 2*). The major findings of *chapter 2* were:

1. P65 is a reliable, detectable and reproducible way of measuring activation of the NFκB pathway in human and murine immune cell lines.
2. Activation of the NFκB pathway (via TLR 4) by *in vitro* dosing with LPS represents a dose-response relationship.
3. Human cells respond to lower concentrations of LPS than murine cells.
4. Human cells had a higher overall increase in nuclear p65 compared with murine cells.
5. Murine cells show a molecular resilience to LPS dosing, but when activated become very sensitive to changes in concentration.

One hour was chosen as a time point as activation of the p65 pathway is known to take a short time[80]. A major limitation of this study was that it only looked at a single time point. In future work it is hoped to look at a time course in order to ascertain whether or not high doses reflect the maximum activation of the pathway. Also further analysis is needed in order to investigate how the activation of the pathway translates to cytokine production.

5.2 Understanding in vivo models of sepsis and their limitations

More robust models are superseding the LPS model of endotoxaemia in mice, and histopathological analysis of the faecal inoculation model has shown it to be more representative of the gradual rising and sustaining response cytokine response, as oppose to boom and bust seen with LPS (see *Chapter 3*). The major findings of chapter 3 were:

1. LPS use *in vivo* represents a technique for inducing sterile information and doesn't meet the ACCP/SCCM[1] definition of sepsis.
2. Both models (LPS and faecal inoculation) showed principal changes consistent with neutrophil recruitment into tissues; LPS animals had a tendency to show greater numbers of neutrophils than the faeces dosed animals. This is probably related to the higher concentrations of cytokines that are seen with the LPS model[8].
3. Faecal inoculated animals demonstrated occasional recruitment of neutrophils into adipose tissue and skeletal muscle (although still minimal, to a greater extent than LPS animals). This reflects the diffuse systemic recruitment seen in human sepsis and highlights the superiority of this model in recapitulating a human sepsis environment *in vivo*.

Further analysis is needed in order to identify whether or not the histopathological changes seen in the tissues are reflected in serum cytokine levels. Furthermore, a time-course investigation of the progressive nature of both models is needed.

5.3 New biomarkers and their translatability

HMGB1 and cleaved/uncleaved CK18 have been shown to be accurate ways of monitoring the level of inflammation, necrosis and apoptosis *in vitro* and *in vivo*[4, 35, 55, 122, 125]. Their application to defined groups of ICU patients, who could potentially benefit from them, has shown that there is potential for a clinical application (see *chapter 4*). Their use alongside currently used markers of liver function could enhance the overall picture that clinicians have when approaching these patients. However, further research is needed involving larger sample sizes and more scrupulous statically analysis before widespread application can occur. The major findings of this chapter were:

1. HMGB1 and cleaved/uncleaved CK18 can be used as markers of sepsis in the defined patient groups;
2. They were significantly elevated in all patients admitted to ICU compared with healthy controls.
3. HMGB1 is markedly elevated in patients with sepsis; however having an underlying condition, such as ALD, impairs its release.
4. Uncleaved CK18 was found to be a reliable marker of necrosis and highlighted the significance of necrosis in septic patients.
5. Patients with decompensated ALD (secondary to variceal haemorrhage) may benefit from measuring uncleaved CK18 as a measurement of severity of disease.
6. Using HMGB1 and CK18 alongside routine biochemistry can enhance the potential "liver profile" available to clinicians and help in diagnosis, treatment and prognosis of patients with sepsis.

5.4 Sepsis, translational medicine & the future

Figure 5.1 describes the process of translational science in the development of effective biomarkers and treatments in the study of sepsis. Understanding the cellular signalling pathways involved in the development of an inflammatory response and the differences between human and murine cells, leads to the development of effective, representative models of sepsis in mice. This allows for reliable, valid *in vivo* studies to be done in order to develop a model of sepsis that is closest to that of the human condition. The final step is the development of effective, efficacious treatment based on these reliable models. This thesis has shown that the bridge between *in vivo* and human models is the most significant hurdle to overcome in the cross between laboratory science and clinical medicine.

Dieterle et al[136], published a landmark paper on the first formal qualification of safety biomarkers for regulatory decision making and the application of biomarkers to drug development with regards to the kidney. They summarize the Predictive Safety Testing Consortiums (PSTC) biomarkers submission, analyses and conclusions, and then go on to discuss the new standards and optimal practices identified through the qualification review process at the Food and Drug Agency (FDA) and the European Medicines Agency (EMEA). Looking at this paper as a

translational model, they have provided guidance and a framework that could be used for future biomarker qualifications (i.e. HMGB1 and CK18).

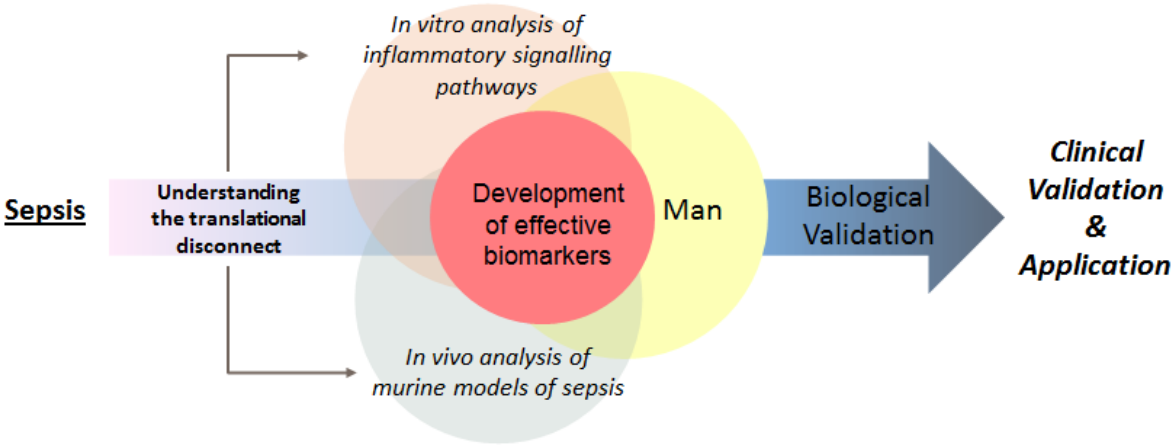

Figure 5.1: Translational model for research in sepsis. Effective In vitro and in vivo systems that are representative of humans, will lead to the development of biomarkers such as HMGB1 and CK18 which can prove efficacious in the treatment and diagnosis of disease.

VI References

1. Bone RC, Balk RA, Cerra FB, Dellinger RP, Fein AM, Knaus WA, et al. Definitions for sepsis and organ failure and guidelines for the use of innovative therapies in sepsis. The ACCP/SCCM Consensus Conference Committee. American College of Chest Physicians/Society of Critical Care Medicine. 1992. *Chest* 2009;136(5 Suppl):e28.
2. Angus DC, Linde-Zwirble WT, Lidicker J, Clermont G, Carcillo J, Pinsky MR. Epidemiology of severe sepsis in the United States: analysis of incidence, outcome, and associated costs of care. *Critical Care Medicine* 2001;29(7):1303-10.
3. Sasse KC, Nauenberg E, Long A, Anton B, Tucker HJ, Hu TW. Long-term survival after intensive care unit admission with sepsis. *Critical Care Medicine* 1995;23(6):1040-7.
4. Kibe S, Adams K, Barlow G. Diagnostic and prognostic biomarkers of sepsis in critical care. *J Antimicrob Chemother* 2011;66 Suppl 2:ii33-40.
5. Alberti C, Brun-Buisson C, Burchardi H, Martin C, Goodman S, Artigas A, et al. Epidemiology of sepsis and infection in ICU patients from an international multicentre cohort study (vol 28, pg 108, 2002). *Intensive Care Medicine* 2002;28(4):525-6.
6. Padkin A, Goldfrad C, Brady AR, Young D, Black N, Rowan K. Epidemiology of severe sepsis occurring in the first 24 hrs in intensive care units in England, Wales, and Northern Ireland. *Critical Care Medicine* 2003;31(9):2332-8.
7. Linde-Zwirble WT, Rickert T. The changing epidemiology of severe sepsis in the US. *Critical Care Medicine* 2002;30(12):A29-A.
8. Remick DG, Ward PA. Evaluation of endotoxin models for the study of sepsis. *Shock* 2005;24 Suppl 1:7-11.
9. Tracey KJ, Fong Y, Hesse DG, Manogue KR, Lee AT, Kuo GC, et al. Anti-cachectin/TNF monoclonal antibodies prevent septic shock during lethal bacteraemia. *Nature* 1987;330(6149):662-4.
10. Fisher CJ, Jr., Agosti JM, Opal SM, Lowry SF, Balk RA, Sadoff JC, et al. Treatment of septic shock with the tumor necrosis factor receptor:Fc fusion protein. The Soluble TNF Receptor Sepsis Study Group. *N Engl J Med* 1996;334(26):1697-702.
11. Hotchkiss RS, Coopersmith CM, McDunn JE, Ferguson TA. The sepsis seesaw: tilting toward immunosuppression. *Nat Med* 2009;15(5):496-7.
12. Muenzer JT, Davis CG, Chang K, Schmidt RE, Dunne WM, Coopersmith CM, et al. Characterization and modulation of the immunosuppressive phase of sepsis. *Infect Immun* 2010;78(4):1582-92.
13. Bianchi ME. DAMPs, PAMPs and alarmins: all we need to know about danger. *Journal of Leukocyte Biology* 2007;81(1):1-5.
14. Medzhitov R, PrestonHurlburt P, Janeway CA. A human homologue of the Drosophila Toll protein signals activation of adaptive immunity. *Nature* 1997;388(6640):394-7.
15. Kawai T, Akira S. Signaling to NF-kappaB by Toll-like receptors. *Trends Mol Med* 2007;13(11):460-9.
16. Armstrong L, Medford AR, Hunter KJ, Uppington KM, Millar AB. Differential expression of Toll-like receptor (TLR)-2 and TLR-4 on monocytes in human sepsis. *Clin Exp Immunol* 2004;136(2):312-9.
17. Tsujimoto H, Ono S, Efron PA, Scumpia PO, Moldawer LL, Mochizuki H. Role of Toll-like receptors in the development of sepsis. *Shock* 2008;29(3):315-21.
18. Sun Z, Andersson R. NF-kappaB activation and inhibition: a review. *Shock* 2002;18(2):99-106.

19. Bonizzi G, Karin M. The two NF-kappaB activation pathways and their role in innate and adaptive immunity. *Trends Immunol* 2004;25(6):280-8.
20. May MJ, Ghosh S. Signal transduction through NF-kappa B. *Immunol Today* 1998;19(2):80-8.
21. Cohen J. The immunopathogenesis of sepsis. *Nature* 2002;420(6917):885-91.
22. Keller ET, Wanagat J, Ershler WB. Molecular and cellular biology of interleukin-6 and its receptor. *Front Biosci* 1996;1:d340-57.
23. Dinarello CA. The biological properties of interleukin-1. *Eur Cytokine Netw* 1994;5(6):517-31.
24. Fiers W. Tumor necrosis factor. Characterization at the molecular, cellular and in vivo level. *FEBS Lett* 1991;285(2):199-212.
25. Dinarello CA. Proinflammatory and anti-inflammatory cytokines as mediators in the pathogenesis of septic shock. *Chest* 1997;112(6 Suppl):321S-9S.
26. Trinchieri G. Interleukin-12 and the regulation of innate resistance and adaptive immunity. *Nat Rev Immunol* 2003;3(2):133-46.
27. Fehniger TA, Caligiuri MA. Interleukin 15: biology and relevance to human disease. *Blood* 2001;97(1):14-32.
28. Gracie JA, Robertson SE, McInnes IB. Interleukin-18. *J Leukoc Biol* 2003;73(2):213-24.
29. Wang H, Bloom O, Zhang M, Vishnubhakat JM, Ombrellino M, Che J, et al. HMG-1 as a late mediator of endotoxin lethality in mice. *Science* 1999;285(5425):248-51.
30. Wang H, Yang H, Tracey KJ. Extracellular role of HMGB1 in inflammation and sepsis. *J Intern Med* 2004;255(3):320-31.
31. Waage A, Halstensen A, Espevik T. Association between tumour necrosis factor in serum and fatal outcome in patients with meningococcal disease. *Lancet* 1987;1(8529):355-7.
32. Bone RC. Sir Isaac Newton, sepsis, SIRS, and CARS. *Critical Care Medicine* 1996;24(7):1125-8.
33. Park JS, Svetkauskaite D, He Q, Kim JY, Strassheim D, Ishizaka A, et al. Involvement of toll-like receptors 2 and 4 in cellular activation by high mobility group box 1 protein. *J Biol Chem* 2004;279(9):7370-7.
34. Lotze MT, Tracey KJ. High-mobility group box 1 protein (HMGB1): nuclear weapon in the immune arsenal. *Nat Rev Immunol* 2005;5(4):331-42.
35. Andersson U, Tracey KJ. HMGB1 is a therapeutic target for sterile inflammation and infection. *Annu Rev Immunol* 2011;29:139-62.
36. Wu CX, Sun H, Liu Q, Guo H, Gong JP. LPS induces HMGB1 relocation and release by activating the NF-kappaB-CBP signal transduction pathway in the murine macrophage-like cell line RAW264.7. *Journal of Surgical Research* 2012;175(1):88-100.
37. Yang H, Ochani M, Li J, Qiang X, Tanovic M, Harris HE, et al. Reversing established sepsis with antagonists of endogenous high-mobility group box 1. *Proc Natl Acad Sci U S A* 2004;101(1):296-301.
38. Tang D, Kang R, Livesey KM, Cheh CW, Farkas A, Loughran P, et al. Endogenous HMGB1 regulates autophagy. *J Cell Biol* 2010;190(5):881-92.
39. Erlandsson Harris H, Andersson U. Mini-review: The nuclear protein HMGB1 as a proinflammatory mediator. *Eur J Immunol* 2004;34(6):1503-12.
40. Amadori M, Bonizzi L. Biological activities of interleukin-2 and gamma-interferon in bovine T lymphocyte conditioned media. *J Biol Regul Homeost Agents* 1989;3(4):139-45.

41. Larson AM, Polson J, Fontana RJ, Davern TJ, Lalani E, Hynan LS, et al. Acetaminophen-induced acute liver failure: results of a United States multicenter, prospective study. *Hepatology* 2005;42(6):1364-72.
42. Poli-De-Figueiredo LF, Garrido AG, Nakagawa N, Sannomiya P. Experimental models of sepsis and their clinical relevance. *Shock* 2008;30:53-9.
43. Marshall JC, Deitch E, Moldawer LL, Opal S, Redl H, van der Poll T. Preclinical models of shock and sepsis: What can they tell us? *Shock* 2005;24:1-6.
44. Redl H, Bahrami S, Schlag G, Traber DL. Clinical Detection of Lps and Animal-Models of Endotoxemia. *Immunobiology* 1993;187(3-5):330-45.
45. Mathiak G, Szewczyk D, Abdullah F, Ovadia P, Feuerstein G, Rabinovici R. An improved clinically relevant sepsis model in the conscious rat. *Critical Care Medicine* 2000;28(6):1947-52.
46. Maier S, Traeger T, Entleutner M, Westerholt A, Kleist B, Huser N, et al. Cecal ligation and puncture versus colon ascendens stent peritonitis: two distinct animal models for polymicrobial sepsis. *Shock* 2004;21(6):505-11.
47. Remick DG, Newcomb DE, Bolgos GL, Call DR. Comparison of the mortality and inflammatory response of two models of sepsis: lipopolysaccharide vs. cecal ligation and puncture. *Shock* 2000;13(2):110-6.
48. Gonnert FA, Recknagel P, Seidel M, Jbeily N, Dahlke K, Bockmeyer CL, et al. Characteristics of clinical sepsis reflected in a reliable and reproducible rodent sepsis model. *Journal of Surgical Research* 2011;170(1):e123-34.
49. Abraham E, Singer M. Mechanisms of sepsis-induced organ dysfunction. *Critical Care Medicine* 2007;35(10):2408-16.
50. Donnelly SC, Strieter RM, Reid PT, Kunkel SL, Burdick MD, Armstrong I, et al. The association between mortality rates and decreased concentrations of interleukin-10 and interleukin-1 receptor antagonist in the lung fluids of patients with the adult respiratory distress syndrome. *Ann Intern Med* 1996;125(3):191-6.
51. Meduri GU, Headley S, Kohler G, Stentz F, Tolley E, Umberger R, et al. Persistent elevation of inflammatory cytokines predicts a poor outcome in ARDS. Plasma IL-1 beta and IL-6 levels are consistent and efficient predictors of outcome over time. *Chest* 1995;107(4):1062-73.
52. Brown KA, Brain SD, Pearson JD, Edgeworth JD, Lewis SM, Treacher DF. Neutrophils in development of multiple organ failure in sepsis. *Lancet* 2006;368(9530):157-69.
53. Weiss M, Elsharkawi M, Welt K, Schneider EM. Transient leukocytosis, granulocyte colony-stimulating factor plasma concentrations, and apoptosis determined by binding of annexin V by peripheral leukocytes in patients with severe sepsis. *Ann N Y Acad Sci* 2003;1010:742-7.
54. Elmore S. Apoptosis: a review of programmed cell death. *Toxicol Pathol* 2007;35(4):495-516.
55. Roth GA, Krenn C, Brunner M, Moser B, Ploder M, Spittler A, et al. Elevated serum levels of epithelial cell apoptosis-specific cytokeratin 18 neoepitope m30 in critically ill patients. *Shock* 2004;22(3):218-20.
56. Ku NO, Liao J, Omary MB. Apoptosis generates stable fragments of human type I keratins. *J Biol Chem* 1997;272(52):33197-203.
57. Rock KL, Latz E, Ontiveros F, Kono H. The sterile inflammatory response. *Annu Rev Immunol* 2010;28:321-42.
58. Chen GY, Nunez G. Sterile inflammation: sensing and reacting to damage. *Nat Rev Immunol* 2010;10(12):826-37.
59. Packham G. The role of NF-kappaB in lymphoid malignancies. *Br J Haematol* 2008;143(1):3-15.

60. Dejardin E. The alternative NF-kappaB pathway from biochemistry to biology: pitfalls and promises for future drug development. *Biochem Pharmacol* 2006;72(9):1161-79.
61. Xiao G, Rabson AB, Young W, Qing G, Qu Z. Alternative pathways of NF-kappaB activation: a double-edged sword in health and disease. *Cytokine Growth Factor Rev* 2006;17(4):281-93.
62. Kaplanski G, Marin V, Montero-Julian F, Mantovani A, Farnarier C. IL-6: a regulator of the transition from neutrophil to monocyte recruitment during inflammation. *Trends Immunol* 2003;24(1):25-9.
63. Munoz C, Carlet J, Fitting C, Misset B, Bleriot JP, Cavaillon JM. Dysregulation of in vitro cytokine production by monocytes during sepsis. *J Clin Invest* 1991;88(5):1747-54.
64. Chensue SW, Terebuh PD, Remick DG, Scales WE, Kunkel SL. In vivo biologic and immunohistochemical analysis of interleukin-1 alpha, beta and tumor necrosis factor during experimental endotoxemia. Kinetics, Kupffer cell expression, and glucocorticoid effects. *Am J Pathol* 1991;138(2):395-402.
65. Aderem A, Underhill DM. Mechanisms of phagocytosis in macrophages. *Annu Rev Immunol* 1999;17:593-623.
66. Tilley R, Mackman N. Tissue factor in hemostasis and thrombosis. *Semin Thromb Hemost* 2006;32(1):5-10.
67. Ge Y, Ezzell RM, Clark BD, Loiselle PM, Amato SF, Warren HS. Relationship of tissue and cellular interleukin-1 and lipopolysaccharide after endotoxemia and bacteremia. *J Infect Dis* 1997;176(5):1313-21.
68. Bradford MM. A rapid and sensitive method for the quantitation of microgram quantities of protein utilizing the principle of protein-dye binding. *Anal Biochem* 1976;72:248-54.
69. Altshuler B. Modeling of dose-response relationships. *Environ Health Perspect* 1981;42:23-7.
70. Hajjar AM, Ernst RK, Tsai JH, Wilson CB, Miller SI. Human Toll-like receptor 4 recognizes host-specific LPS modifications. *Nat Immunol* 2002;3(4):354-9.
71. Lu YC, Yeh WC, Ohashi PS. LPS/TLR4 signal transduction pathway. *Cytokine* 2008;42(2):145-51.
72. Matsuguchi T, Musikacharoen T, Ogawa T, Yoshikai Y. Gene expressions of Toll-like receptor 2, but not Toll-like receptor 4, is induced by LPS and inflammatory cytokines in mouse macrophages. *J Immunol* 2000;165(10):5767-72.
73. Rehli M. Of mice and men: species variations of Toll-like receptor expression. *Trends Immunol* 2002;23(8):375-8.
74. Visintin A, Mazzoni A, Spitzer JA, Segal DM. Secreted MD-2 is a large polymeric protein that efficiently confers lipopolysaccharide sensitivity to Toll-like receptor 4. *Proc Natl Acad Sci U S A* 2001;98(21):12156-61.
75. Ernst RK, Hajjar AM, Tsai JH, Moskowitz SM, Wilson CB, Miller SI. Pseudomonas aeruginosa lipid A diversity and its recognition by Toll-like receptor 4. *J Endotoxin Res* 2003;9(6):395-400.
76. Warren HS, Fitting C, Hoff E, Adib-Conquy M, Beasley-Topliffe L, Tesini B, et al. Resilience to bacterial infection: difference between species could be due to proteins in serum. *J Infect Dis* 2010;201(2):223-32.
77. Takashiba S, Van Dyke TE, Amar S, Murayama Y, Soskolne AW, Shapira L. Differentiation of monocytes to macrophages primes cells for lipopolysaccharide stimulation via accumulation of cytoplasmic nuclear factor kappaB. *Infect Immun* 1999;67(11):5573-8.

78. Schaedler RW, Dubos RJ. The susceptibility of mice to bacterial endotoxins. *J Exp Med* 1961;113:559-70.
79. Copeland S, Warren HS, Lowry SF, Calvano SE, Remick D, Inflammation, et al. Acute inflammatory response to endotoxin in mice and humans. *Clin Diagn Lab Immunol* 2005;12(1):60-7.
80. Shukla S, MacLennan GT, Fu P, Patel J, Marengo SR, Resnick MI, et al. Nuclear factor-kappaB/p65 (Rel A) is constitutively activated in human prostate adenocarcinoma and correlates with disease progression. *Neoplasia* 2004;6(4):390-400.
81. Doi K, Leelahavanichkul A, Yuen PS, Star RA. Animal models of sepsis and sepsis-induced kidney injury. *J Clin Invest* 2009;119(10):2868-78.
82. Dyson A, Singer M. Animal models of sepsis: why does preclinical efficacy fail to translate to the clinical setting? *Crit Care Med* 2009;37(1 Suppl):S30-7.
83. Butcher EC. Leukocyte-endothelial cell recognition: three (or more) steps to specificity and diversity. *Cell* 1991;67(6):1033-6.
84. Delaigle AM, Senou M, Guiot Y, Many MC, Brichard SM. Induction of adiponectin in skeletal muscle of type 2 diabetic mice: In vivo and in vitro studies. *Diabetologia* 2006;49(6):1311-23.
85. Van Amersfoort ES, Van Berkel TJ, Kuiper J. Receptors, mediators, and mechanisms involved in bacterial sepsis and septic shock. *Clin Microbiol Rev* 2003;16(3):379-414.
86. Dear JW, Yasuda H, Hu X, Hieny S, Yuen PS, Hewitt SM, et al. Sepsis-induced organ failure is mediated by different pathways in the kidney and liver: acute renal failure is dependent on MyD88 but not renal cell apoptosis. *Kidney Int* 2006;69(5):832-6.
87. Feterowski C, Emmanuilidis K, Miethke T, Gerauer K, Rump M, Ulm K, et al. Effects of functional Toll-like receptor-4 mutations on the immune response to human and experimental sepsis. *Immunology* 2003;109(3):426-31.
88. Hotchkiss RS, Swanson PE, Freeman BD, Tinsley KW, Cobb JP, Matuschak GM, et al. Apoptotic cell death in patients with sepsis, shock, and multiple organ dysfunction. *Crit Care Med* 1999;27(7):1230-51.
89. Liu LM, Zhang JX, Luo J, Guo HX, Deng H, Chen JY, et al. A role of cell apoptosis in lipopolysaccharide (LPS)-induced nonlethal liver injury in D-galactosamine (D-GalN)-sensitized rats. *Dig Dis Sci* 2008;53(5):1316-24.
90. Jirillo E, Caccavo D, Magrone T, Piccigallo E, Amati L, Lembo A, et al. The role of the liver in the response to LPS: experimental and clinical findings. *J Endotoxin Res* 2002;8(5):319-27.
91. Koskinas J, Gomatos IP, Tiniakos DG, Memos N, Boutsikou M, Garatzioti A, et al. Liver histology in ICU patients dying from sepsis: a clinico-pathological study. *World J Gastroenterol* 2008;14(9):1389-93.
92. Abraham E, Carmody A, Shenkar R, Arcaroli J. Neutrophils as early immunologic effectors in hemorrhage- or endotoxemia-induced acute lung injury. *Am J Physiol Lung Cell Mol Physiol* 2000;279(6):L1137-45.
93. Fantuzzi G. Adipose tissue, adipokines, and inflammation. *J Allergy Clin Immunol* 2005;115(5):911-9; quiz 20.
94. Diez JJ, Iglesias P. The role of the novel adipocyte-derived hormone adiponectin in human disease. *Eur J Endocrinol* 2003;148(3):293-300.
95. Wang SD, Huang KJ, Lin YS, Lei HY. Sepsis-induced apoptosis of the thymocytes in mice. *J Immunol* 1994;152(10):5014-21.
96. Hinson JA, Roberts DW, James LP. Mechanisms of acetaminophen-induced liver necrosis. *Handb Exp Pharmacol* 2010(196):369-405.

97. Blazka ME, Elwell MR, Holladay SD, Wilson RE, Luster MI. Histopathology of acetaminophen-induced liver changes: role of interleukin 1 alpha and tumor necrosis factor alpha. *Toxicol Pathol* 1996;24(2):181-9.
98. Ley K. Integration of inflammatory signals by rolling neutrophils. *Immunol Rev* 2002;186:8-18.
99. Teoh H, Quan A, Bang KW, Wang G, Lovren F, Vu V, et al. Adiponectin deficiency promotes endothelial activation and profoundly exacerbates sepsis-related mortality. *Am J Physiol Endocrinol Metab* 2008;295(3):E658-64.
100. Blazka ME, Wilmer JL, Holladay SD, Wilson RE, Luster MI. Role of proinflammatory cytokines in acetaminophen hepatotoxicity. *Toxicol Appl Pharmacol* 1995;133(1):43-52.
101. Jaeschke H. Mechanisms of Liver Injury. II. Mechanisms of neutrophil-induced liver cell injury during hepatic ischemia-reperfusion and other acute inflammatory conditions. *Am J Physiol Gastrointest Liver Physiol* 2006;290(6):G1083-8.
102. Harris BA. Editorial: Some thoughts on teaching obstetrics and gynecology in a family practice program. *Ala J Med Sci* 1976;13(2):133.
103. Wei Y, Chen K, Whaley-Connell AT, Stump CS, Ibdah JA, Sowers JR. Skeletal muscle insulin resistance: role of inflammatory cytokines and reactive oxygen species. *Am J Physiol Regul Integr Comp Physiol* 2008;294(3):R673-80.
104. Ayala A, Herdon CD, Lehman DL, Ayala CA, Chaudry IH. Differential induction of apoptosis in lymphoid tissues during sepsis: variation in onset, frequency, and the nature of the mediators. *Blood* 1996;87(10):4261-75.
105. Baggiolini M. Chemokines and leukocyte traffic. *Nature* 1998;392(6676):565-8.
106. Antoine DJ, Williams DP, Kipar A, Laverty H, Park BK. Diet restriction inhibits apoptosis and HMGB1 oxidation and promotes inflammatory cell recruitment during acetaminophen hepatotoxicity. *Mol Med* 2010;16(11-12):479-90.
107. Haslett C. Resolution of acute inflammation and the role of apoptosis in the tissue fate of granulocytes. *Clin Sci (Lond)* 1992;83(6):639-48.
108. Andonegui G, Bonder CS, Green F, Mullaly SC, Zbytnuik L, Raharjo E, et al. Endothelium-derived Toll-like receptor-4 is the key molecule in LPS-induced neutrophil sequestration into lungs. *J Clin Invest* 2003;111(7):1011-20.
109. Zhang YH, Takahashi K, Jiang GZ, Kawai M, Fukada M, Yokochi T. In vivo induction of apoptosis (programmed cell death) in mouse thymus by administration of lipopolysaccharide. *Infect Immun* 1993;61(12):5044-8.
110. Hiramatsu M, Hotchkiss RS, Karl IE, Buchman TG. Cecal ligation and puncture (CLP) induces apoptosis in thymus, spleen, lung, and gut by an endotoxin and TNF-independent pathway. *Shock* 1997;7(4):247-53.
111. Huston JM, Wang H, Ochani M, Ochani K, Rosas-Ballina M, Gallowitsch-Puerta M, et al. Splenectomy protects against sepsis lethality and reduces serum HMGB1 levels. *J Immunol* 2008;181(5):3535-9.
112. Fleming KM, West J, Aithal GP, Fletcher AE. Abnormal liver tests in people aged 75 and above: prevalence and association with mortality. *Aliment Pharmacol Ther* 2011;34(3):324-34.
113. Williams R. Global challenges in liver disease. *Hepatology* 2006;44(3):521-6.
114. Thomson SJ, Westlake S, Rahman TM, Cowan ML, Majeed A, Maxwell JD, et al. Chronic liver disease--an increasing problem: a study of hospital admission and mortality rates in England, 1979-2005, with particular reference to alcoholic liver disease. *Alcohol Alcohol* 2008;43(4):416-22.
115. Canabal JM, Kramer DJ. Management of sepsis in patients with liver failure. *Curr Opin Crit Care* 2008;14(2):189-97.

116. Nagata K, Suzuki H, Sakaguchi S. Common pathogenic mechanism in development progression of liver injury caused by non-alcoholic or alcoholic steatohepatitis. *J Toxicol Sci* 2007;32(5):453-68.
117. Berry PA, Wendon JA. The management of severe alcoholic liver disease and variceal bleeding in the intensive care unit. *Curr Opin Crit Care* 2006;12(2):171-7.
118. Kavli M, Strom T, Carlsson M, Dahler-Eriksen B, Toft P. The outcome of critical illness in decompensated alcoholic liver cirrhosis. *Acta Anaesthesiol Scand* 2012;56(8):987-94.
119. Gerhardt W, Keller H. Evaluation of test data from clinical studies. I. Terminology, graphic interpretation, diagnostic strategies, and selection of sample groups. II. Critical review of the concepts of efficiency, receiver operated characteristics (ROC), and likelihood ratios. *Scand J Clin Lab Invest Suppl* 1986;181:1-74.
120. Child CG, Turcotte JG. Surgery and portal hypertension. *Major Probl Clin Surg* 1964;1:1-85.
121. Wang CS, Chang TT, Yao WJ, Wang ST, Chou P. Impact of increasing alanine aminotransferase levels within normal range on incident diabetes. *J Formos Med Assoc* 2012;111(4):201-8.
122. Andersson U, Tracey KJ. HMGB1 in sepsis. *Scand J Infect Dis* 2003;35(9):577-84.
123. Liu Z, Zhang J, Huang X, Huang L, Li S, Wang Z. Magnesium sulfate inhibits the secretion of high mobility group box 1 from lipopolysaccharide-activated RAW264.7 macrophages in vitro. *J Surg Res* 2012.
124. Sunden-Cullberg J, Norrby-Teglund A, Rouhiainen A, Rauvala H, Herman G, Tracey KJ, et al. Persistent elevation of high mobility group box-1 protein (HMGB1) in patients with severe sepsis and septic shock. *Crit Care Med* 2005;33(3):564-73.
125. Angus DC, Yang L, Kong L, Kellum JA, Delude RL, Tracey KJ, et al. Circulating high-mobility group box 1 (HMGB1) concentrations are elevated in both uncomplicated pneumonia and pneumonia with severe sepsis. *Crit Care Med* 2007;35(4):1061-7.
126. Karlsson S, Pettila V, Tenhunen J, Laru-Sompa R, Hynninen M, Ruokonen E. HMGB1 as a predictor of organ dysfunction and outcome in patients with severe sepsis. *Intensive Care Med* 2008;34(6):1046-53.
127. Qin S, Wang H, Yuan R, Li H, Ochani M, Ochani K, et al. Role of HMGB1 in apoptosis-mediated sepsis lethality. *J Exp Med* 2006;203(7):1637-42.
128. Peltz ED, Moore EE, Eckels PC, Damle SS, Tsuruta Y, Johnson JL, et al. HMGB1 is markedly elevated within 6 hours of mechanical trauma in humans. *Shock* 2009;32(1):17-22.
129. Albayrak A, Uyanik MH, Cerrah S, Altas S, Dursun H, Demir M, et al. Is HMGB1 a new indirect marker for revealing fibrosis in chronic hepatitis and a new therapeutic target in treatment? *Viral Immunol* 2010;23(6):633-8.
130. Rosa H, Silverio AO, Perini RF, Arruda CB. Bacterial infection in cirrhotic patients and its relationship with alcohol. *Am J Gastroenterol* 2000;95(5):1290-3.
131. Takano K, Shinoda M, Tanabe M, Miyasho T, Yamada S, Ono S, et al. Protective effect of high-mobility group box 1 blockade on acute liver failure in rats. *Shock* 2010;34(6):573-9.
132. Zhou RR, Liu HB, Peng JP, Huang Y, Li N, Xiao MF, et al. High mobility group box chromosomal protein 1 in acute-on-chronic liver failure patients and mice with ConA-induced acute liver injury. *Exp Mol Pathol* 2012;93(2):213-9.
133. Nanji AA, Hiller-Sturmhofel S. Apoptosis and necrosis: two types of cell death in alcoholic liver disease. *Alcohol Health Res World* 1997;21(4):325-30.
134. Bantel H, Schulze-Osthoff K. Cell death in sepsis: a matter of how, when, and where. *Crit Care* 2009;13(4):173.

135. Hofer S, Brenner T, Bopp C, Steppan J, Lichtenstern C, Weitz J, et al. Cell death serum biomarkers are early predictors for survival in severe septic patients with hepatic dysfunction. *Crit Care* 2009;13(3):R93.
136. Dieterle F, Sistare F, Goodsaid F, Papaluca M, Ozer JS, Webb CP, et al. Renal biomarker qualification submission: a dialog between the FDA-EMEA and Predictive Safety Testing Consortium. *Nat Biotechnol* 2010;28(5):455-62.

VII Appendix I

Below is an Index of all histopathological analysis of organs from each animal. Animals are indexed by their case number, and this is given along with the study number, intervention and a summary of the major histological findings from each individual tissue.

Case No	Animal	Treatment/ cull	Tissue	Histology
Samples from the University of Liverpool				
12L-1393	1	25mg/kg LPS; 6h	Heart	NHAIR
			Lung	Capillaries and veins packed with NL (and monocytes?), activation of endothelial cells (EC), some NL rolling on arterial walls
			Liver	No glycogen (NG; PAS), but often one to several smaller, well delineated vacuoles in hepatocytes; small NL aggregate in parenchyma and mild increase in individual NL between hepatic cords (HC); several NL in central and portal veins (CV, PV) [PHOTO]
			Pancreas	NHAIR; interstitial vein with numerous NL
			Kidney	NHAIR
			Spleen	Mod. sized follicles with several apoptotic cells; red pulp with mod. cellularity and numerous apoptotic cells
			Thymus	Numerous apoptotic cells, in particular in cortex [PHOTO]
			BM	Mod. cellularity, some apoptotic cells
			Brain	NHAIR; several NL in capillaries, occ. packed [PHOTO]
			MG	NHAIR (mainly L)
			EF	NHAIR
			BF	NHAIR
			Skin	NHAIR (no fat included)
12L-1394	2	25mg/kg LPS; 6h	Heart	NHAIR
			Lung	Numerous NL in vessels and capillaries, with some NL rolling
			Liver	NG (PAS); increased number of individual and small groups of NL between HC; some NL rolling in CV and PV
			Pancreas	NHAIR
			Kidney	NHAIR
			Spleen	Mod. sized follicles with several apoptotic cells; red pulp with low cellularity, numerous apoptotic cells and some NL aggregates [PHOTO]
			BM	Mod. cellularity, some apoptotic cells
			Brain	NHAIR; some NL in veins
			MG	NHAIR
			EF	NHAIR, apart from focal extensive acute haemorrhage
			BF	NHAIR
			Skin	NHAIR; small veins in sc fat partly packed with NL
12L-1395	3	25mg/kg LPS; 6h	Heart	NHAIR
			Lung	Often numerous NL in veins and capillaries, partly packed, with some NL rolling
			Liver	NG (PAS); increased number of individual and small groups of NL between HC; some NL rolling in CV and PV
			Pancreas	NHAIR
			Kidney	NHAIR
			Spleen	Mod. sized follicles with some apoptotic cells; red pulp with very low cellularity, some apoptotic cells and some NL
			Thymus	Numerous apoptotic cells, in particular in cortex

			Popl. ln	NHAIR
			BM	Mod. cellularity; occ. apoptotic cell
			Brain	NHAIR; some leptomeningeal veins with numerous NL
			MG	NHAIR
			EF	NHAIR
			BF	NHAIR; small veins with numerous NL
			Skin	NHAIR (hardly any fat)
12L-1396	4	25mg/kg LPS; 6h	Heart	NHAIR
			Lung	Often numerous NL in veins and capillaries, partly packed, with some NL rolling
			Liver	NG (PAS); mildly increased number of individual and small groups of NL between HC; some NL rolling in CV and PV
			Pancreas	NHAIR
			Kidney	NHAIR
			Spleen	Mod. sized follicles with several apoptotic cells; red pulp with mod. cellularity and numerous apoptotic cells
			Thymus	Numerous apoptotic cells, in particular in cortex
			BM	Mod. cellularity; occ. apoptotic cell
			Brain	NHAIR; some NL in veins
			MG	NHAIR
			EF	NHAIR; small veins with numerous NL
			BF	NHAIR
12L-1397	5	25mg/kg LPS; 6h	Heart	NHAIR
			Lung	Often numerous NL in veins and capillaries, partly packed, with some NL rolling
			Liver	Patchy aggregates of hepatocytes with glycogen, else NG (PAS); mildly increased number of individual and small groups of NL between HC; some NL in CV and PV
			Pancreas	NHAIR
			Kidney	Focal interstitial mononuclear infiltration, otherwise NAIR
			Brain	NHAIR; several NL in veins, some rolling
			Spleen	Rel large secondary? follicles with numerous apoptotic cells; red pulp with mod. cellularity and numerous apoptotic cells and NL
			Thymus	Numerous apoptotic cells, in particular in cortex
			BM	High cellularity; occ. apoptotic cell
			MG	NHAIR
			EF	NHAIR
			BF	NHAIR; small veins with numerous NL [PHOTO]
			Skin	Dermal and sc vessels often with numerous NL [PHOTO]
12L-1398	6	25mg/kg LPS; 6h	Heart	NHAIR
			Lung	Often numerous NL in veins and capillaries, often packed, with some NL rolling
			Liver	NG (PAS); mildly increased number of individual and small groups of NL between HC
			Pancreas	NHAIR
			Kidney	NHAIR
			BM	High cellularity; occ. apoptotic cell
			MG	NHAIR
			EF	NHAIR
			PF	NHAIR
			Skin	NHAIR, one sc vein with several NL
12L-1399	7	25mg/kg LPS; 6h	Heart	NHAIR; a few NL attached to EC in atrium
			Lung	Often numerous NL in veins and capillaries, often packed, with some NL rolling
			Liver	NG (PAS); mod. increased number of individual and scattered larger groups of NL (with necrotic hepatocytes) between HC

			Kidney	NHAIR
			Brain	Several NL in small veins
			Spleen	Mod sized follicles with numerous apoptotic cells; red pulp with mod. cellularity and numerous apoptotic cells
			Thymus	Very numerous apoptotic cells, in particular in cortex
			Ln	Small follicles and T cell zones, no apoptotic cells
			BM	High cellularity; occ. apoptotic cell
			MG	NHAIR (mainly L)
			EF	NHAIR; veins with several NL
			Skin	NHAIR
12L-1400	8	25mg/kg LPS; 6h	Heart	NHAIR
			Lung	Often numerous NL in veins and capillaries, with some NL rolling
			Liver	Mod number of hepatocytes with glycogen, patchy (PAS); mod. increased number of individual and scattered larger groups of NL between HC
			Kidney	NHAIR
			Brain	NHAIR
			Spleen	Mod sized follicles with mod. number of apoptotic cells; red pulp with mod. cellularity and some apoptotic cells and numerous NL
			Thymus	Mod number of apoptotic cells, in particular in cortex
			BM	High cellularity; occ. apoptotic cell
			MG	NHAIR (mainly L)
			EF	Mild multifocal mononuclear (LC, PC, mØ) infiltration, some NL in vein
			PF	NHAIR
			Skin	NHAIR; veins with numerous NL
12L-1401	9	25mg/kg LPS; 6h	Heart	NHAIR
			Lung	Small veins often packed with NL, also numerous in arteries, with some NL rolling and EC activation; mild focal alveolar haemorrhage [PHOTO]
			Liver	Scattered hepatocytes with glycogen (PAS); increased number of individual and very small groups of NL between HC, some NL in CV and PV
			Kidney	NHAIR
			Brain	NHAIR
			Spleen	Rel large follicles with a few apoptotic cells; red pulp with low cellularity and occ. apoptotic cells and several NL
			Thymus	Rel. numerous apoptotic cells, in particular in cortex
			BM	High cellularity; occ. apoptotic cell
			MG	NHAIR (mainly L)
			EF	NHAIR, apart from several veins with numerous NL, some rolling? [PHOTOS]
			BF	NHAIR
			Skin	NHAIR
12L-1402	10	25mg/kg LPS; 6h	Heart	NHAIR
			Lung	Small veins often packed with NL, also numerous in arteries, with some NL rolling and EC activation [PHOTO]
			Liver	NG (PAS); increased number of individual and some small groups of NL with occ. necrotic hepatocyte between HC, some NL in CV and PV, occ. rolling [PHOTO]
			Kidney	Glomerula with occ. homogenous eosinophilic material in tufts (PAS: slightly pos.) [PHOTO]
			Spleen	Mod sized follicles with several apoptotic cells; red pulp with low cellularity and some apoptotic cells
			Thymus	Numerous apoptotic cells, in particular in cortex
			BM	Mod cellularity; some apoptotic cells

			MG	NHAIR
			EF	NHAIR
			BF	NHAIR
			Skin	NHAIR
12L-1403	11	25mg/kg LPS; 6h	Lung	Small veins with numerous NL, partly packed, with some NL rolling
			Liver	NG (PAS); mildly increased number of individual and occ. group of NL with necrotic hepatocyte between HC, some NL in CV and PV
			Kidney	NHAIR
			Brain	NHAIR
			Spleen	Mod sized follicles with several apoptotic cells; red pulp with low cellularity and several apoptotic cells and NL
			BM	Mod cellularity; some apoptotic cells
			MG	NHAIR
			EF	NHAIR
			BF	NHAIR
			Skin	NHAIR
12L-1404	12	Inter-peritoneal saline (control); 6h	Heart	NHAIR
			Lung	NHAIR
			Liver	Diffuse glycogen (DG; PAS); one small mixed cellular aggregate
			Kidney	Occ. tubular and glomerular protein casts; otherwise NHAIR
			Spleen	Rel small follicles with a few apoptotic cells; cell rich red pulp
			Thymus	A few disseminated apoptotic cells, in particular in cortex
			BM	High cellularity
			MG	NHAIR (mainly L), apart from the presence of NL in lumen of vessels and occasionally immediately outside capillary
			EF	NHAIR, apart from the presence of numerous NL in lumen of vessels
			BF	Focal attachment of bacteria and debris (from faeces suspension) with NL aggregates to serosa; numerous vessels with NL in lumen
12L-1405	13	Inter-peritoneal saline (control); 6h	Heart	NHAIR
			Lung	NHAIR [PHOTO]
			Liver	DG (PAS); NHAIR [PHOTO]
			Kidney	NHAIR
			Spleen	Rel small follicles; cell rich red pulp [PHOTO]
			Thymus	Occ. apoptotic cell in cortex [PHOTO]
			BM	High cellularity
			MG	NHAIR
			EF	NHAIR
			Skin	NHAIR
12L-1406	14	Inter-peritoneal saline (control); 6h	Heart	NHAIR
			Lung	NHAIR
			Liver	DG (PAS); NHAIR
			Kidney	NHAIR
			Spleen	Rel small follicles; cell rich red pulp
			Thymus	Occ. apoptotic cell in cortex
			BM	High cellularity
			MG	NHAIR
			EF	NHAIR
			BF	NHAIR
			Skin	NHAIR; ln. with a few NL in lumen of vessels and in medulla
12L-1407	15	Inter-peritoneal saline	Heart	NHAIR (cross section)
			Liver	DG (PAS); NHAIR
			Kidney	NHAIR

		(control); 6h	Spleen	Rel small follicles; cell rich red pulp
			Thymus	Occ. apoptotic cell in cortex
			BM	High cellularity
			MG	NHAIR
			EF	NHAIR, apart from the presence of several NL in lumen of vessels
			Skin	NHAIR, apart from the presence of numerous NL in lumen of vessels
12L-1408	16	Inter-peritoneal saline (control); 6h	Heart	NHAIR
			Lung	NHAIR
			Liver	DG (PAS); NHAIR, apart from scattered small NL aggregates with occ. necrotic hepatocyte
			Kidney	NHAIR
			Spleen	Mod sized, partly secondary follicles, often with several apoptotic cells; cell rich red pulp
			Thymus	Some disseminated apoptotic cells in cortex
			BM	High cellularity
			MG	NHAIR
			EF, peri-renal fat	NHAIR, apart from the presence of several NL in lumen of vessels in perirenal fat and focal macrophage infiltration in EF
			BF	NHAIR, apart from focal extensive acute haemorrhage
			Skin	NHAIR (very small section)
12L-1409	17	Inter-peritoneal saline (control); 6h	Heart	NHAIR
			Lung	NHAIR
			Liver	DG (PAS); NHAIR, apart from scattered small NL aggregates with occ. necrotic hepatocyte
			Kidney	NHAIR
			Spleen	Mod sized, partly secondary follicles, with some apoptotic cells; cell rich red pulp
			Thymus	Some disseminated apoptotic cells in cortex
			BM	High cellularity
			MG with fat	Presence of several NL in lumen of vessels and multifocal mild to mod NL infiltration (focal neutrophilic interstitial myositis and steatitis)
			Skin	NHAIR
12L-1410	18	350mg/kg APAP; 6h	Heart	NHAIR
			Lung	NHAIR, apart from scattered apoptotic alveolar epithelial cells
			Liver	NG (PAS), but delineated cytoplasmic vacuoles in hepatocytes, often larger centrilobular; scattered centrilobular apoptotic/necrotic hepatocytes; occ. NL in central vein and occ. a few leukocytes in adjacent sinuses
			Kidney	NHAIR
			Spleen	Mod sized, partly secondary follicles, with numerous apoptotic cells; cell rich red pulp with numerous apoptotic cells
			BM	High cellularity; a few apoptotic cells
			MG	NHAIR
			EF	NHAIR
			BF	NHAIR (perirenal, subcutaneous)
			Skin	NHAIR
12L-1411	19	350mg/kg APAP; 6h	Heart	NHAIR
			Lung	NHAIR, apart from scattered apoptotic cells (where?)
			Liver	NG (PAS), but delineated cytoplasmic vacuoles in hepatocytes, larger centrilobular (1-2 cell layers, hydropic degeneration); scattered centrilobular apoptotic/necrotic hepatocytes; a few NL and some activated EC (?) in central

				veins [PHOTO]
			Kidney	NHAIR
			Spleen	Rel small follicles, with numerous apoptotic cells; cell rich red pulp with numerous apoptotic cells [PHOTO]
			Thymus	Numerous apoptotic cells, in particular in cortex [PHOTO]
			BM	High cellularity; some apoptotic cells
			MG	NHAIR
			EF	NHAIR
			BF	NHAIR
			Skin	NHAIR
12L-1412	20	350mg/kg APAP; 6h	Heart	NHAIR
			Lung	NHAIR
			Liver	NG (PAS), but delineated cytoplasmic vacuoles in hepatocytes; centrilobular cell loss and hydropic swelling/degeneration of remaining hepatocytes [Grade 2] [PHOTO]
			Kidney	NHAIR
			Spleen	Rel small follicles with numerous apoptotic cells; cell rich red pulp with numerous apoptotic cells
			Thymus	Numerous apoptotic cells, in particular in cortex
			BM	High cellularity; some apoptotic cells
			MG	NHAIR
			EF	NHAIR, apart from focal mononuclear infiltrate (ln.?)
			BF	NHAIR
			Skin	NHAIR
12L-1413	21	350mg/kg APAP; 6h	Heart	NHAIR
			Lung	NHAIR
			Liver	NG (PAS), but delineated cytoplasmic vacuoles in hepatocytes; centrilobular cell loss and hydropic swelling/degeneration of remaining hepatocytes [Grade 2-3]
			Kidney	NHAIR
			Spleen	Rel small follicles with very numerous apoptotic cells; cell rich red pulp with numerous apoptotic cells
			Thymus	Very numerous apoptotic cells, in particular in cortex
			BM	High cellularity; some apoptotic cells
			MG	NHAIR
			EF	NHAIR
			BF	NHAIR
			Skin	NHAIR
12L-1414	22	350mg/kg APAP; 6h	Heart	NHAIR
			Lung	NHAIR
			Liver	NG (PAS), but delineated cytoplasmic vacuoles in hepatocytes; centrilobular cell loss and hydropic swelling/degeneration of remaining hepatocytes [Grade 2-3]
			Kidney	NHAIR
			Spleen	Rel small follicles with very numerous apoptotic cells; cell rich red pulp with numerous apoptotic cells
			Thymus	Numerous apoptotic cells, in particular in cortex
			BM	High cellularity; a few apoptotic cells
			MG	NHAIR
			EF	NHAIR, apart from the presence of several NL in lumen of vessels and some outside vessels
			BF	NHAIR
			Skin	NHAIR, apart from focal mononuclear infiltration in subcutis
12L-1415	23	350mg/kg APAP; 6h	Heart	NHAIR
			Lung	NHAIR
			Liver	NG (PAS), but delineated cytoplasmic vacuoles in hepatocytes; centrilobular cell loss and hydropic

				swelling/degeneration of remaining hepatocytes [Grade 1-2]
			Kidney	NHAIR
			Spleen	Rel small follicles with numerous apoptotic cells; cell rich red pulp with several apoptotic cells
			BM	High cellularity; numerous apoptotic cells
			MG	NHAIR
			EF	NHAIR
			BF	NHAIR
			Skin	NHAIR
Samples from the University of Jena				
12L-1073	1	Inter-peritoneal saline (control); 6h	Liver	Diffuse glycogen (DG), most pronounced centrilobular (PAS); NHAIR
			MG	NHAIR (mainly L)
			EF	NHAIR
			PF	NHAIR
			SF	NHAIR (with skeletal muscle, NHAIR)
12L-1074	2	Inter-peritoneal saline (control); 6h	Liver	DG, most pronounced centrilobular (PAS); NHAIR, apart from small random focal leukocyte aggregate
			MG	NHAIR (mainly L)
			EF	NHAIR
			PF	NHAIR
			SF	NHAIR
12L-1075	3	Inter-peritoneal saline (control); 6h	Liver	DG, most pronounced centrilobular (PAS); NHAIR
			MG	NHAIR (mainly L)
			EF	NHAIR
			PF	NHAIR
			SF	NHAIR, with larger artery exhibiting activated (?) endothelial cells (EC)
12L-1076	4	Inter-peritoneal saline (control); 6h	Liver	DG, most pronounced centrilobular (PAS); focal area of coagulative necrosis with a few leukocytes (NL); two random focal leukocyte aggregates
			MG	NHAIR (mainly L)
			EF	NHAIR
			PF	NHAIR
			SF	NHAIR
12L-1077	5	Inter-peritoneal saline (control); 6h	Liver	DG, most pronounced centrilobular (PAS); NHAIR
			MG	NHAIR (mainly L)
			EF	NHAIR
			PF	NHAIR, apart from small focal subserosal LC aggregate
			SF	NHAIR (with skeletal muscle, NHAIR)
12L-1078	6	Inter-peritoneal saline (control); 6h	Liver	DG, most pronounced centrilobular (PAS); NHAIR
			MG	NHAIR
			EF	NHAIR
			PF	NHAIR
			SF	NHAIR, apart from a small loose focal aggregates of mØ
12L-1079	7	Inter-peritoneal saline (control); 6h	Liver	DG, most pronounced centrilobular (PAS); one small focal aggregates of 5-6 NL beside central vein (CV); occasionally a few leukocytes in CV
			MG	NHAIR (mainly L)
			EF	NHAIR
			PF	NHAIR
			SF	Some arteries with mild EC activation; a few leukocytes in lumen of small veins; slight multifocal PC/LC infiltration (with skeletal muscle, NHAIR)
12L-1080	8	Inter-peritoneal saline (control); 6h	Liver	DG, most pronounced centrilobular (PAS); scattered random small focal leukocyte aggregates
			MG	NHAIR (mainly L)
			EF	NHAIR

			PF	NHAIR
			SF	NHAIR
12L-1081	9	Inter-peritoneal saline (control); 6h	Liver	DG, most pronounced centrilobular (PAS); NHAIR
			MG	NHAIR (mainly L)
			EF	NHAIR, apart from focal subserosal LC aggregate
			PF	NHAIR
			SF	Focal, poorly delineated area with small vessel EC activation and mild to moderate perivascular and interstitial mixed cellular (mØ, fewer NL and LC) infiltration
12L-1082	10	Inter-peritoneal saline (control); 6h	Liver	DG, most pronounced centrilobular (PAS); NHAIR, apart from one random focal leukocyte aggregate
			MG	NHAIR (mainly L)
			EF	NHAIR
			PF	NHAIR
			SF	NHAIR
12L-1083	11	Inter-peritoneal saline (control); 6h	Liver	DG, most pronounced centrilobular (PAS); scattered random small leukocyte aggregates, one focal large area of LC infiltration around a CV
			MG	NHAIR (mainly L)
			EF	NHAIR
			PF	NHAIR, apart from marked multifocal acute interstitial haemorrhage
			SF	NHAIR
12L-1084	12	1.75 mL/kg body weight stool suspension; 6h	Liver	DG, most pronounced centrilobular (PAS); multifocal patchy subserosal NL infiltration and focal attachment of bacteria and debris (from faeces suspension) to serosa; a few to several NL in the lumen of CVs and portal veins (PV)
			MG	NHAIR (mainly L), apart from the presence of NL in lumen of vessels and occasionally immediately outside capillary
			EF	NHAIR, apart from the presence of numerous NL in lumen of vessels
			PF	Focal attachment of bacteria and debris (from faeces suspension) with NL aggregates to serosa; numerous vessels with NL in lumen
			SF	NHAIR, apart from the presence of numerous NL in lumen of vessels
12L-1085	13	1.75 mL/kg body weight stool suspension; 6h	Liver	DG (variable intensity; PAS); subserosal (multifocally) one layer of NL infiltration; several NL in the lumen of CVs and PVs and a few in sinusoids immediately outside CV
			MG	NHAIR (mainly L), apart from the presence of some NL in lumen of vessels
			EF	NHAIR, apart from the presence of numerous NL in lumen of vessels
			PF	Focal subserosal LC aggregate; attachment of bacteria and debris (from faeces suspension) with NL to serosa; several vessels with NL in lumen
			SF	NHAIR, apart from the presence of occasional NL in lumen of vessels
12L-1086	14	1.75 mL/kg body weight stool suspension; 6h	Liver	Mutifocal patchy (sub)serosal NL infiltration, partly with fibrin/cell debris and bacteria (from faeces suspension); several NL in the lumen of CVs and PVs; DG, most pronounced centrilobular (PAS)
			MG	NHAIR (mainly L)
			EF	NHAIR, apart from the presence of numerous NL in lumen of vessels
			PF	Focal attachment of bacteria and debris (from faeces suspension) with NL and blood to serosa; vessels with NL in lumen
			SF	NHAIR, apart from the presence of NL in lumen of vessels

12L-1087	15	1.75 mL/kg body weight stool suspension; 6h	Liver	Slight focal subserosal NL infiltration; several NL in the lumen of CVs and PVs and a few in sinusoids immediately outside CV; DG (variable intensity, PAS)
			MG	NHAIR (mainly L), apart from the presence of some NL in lumen of vessels
			EF	NHAIR, apart from the presence of several NL in vessels
			PF	NHAIR, apart from the presence of some NL in lumen of vessels
			SF	NHAIR, apart from the presence of some NL in lumen of vessels
12L-1088	16	1.75 mL/kg body weight stool suspension; 6h	Liver	Slight focal subserosal NL infiltration; several NL in the lumen of CVs and PVs and a few in sinusoids immediately outside CV; DG (variable, but generally reduced intensity, PAS)
			MG	NHAIR (mainly L), apart from the presence of several NL in lumen of vessels
			EF	NHAIR, apart from the presence of numerous NL in lumen of vessels
			PF	Focal attachment of NL with bacteria and debris (from faeces suspension) to serosa and (sub)serosal infiltration by mØ and NL; vessels with numerous NL in lumen
			SF	NHAIR, apart from the presence of often numerous NL in lumen of vessels
12L-1089	17	1.75 mL/kg body weight stool suspension; 6h	Liver	Subserosal (multifocally) one layer of NL infiltration and focal attachment of NL with debris and bacteria (from faecal suspension); several NL in the lumen of CVs and PVs and a few in sinusoids immediately outside CV; DG (variable intensity, reduced amount, PAS)
			MG	NHAIR (mainly L), apart from the presence of a few NL in lumen of vessels
			EF	NHAIR, apart from the presence of NL in lumen of some vessels and slight focal subserosal LC infiltration
			PF	NHAIR, apart from the presence of NL in lumen of vessels
			SF	NHAIR, apart from the presence of several NL in lumen of vessels and focal mild perivascular LC infiltrate
12L-1090	18	1.75 mL/kg body weight stool suspension; 6h	Liver	Subserosal (multifocally) one layer of NL infiltration and focal attachment of NL with debris and bacteria (from faecal suspension), in one subserosal area focal hepatocellular coagulative necrosis; several NL in the lumen of CVs and PVs and a few in sinusoids immediately outside CV; DG (variable intensity, reduced amount, PAS)
			MG	NHAIR (mainly L), apart from the presence of a few NL in lumen of vessels
			EF	NHAIR, apart from the presence of NL in lumen of vessels
			PF	NHAIR, apart from the presence of NL in lumen of vessels
			SF	NHAIR, apart from the presence of NL in lumen of vessels
12L-1091	19	1.75 mL/kg body weight stool suspension; 6h	Liver	Multifocal (sub)serosal NL infiltration (very superficial), often with attached NL with fibrin and bacteria (from faeces suspension); several NL in the lumen of CVs and PVs; DG (variable intensity, reduced amount, PAS)
			MG	NHAIR (mainly L), apart from the presence of a few NL in lumen of vessels
			EF	NHAIR, apart from the presence of some NL in lumen of vessels
			PF	NHAIR, apart from the presence of some NL in lumen of vessels
			SF	NHAIR, apart from the presence of several NL in lumen of vessels
12L-	20	1.75 mL/kg	Liver	A few (sub)serosal NL; some NL in the lumen of CVs and

1092		body weight stool suspension; 6h		PVs; DG (variable intensity, PAS)
			MG	NHAIR (mainly L)
			EF	NHAIR, apart from the presence of a few NL in lumen of vessels
			PF	NHAIR
			SF	NHAIR, apart from the presence of a few NL in vessels
12L-1093	21	1.75 mL/kg body weight stool suspension; 6h	Liver	Multifocal mild (sub)serosal NL infiltration (very superficial), occasionally attached NL with fibrin and bacteria (from faeces suspension); several NL in the lumen of CVs and PVs; DG (variable intensity, reduced amount, PAS) [PHOTOS]
			MG	Apart from the presence of several NL in the lumen of a larger artery, NHAIR (mainly L); **no** rolling! [PHOTOS]
			EF	NHAIR, apart from the presence of some NL in lumen of vessels[PHOTOS]
			PF	Focal serosal NL infiltration with some bacteria; vessels often with a few NL in lumen [PHOTOS]
			SF	NHAIR, apart from the presence of several NL in lumen of vessels [PHOTOS]
12L-1094	22	1.75 mL/kg body weight stool suspension; 6h	Liver	Multifocal mild (sub)serosal NL infiltration (very superficial), occasionally attached NL with fibrin and bacteria (from faeces suspension); several NL in the lumen of CVs and PVs and a few in sinuses immediately adjacent to CV; DG (variable intensity, reduced amount, PAS)
			MG	NHAIR (mainly L), apart from the presence of several NL in lumen of vessels
			EF	NHAIR, apart from the presence of numerous NL in lumen of vessels
			PF	NHAIR, apart from the presence of some NL in lumen of vessels and focal attachment of a small amount of NL with debris and bacteria to the serosa
			SF	NHAIR, apart from the presence of numerous NL in lumen of vessels

* MG – Musculus gastrocnemius; EF – epididymal fat; BF – brown fat; SF – subcutaneous fat; BM – bone marrow (sternum, femoro-tibial joint); NHAIR – no histological abnormality is recognised; L – longitudinal section; NL – neutrophils, LC – lymphocytes, mØ – macrophages .